

FORECASTING DOWNDRAFT WIND SPEEDS
ASSOCIATED WITH AIRMASS
THUNDERSTORMS FOR PETERSON AIR FORCE
BASE, COLORADO, USING THE WSR-88D

THESIS

Travis A Steen, Captain, USAF
AFIT/GM/ENP/99M-10

DEPARTMENT OF THE AIR FORCE
AIR UNIVERSITY
AIR FORCE INSTITUTE OF TECHNOLOGY

Wright-Patterson Air Force Base, Ohio

DISTRIBUTION STATEMENT A

Approved for Public Release
Distribution Unlimited

DISTRIBUTION STATEMENT

DTIC QUALITY INSPECTED 2

19990402 013

AFIT/GM/ENP/99M-10

FORECASTING DOWNDRAFT WIND SPEEDS ASSOCIATED WITH AIRMASS
THUNDERSTORMS FOR PETERSON AIR FORCE BASE, COLORADO, USING
THE WSR-88D

THESIS

Presented to the Faculty of the Graduate School of Engineering

of the Air Force Institute of Technology

Air University

Air Education and Training Command

In Partial Fulfillment of the Requirements for the

Degree of Master of Science in Meteorology

Travis A. Steen, B.S.

Captain, USAF

March, 1999

Approved for Public Release – Distribution Unlimited

AFIT/GM/ENP/99M-10

FORECASTING DOWNDRAFT WIND SPEEDS ASSOCIATED WITH AIRMASS
THUNDERSTORMS FOR PETERSON AIR FORCE BASE, COLORADO, USING
THE WSR-88D

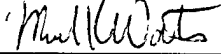
Travis A. Steen, B.S.
Captain, USAF

Approved:



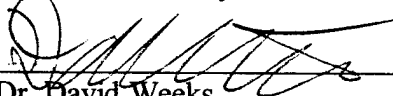
Lt Col Cecilia A. Miner
Chair, Advisory Committee

1 Mar 99
Date



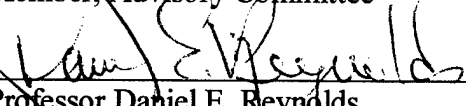
Lt Col Michael K. Walters
Member, Advisory Committee

1 Mar 99
Date



Dr. David Weeks
Member, Advisory Committee

2 Mar 99
Date



Professor Daniel E. Reynolds
Member, Advisory Committee

1 Mar 99
Date

The views expressed in this thesis are those of the author and do not reflect the official policy or position of the Department of Defense or the U.S. Government.

Acknowledgments

I would like to express my sincere appreciation to my faculty advisors, Lt Col Cecilia Miner and Lt Col Michael Walters, for their guidance and support throughout the course of this thesis effort. Their help and experience was greatly appreciated. I would also like to thank Professor Daniel Reynolds for his guidance and assistance in the statistical portion of this research. Your classes helped a great deal. Finally, I would like to thank MSgt Pete Rahe for all his help during this research including keeping me in business with WATADS and the forecast contest. You made the process run much smoother. Thank you.

Travis A. Steen

Table of Contents

Acknowledgments.....	ii
Table of Contents.....	iii
List of Figures.....	vi
List of Tables.....	viii
Abstract.....	x
1 Introduction.....	1
1.1 Background.....	1
1.2 Problem Statement.....	6
1.3 Research Objectives.....	6
1.4 Research Focus.....	7
1.5 Overall Approach.....	9
1.6 Summary of Results.....	10
1.7 Preview.....	12
2 Literature Review.....	14
2.1 Downdraft Theory.....	14
2.1.1 Foster (1958).....	14
2.1.2 Fujita (1985).....	15
2.1.3 NIMROD (1978).....	15
2.1.4 JAWS (1982).....	16
2.1.5 Results of NIMROD and JAWS.....	17
2.1.6 Emanuel (1981).....	18
2.1.7 Brown, Knupp and Caracena (1982).....	18
2.1.8 Srivastava (1985).....	19
2.1.9 Wakimoto (1985).....	21
2.2 Radar Applications to Downdraft Forecasting.....	22
2.2.1 McCarthy and Wilson (1985).....	22
2.2.2 Roberts and Wilson (1989).....	23
2.2.3 Greene and Clark (1972).....	24
2.3 Downdraft Studies.....	25
2.3.1 Stewart (1991).....	25
2.3.2 Frazier (1992).....	27
2.3.3 United States Air Force, Headquarters Air Weather Service (1996).....	29
2.3.4 Stewart (1996).....	30
2.3.5 Stewart and Vasiloff (1998).....	33

3	Methodology	35
3.1	Data Set Selection	35
3.1.1	Type of Convective Event.....	35
3.1.2	Time Period.....	36
3.1.3	Identification of Airmass Thunderstorm Days.....	36
3.1.3.1	Screening Surface Observations.....	37
3.1.3.2	Screening Lightning Data.....	39
3.1.3.3	Screening Surface Observations: Part II.....	40
3.1.3.4	Screening Daily Surface Weather Maps.....	41
3.1.3.5	Acquiring WSR-88D Data.....	42
3.2	Radar Products.....	42
3.3	Data Collection	43
3.4	Data Processing.....	44
3.5	Development of Research Method.....	49
4	Results and Analysis.....	51
4.1	Description of Data Set	51
4.2	Evaluation of Techniques	54
4.2.1	Stewart's VIL/TOP Technique (1991).....	54
4.2.2	Headquarters AWS' VIL/TOP Technique (1996).....	59
4.2.3	Stewart's Maximum dBZ/Height of Maximum dBZ Technique (1996).....	62
4.2.4	Stewart and Vasiloff's Dry Microburst Prediction Technique (1998).....	64
4.3	Description of Wind Data Set.....	67
4.4	Regression of Wind Techniques	68
4.4.1	Regression of VIL and TOP.....	68
4.4.2	Regression of Maximum dBZ and Height of Maximum dBZ.....	72
4.4.3	Regression of Maximum dBZ and Sub-Cloud Temperature Lapse Rate.....	75
4.5	Regression of Radar Products.....	76
4.6	Validation of the Developed Regression Models	91
4.7	A Second Validation of the Developed Regression Models	95
5	Conclusion.....	98
5.1	Problem Statement Review.....	98
5.2	Review of Methodology	99
5.3	Review of Results	100
5.4	Possible Sources of Error	101
5.5	Recommendations	104
	Appendix A: Acronyms.....	107
	Appendix B: Radar Worksheets	109
	Appendix C: Sample WSR-88D Images.....	119
	Bibliography	122

Vita..... 125

List of Figures

Figure 1. A schematic model of a surface microburst (Fujita, 1985).	2
Figure 2. Plot of predicted wind gust (kts) obtained from equation (3) using Maximum dBZ and Height of Maximum dBZ values. Adapted from Stewart (1996).	32
Figure 3. Sample surface observation for PAFB recording a thunderstorm (TS).	38
Figure 4. Sample lightning flash observation for PAFB.	39
Figure 5. Radar products collected and research relevance.	43
Figure 6. Scatter plot of computed wind speeds using Stewart's (1991) VIL/TOP technique versus observed wind speeds.	58
Figure 7. Scatter plot of computed wind speeds using Headquarters AWS' (1996) VIL/TOP technique versus observed wind speeds.	61
Figure 8. Scatter plot of computed wind speeds using Stewart's (1996) Maximum dBZ/Height of Maximum dBZ technique versus observed wind speeds.	64
Figure 9. Scatter plot of the computed wind speeds using Stewart and Vasiloff's (1998) DMP technique versus observed wind speeds.	66
Figure 10. Scatter plot of Grid Based VIL vs. observed wind speeds.	69
Figure 11. Scatter plot of EchoTop Height vs. observed wind speeds.	70
Figure 12. Statistical nonlinear regression models used.	71
Figure 13. Scatter plot of Maximum dBZ value vs. observed wind speeds.	73
Figure 14. Scatter plot of Height of Maximum dBZ vs. observed wind speeds.	73
Figure 15. Scatter plot of Cell Based VIL vs. observed wind speeds.	77
Figure 16. Scatter plot of Storm Top Heights vs. observed wind gust speeds.	77
Figure 17. Scatter plot of Cloud Base Heights vs. observed wind speeds.	78
Figure 18. Regression residual plot for equation (4).	82
Figure 19. Plot of observed wind speeds vs. computed wind speeds using equation (4).	83

Figure 20. Wilk-Shapiro/Rankit Plot for residuals of equation (4).	84
Figure 21. Regression residual plot for equation (5).	88
Figure 22. Plot of observed wind speeds vs. computed wind speeds using equation (5).	89
Figure 23. Wilk-Shapiro/Rankit Plot for residuals of equation (5).	90

List of Tables

Table 1. Results from the evaluation of the four potential wind gust prediction techniques.....	11
Table 2. Vertical air velocities (kts) at $z=3.7$ km for Marshall-Palmer raindrop size distribution, at the top of the downdraft column, as a function of environmental lapse rate and reflectivity. Adapted from Srivastava (1985).	21
Table 3. Potential wind gust (kts) as a function of VIL and TOP. Adapted from Stewart (1991).....	26
Table 4. Potential wind gust (kts) as a function of VIL and TOP. Adapted from Headquarters Air Weather Service (1996).....	29
Table 5. Potential wind gusts (kts) as a function of peak radar reflectivity (observed at or just above cloud base) and the sub-cloud lapse rate [after Srivastava (1985)] for a penetrative depth of 3800m. Adapted from Stewart (1998).	33
Table 6. Summary statistics for collected radar products.	52
Table 7. Pearson correlation (top value in each block) and P-values (bottom value) for collected radar products.	53
Table 8. Summary statistics for sub-cloud temperature lapse rate ($K\ km^{-1}$).	54
Table 9. Predicted and observed wind gust speeds.....	55
Table 10. Mean absolute error, root mean-squared error and bias for the four potential wind gust prediction techniques.	57
Table 11. Summary statistics for predicted and observed wind gust speeds (kts).	67
Table 12. Results of the multiple regression model using VIL and TOP products.	71
Table 13. Results of multiple regression model using Maximum dBZ and Height of Maximum dBZ products.	74
Table 14. Results of multiple regression model using Maximum dBZ and sub-cloud temperature lapse rate products.	75
Table 15. Results of multiple regression model using VIL, Cell Based VIL, TOP, ST, Maximum dBZ, Height of Maximum dBZ, Cloud Base Height and sub-cloud temperature lapse rate products.	79

Table 16. Observed and predicted wind gust speeds computed using Grid Based VIL, Height of Maximum dBZ and equation (4).	81
Table 17. Observed and predicted wind gust speeds computed using Grid Based VIL, Height of Maximum dBZ and equation (5).	87
Table 18. Results of sixteen full quadratic regression models using Grid Based VIL and Height of Maximum dBZ.....	96
Table 19. Results of sixteen first-order interaction regression models using Grid Based VIL and Height of Maximum dBZ.....	97

Abstract

During the period Jun-Aug 96, four Air Force installations suffered over \$4.8 million in damage from convective winds. During the same summer, Air Force Space Command units issued nearly 65% of their weather warnings for convective winds, making the forecasting of convective winds the most frequent challenge to forecasters. This thesis seeks to assist Air Force forecasters at Peterson Air Force Base (PAFB), Colorado, in forecasting airmass thunderstorm downdraft wind speeds using the Weather Surveillance Radar-1988 Doppler (WSR-88D).

To accomplish this purpose, several existing potential downdraft wind speed prediction techniques were evaluated against the observed wind speeds of nineteen airmass thunderstorms. The nineteen airmass thunderstorms studied accounted for all airmass thunderstorms occurring within 10.5 nm of PAFB from 1 Apr-30 Sep 96 and 1 Apr-30 Sep 97 and for which archived WSR-88D data was available. The results of the evaluations suggested the prediction techniques in operational use are not accurate in forecasting downdraft wind speeds at PAFB. Moreover, it was discovered during this research that the technique developed by the Air Force's Air Weather Service (AWS) to predict wind gust potential has no scientific basis and its use by Air Force forecasters should be discontinued. A statistical analysis of these prediction techniques using WSR-88D data collected from the airmass thunderstorms provided no accurate means by which to statistically modify these techniques for application at PAFB. Finally, 112 regression models were developed and tested to identify a possible relationship between WSR-88D

products and observed wind gusts resulting from the airmass thunderstorms. Of these 112 regression models, only two models incorporating Grid Based VIL and Height of Maximum dBZ were determined to be both valid and statistically significant in explaining the variation in observed wind gust speeds. Using data collected from sixteen storms, the two regression models were evaluated and predicted a wind speed within ± 5 kts of the observed wind speed for twelve of the sixteen storms. This successful potential wind gust forecast was significantly better than the potential wind gust forecasts of the four techniques evaluated and currently in operational use. Although the results obtained are inconclusive due to the small data set of airmass thunderstorms used, the results appear promising. Consequently, further research should be conducted using a larger data set of airmass thunderstorms to evaluate the two regression models developed for application at PAFB.

FORECASTING DOWNDRAFT WIND SPEEDS ASSOCIATED WITH AIRMASS THUNDERSTORMS FOR PETERSON AIR FORCE BASE, COLORADO, USING THE WSR-88D

1 Introduction

1.1 Background

A downdraft is defined as “a relatively small-scale current of air with marked [downward] vertical motion” (Huschke, 1989:177). The magnitude wind gusts could attain as a result of thunderstorm downdrafts reaching the surface was not completely accepted by the meteorological community until Dr. T. Theodore Fujita surveyed damage associated with an outbreak of tornadoes on 3-4 April 1974. Fujita hypothesized that some of the damage was the result of a thunderstorm downdraft and not a tornado. However, it was not until over a year later when Fujita first used the term “downburst” while investigating the Eastern Airlines Flight 66 accident on 24 June 1975 at John F. Kennedy Airport, New York City, to describe this meteorological phenomenon. At the time, Fujita defined a downburst as “a strong downdraft which induces an outburst of damaging winds on or near the ground.” The identification of this atmospheric phenomenon led Fujita to conduct the first field investigation of downbursts in 1978 titled Northern Illinois Meteorological Research On Downbursts (NIMROD). During 42 days of research Fujita identified the fact that downbursts did exist, and they were of both large and small horizontal scale (Fujita, 1985:2-4). As a result, Fujita sub-classified downbursts into two types based on their horizontal scale length; he defined a

“microburst” as a small downburst less than 4 km in horizontal dimension, and a “macroburst” as a downburst greater than 4 km in horizontal dimension (Fujita, 1985:8).

Figure 1 is schematic model of a surface microburst.

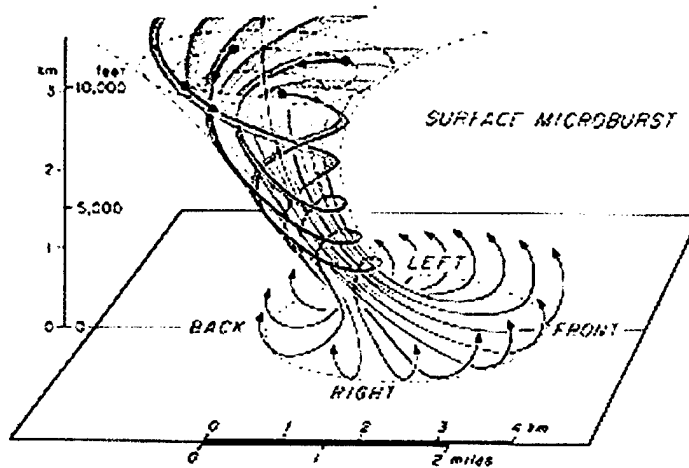


Figure 1. A schematic model of a surface microburst (Fujita, 1985).

A second field investigation of downbursts was conducted in 1982 by Fujita just north of Denver, Colorado. At the time, it appeared microburst-related aircraft accidents were on the rise throughout the world; thus, the Joint Airport Weather Studies (JAWS) was undertaken to further research on microbursts (Fujita, 1985:49). From this experiment it was discovered that microbursts could occur with or without measurable rain occurring from the parent cell. As a result of this experiment and this newly identified phenomenon, microbursts were further sub-classified into “dry” and “wet” microbursts (Fujita, 1985:70-71). Although these are the two basic subcategories, Read and Elmore (1989) later discovered while analyzing atmospheric soundings for microbursts in northern Texas that downbursts existed in environmental conditions

between those of the wet and dry microburst. These newly discovered microbursts were termed “hybrid” microbursts (National Weather Service Training Center Hydrometeorology and Management Division, 1993: 62).

With the identification and verification of downbursts as a meteorological phenomenon in the late 1970s and early 1980s, Dr. Kerry Emmanuel conducted further research dealing with downdraft theory. He built upon Squires (1958) theory that unsaturated downdrafts introduced at cloud top, and driven by evaporative cooling, could penetrate to great depths through the cloud. Emanuel developed a theory suggesting that these in-cloud downdrafts could penetrate throughout the entire thunderstorm and reach the surface at great velocities and were very capable of causing considerable damage. Finally, Emmanuel suggested that these downdrafts might be related to downbursts (Emanuel, 1981:1541,1556).

With the increased use of weather models in the 1980s to predict wind gust speeds associated with thunderstorm downdrafts, the difficult part became the ability of forecasters to quickly obtain values for the model’s parameters. The increased use of radar, and later the widespread use of Doppler radar, held potential in solving this problem. Two of the first researchers to recognize this fact were McCarthy and Wilson (1985) during the Classify, Locate and Avoid Wind Shear (CLAWS) Project. Doppler radar was utilized throughout this project, and they concluded that Doppler radar was a very useful tool in microburst warning during their project, and could possibly be very effective in forecasting thunderstorm downdrafts (McCarthy and Wilson, 1985:255). In 1989, Roberts and Wilson used Doppler radar data collected from the CLAWS Project to identify radar signatures characteristic of the microburst-producing storms. They

concluded from their research that Doppler radar could provide a 0-10 minute warning prior to the onset of microbursts (Roberts and Wilson, 1989:285).

In 1991, Stewart attempted to quantify downdraft wind gust potential using weather radar. Stewart modified Emmanuel's (1981) equation, and using products obtained by the Weather Surveillance Radar-1957 (WSR-57) (a non-Doppler radar which was the precursor to the WSR-88D) empirically developed an equation using the WSR-57's Vertically Integrated Liquid Water Content (VIL) and Echo Top (TOP) products to forecast wind gust potential for airmass thunderstorms. (VIL is a product which estimates the amount of liquid water contained in a storm. TOP is a reflectivity-based product depicting the highest level of the 18.5 dBZ return detected over a specific location.) His verification rate using VIL, TOP and his technique to forecast wind gust speeds was 82 percent (Stewart, 1991:15). Therefore, his research strongly suggested that a possible method existed which used WSR-57 VIL and TOP products to forecast wind gust speeds.

With the fielding of the WSR-88D in the late eighties and early nineties, the entire continental United States experienced complete Doppler coverage (with the exception of a few sparsely populated areas in the western United States). As a result of this widespread fielding of the WSR-88D, meteorologists were better equipped to conduct downburst studies that used Doppler radar. One such use of the WSR-88D to forecast downbursts and predict their resultant wind gust speeds was the Air Force Air Weather Service's adaptation of Stewart's (1991) VIL/TOP table. Stewart's table was originally created for the non-Doppler WSR-57 used prior to the fielding of the WSR-88D. However, the Air Weather Service (AWS) table was recommended for use by operational

Air Force forecasters to obtain a forecasted wind gust potential for pulse-type (i.e., airmass) thunderstorms using the WSR-88D. Like Stewart's (1991) table, the AWS table provided specific wind gust speeds based on different values of VIL and TOP heights (Headquarters Air Weather Service, January 1996).

In an effort to develop a wind gust potential technique for the WSR-88D, Stewart developed a method to predict wind gust speeds for airmass thunderstorms using the maximum reflectivity value of a storm and the height of this maximum reflectivity to determine maximum wind gust potential (Stewart, 1996:324-325).

Finally, recognizing that there are considerable differences between the dry and wet environments, Stewart and Vasiloff (1998) conducted a study in the High Plains to fine tune one of Srivastava's (1985) wind gust prediction techniques. (In the context of this research, the High Plains region of the United States was defined as the elevated terrain starting at the eastern foothills of the Rocky Mountains and extending eastward into the central United States.) In their research, they found a strong correlation in the dry microburst environment between a storm's maximum reflectivity at or just above cloud base and the sub-cloud temperature lapse rate to determine downdraft wind speeds.

With the exception of Stewart and Vasiloff's (1998) technique developed specifically for dry microburst prediction, the problem with the majority of the research already conducted was that little study had been aimed at downdraft wind gust prediction using the WSR-88D in the High Plains region of the United States. Air Force forecasters in this region, like forecasters throughout the United States, face the daunting task of predicting the strength of downdraft winds to assist in personnel safety and resource protection. The importance of this forecast is illustrated in two ways. First, during the

summer of 1996, Air Force Space Command (AFSPC) units issued nearly 65% of their weather warnings for convective winds, making it the most frequent challenge to forecasters. Second, the magnitude of the risk is illustrated by the fact that during the period Jun-Aug 96, four Air Force installations suffered over \$4.8 million in damage from convective winds. The WSR-88D represents a potent tool for assisting Air Force forecasters in overcoming some of the hurdles associated with predicting downdraft wind speeds in this region; thus, this research investigated possible ways the WSR-88D could be used to forecast downdraft wind speeds associated with airmass thunderstorms in the High Plains, specifically Peterson Air Force Base (PAFB), Colorado.

1.2 Problem Statement

How do existing potential wind gust prediction techniques perform in forecasting downdraft induced surface wind speeds for airmass thunderstorms occurring near PAFB? Furthermore, how can WSR-88D products, specifically Vertically Integrated Liquid Water (VIL), Echo Top (TOP), Storm Top (ST) and reflectivity, be used by Air Force forecasters to accurately forecast downdraft induced surface wind speeds at PAFB?

1.3 Research Objectives

Several objectives were accomplished during this research. The first objective was to evaluate the operational effectiveness of the four existing techniques used to forecast potential wind gust speeds for airmass thunderstorms at PAFB. The techniques that were evaluated were Stewart's (1991) VIL/TOP technique, Stewart's (1996) Maximum Reflectivity/Height of Maximum Reflectivity technique, Headquarters Air Weather Service's (1996) VIL/TOP technique, and finally Stewart and Vasiloff's (1998) Dry Microburst Gust Prediction (DMP) technique. The second objective of this research was

to attempt to modify the techniques that did not accurately forecast downdraft wind speeds for PAFB. This modification consisted of statistically analyzing and regressing the WSR-88D data collected during this research in an effort to find a relationship that could be used in forecasting wind gust speeds for airmass thunderstorm occurring near PAFB. The third objective of this research was to identify, through an extensive literature review, other important WSR-88D products not used in the four studies mentioned above, and attempt to find a possible correlation between these newly identified radar products and downdraft wind speeds at PAFB. All three of these objectives attempted to address and solve the original problem of this research which was to provide a method by which Air Force forecasters could accurately forecast airmass thunderstorm downdraft wind speeds, to include downbursts, at PAFB.

1.4 Research Focus

The focus of this research revolved around using the WSR-88D to study downdraft-induced wind gusts equal to or in excess of 15 knots resulting from airmass thunderstorms within a 10.5 nm radius of PAFB, and occurring during the periods 1 April-30 September 1996 and 1 April-30 September 1997. The reason the focus of this research was so specific in its definition was due to several limiting factors. The first of these limiting factors was the time to conduct research. Since a great deal of data was needed to meet the research objectives for a single location, it was necessary to limit this study to airmass thunderstorms occurring at one location, PAFB. A second limitation was the wind sensor network. PAFB had only one wind sensor recording and archiving wind data. As a result, all airmass thunderstorms occurring near PAFB had to be within 10.5 nm of this wind sensor to be of any use, and thus included in this research. A third

limiting factor was the type of thunderstorm to be studied. Since the four studies to be evaluated by this research all dealt solely with airmass thunderstorms, the class of thunderstorm selected for study was airmass.

One non-limiting factor was the occurrence or non-occurrence of microbursts from the airmass thunderstorms being studied. Of the four techniques studied, three were developed using data from microburst producing airmass thunderstorms. (As will be discussed in section 2.3.3, the fourth technique evaluated was not based on any thunderstorm data.) Since the purpose of this research was to assist Air Force forecasters in forecasting downdraft wind speeds, not just those associated with microbursts, all airmass thunderstorms with winds greater than or equal to 15 knots were included in this research. Furthermore, non-microburst cases were used because in an operational environment, forecasters will not know ahead of time if a microburst will occur; thus, a technique that incorporates all airmass thunderstorm days is needed.

A second non-limiting factor for this research was the type of microburst environment in which the airmass thunderstorm occurred. Therefore, the research conducted for this study was to include the investigation of downdraft winds associated with the dry, hybrid and wet microburst environments. However, the final airmass thunderstorm data set did not include any storms occurring in a wet microburst environment; consequently, the wet microburst environment was no longer of interest to this research. The reason the dry and hybrid microburst environments were both investigated was due to the synoptic environment of the High Plains region. In this type of region, dry microbursts can be expected; however, oftentimes this region can

experience an influx of moisture, thus creating a favorable environment for hybrid microbursts.

Finally, the scope of this study was limited to the investigation of just a few of the WSR-88D products, specifically VIL, Cell Based VIL, TOP, ST, Maximum Reflectivity, Height of Maximum Reflectivity and Cloud Base Height. Currently, there are over sixty different WSR-88D products, and although many products deal with convective activity, the products mentioned above provided the most promise, in this researcher's opinion, in identifying correlation between their values and downdraft wind speeds when using the WSR-88D.

1.5 Overall Approach

Based on the research objectives and focus, the overall approach of this research consisted of three phases. The first phase was to identify all airmass thunderstorms occurring within 10.5 nm of PAFB during 1 Apr-30 Sep 96 and 1 Apr-30 Sep 97 for which observed surface winds were greater than or equal to 15 knots. These airmass thunderstorm days comprised the data set from which the radar data was requested.

The second phase was to order and interrogate Level II data (i.e., archived WSR-88D data) from the Pueblo, Colorado WSR-88D corresponding to the airmass thunderstorms days identified in the first phase. (Pueblo, Colorado is the servicing WSR-88D site for PAFB.) The Level II data was then analyzed using the WSR-88D Algorithm Testing and Display System (WATADS). It was through this analysis that the values for the radar products of interest were collected.

The final phase was to conduct a statistical analysis of the collected radar products. This phase included the evaluation of the existing downdraft prediction techniques for

PAFB and the possible modification of these techniques if they were not accurate predictors of downdraft wind speeds at PAFB. Furthermore, the final step of this statistical analysis included the use of other WSR-88D products to possibly identify a new relationship between the radar products collected and observed downdraft wind speeds.

1.6 Summary of Results

The research conducted was based on a data set of nineteen airmass thunderstorms occurring within 10.5 nm of PAFB during 1 Apr-30 Sep 96 and 1 Apr-30 Sep 97 for which observed winds were greater than or equal to 15 knots. From this data set of thunderstorms, the following results were obtained.

The results of the evaluations of Stewart's (1991) VIL/TOP technique, Headquarters AWS' (1996) VIL/TOP technique, Stewart's (1996) Maximum dBZ/Height of Maximum dBZ method and Stewart and Vasiloff's (1998) DMP technique are presented in Table 1. Section 4.2.1 contains a description of a successful potential wind gust forecast, a missed potential wind gust forecast and a no potential wind gust forecast. As can be discerned from the table, these techniques were not very accurate in forecasting downdraft wind speeds associated with airmass thunderstorms at PAFB for the cases used in this study.

Table 1. Results from the evaluation of the four potential wind gust prediction techniques.

	Stewart's (1991) Technique	Headquarters AWS' (1996) Technique	Stewart's (1996) Technique	Stewart and Vasiloff's (1998) Technique
Number of Successful Potential Wind Gust Forecasts	2	1	4	1
Percentage of Successful Potential Wind Gust Forecasts	11.8	5.9	21.0	5.3
Number of Missed Potential Wind Gust Forecasts	9	5	14	11
Percentage of Missed Potential Wind Gust Forecasts	52.9	29.4	73.7	57.9
Number of No Potential Wind Gust Forecasts	6	11	1	7
Percentage of No Potential Wind Gust Forecasts	35.3	64.7	5.3	36.8

The next objective of this research was to attempt to modify these four prediction techniques for use at PAFB. However, no specific forecasting bias could be identified between the predicted and observed wind gust speeds; thus, statistical regression was conducted on the four techniques. Unfortunately, a multiple regression analysis of the techniques was unable to identify a relationship between the radar products and the observed wind gusts. As a result, modification of the gust prediction techniques for forecasting purposes at PAFB could not be accomplished using the data set available.

The last objective of this research was to investigate the use of radar products other than those used in the four wind gust prediction techniques to forecast downdraft wind

speeds at PAFB. Statistical regression was used to identify a possible relationship between these radar products and observed wind gusts. After 112 regression models were tested, two models that incorporated VIL and Height of Maximum dBZ to explain the variation in observed wind gust speeds showed promise. Both regression models were shown to be valid and statistically significant. Furthermore, the two regression models developed using VIL and Height of Maximum dBZ as independent variables and the observed wind gust speed as the dependent variable, would have predicted a wind speed within ± 5 kts of the observed wind speed 75% of the time for the thunderstorms studied in this research. Although the sample set consisted of only sixteen airmass thunderstorms, since VIL values could be obtained for only sixteen of the nineteen storms studied, the results suggested that the two regression models hold some potential in forecasting downdraft wind speeds associated with airmass thunderstorms for PAFB. However, the results obtained from these two regression models should not be considered conclusive until tested with a larger data set.

1.7 Preview

Chapter 2 briefly reviews the theories, the research and the studies dealing with the theory of thunderstorm downdrafts and the prediction of downdraft-induced surface wind speeds. This literature review chapter is divided into three sections: Downdraft Theory, Radar Applications to Downdraft Forecasting, and Downdraft Studies. These three sections provide the reader with a brief discussion of early downdraft modeling and forecasting, introduce radar applications in downdraft forecasting, and conclude by describing the several studies conducted prior to this research which attempted to forecast downdraft speeds.

Chapter 3 describes in detail the techniques and assumptions used to develop the final data set of airmass thunderstorm days for PAFB. Furthermore, it discusses the interrogation of WSR-88D data to identify airmass thunderstorms near PAFB and the subsequent collection of radar data used in the research to develop a method by which to forecast downdraft speeds for PAFB.

Chapter 4 outlines the analysis of the data collected during this research and evaluates and then attempts to modify the various wind gust prediction methods already in use. Furthermore, it attempts to correlate other radar products to observed wind gusts in an effort to develop a new method to forecast downdraft wind speeds at PAFB.

Chapter 5 reviews the methodology and results of this research, to include the two regression models which show promise in the predicting downdraft winds speeds associated with airmass thunderstorms at PAFB. Finally, the conclusions drawn from this research are discussed to include possible sources of error and recommendations for future research.

2 *Literature Review*

2.1 **Downdraft Theory**

2.1.1 **Foster (1958).**

One of the first attempts to calculate downdraft speeds associated with thunderstorm activity was carried out by Foster. He proposed that a thunderstorm downdraft resulted from “the negative buoyancy force acting on a parcel of air entrained into a thunderstorm at some upper level.” The entrained air cools by evaporation, and upon becoming colder than its environment descends to the ground (Foster, 1958:91). To calculate thunderstorm downdraft speeds Foster integrated the buoyancy equation and then used a thermodynamic diagram to calculate the positive energy area of a descending air parcel. The value of the positive energy area was then substituted into the buoyancy equation and used to calculate the downdraft speed. Using this modified buoyancy equation, Foster computed the downdraft speeds for one hundred atmospheric soundings. Upon comparing these one hundred computed downdraft speeds with the observed surface wind gusts, he obtained a correlation coefficient of 0.50 (Foster, 1958:91). Although a correlation coefficient greater than 0.50 would have been desired, it was still statistically significant enough to conclude that the calculated downdraft speeds were related in some way to the surface wind gusts accompanying a thunderstorm (Foster, 1958:94). His belief was the descending air (i.e., the downdraft), cooled by evaporation, created the wind gusts experienced at the surface (Foster, 1958:91). It was this theory, and not necessarily his method of calculating downdraft speeds, which laid the foundation for future research attempting to forecast surface wind gust speeds associated with thunderstorm activity.

2.1.2 Fujita (1985).

While conducting an aerial survey of Beckley, West Virginia, after an outbreak of tornadoes on 3-4 April 1974, Fujita noticed tree damage arranged in a very peculiar pattern. The pattern was “starburst” in shape, which was not typical of the tree damage pattern resulting from a tornado. Fujita hypothesized that this tree damage was actually caused by a thunderstorm downdraft, and that this downdraft was capable of producing tornado-like damage. However, it was not until he was investigating the Eastern Airlines Flight 66 accident on 24 June 1975 at John F. Kennedy Airport, New York City, that Fujita first used the term “downburst” to describe this type of meteorological event (Fujita, 1985:2). This new term was considered extremely controversial at the time. Although the existence of thunderstorm downdrafts was well known, the meteorological community at the time was not convinced that thunderstorm downdrafts were capable of such damage. The meteorological community believed that no matter the strength of the initial downdraft, it would significantly weaken before reaching the ground and would be unable to cause the type of damage proposed by Fujita (Fujita, 1985:2). However, Fujita’s subsequent research and field studies demonstrated that downbursts could indeed produce damaging surface winds. Furthermore, the identification and classification of this atmospheric phenomenon by Fujita also led other scientists to conduct an immense amount of research pertaining to these newly discovered “downbursts” (Fujita, 1985:1-2).

2.1.3 NIMROD (1978).

The first major field study of downburst winds was conducted between 19 May and 1 July 1978 and sponsored by the University of Chicago. The study, named NIMROD (Northern Illinois Meteorological Research On Downbursts), was conceived and

spearheaded by Fujita and Srivastava. During 42 days of research, the team used three Doppler radars and 27 Portable Automated Mesonet (PAM) stations to identify and record downburst events occurring within the research area (Fujita, 1985:4). The PAM stations recorded wind speeds once a minute, 24 hours a day, for the entire period. In the end, each PAM station recorded 61,766 one-minute maximum winds. Use of a microburst identification algorithm, created by the NIMROD meteorologists solely to sort through the PAM data and identify possible microbursts, resulted in 143 possible microburst events being identified. After further examination of the research data by NIMROD meteorologists, the number of possible microburst events was reduced to fifty (Fujita, 1985:53-55).

2.1.4 JAWS (1982).

A second field experiment named JAWS (Joint Airport Weather Studies) was conducted near Denver, Colorado, between 15 May and 9 August 1982. The experiment led by Fujita, McCarthy and Wilson, tested the hypothesis that a deep sub-cloud dry adiabatic lapse rate common to the High Plains region of the United States would result in the identification of a new type of microburst unlike those identified and studied in the NIMROD experiment (Fujita, 1985:49). As in the NIMROD experiment, three Doppler radars were used along with 27 PAM stations. However, the area over which the Doppler radars and PAM stations were employed was much smaller than that of NIMROD study. A smaller research area was created in an attempt to more accurately identify and interrogate microbursts versus macrobursts, since microbursts appeared to be the more prevalent meteorological phenomenon (Fujita, 1985:4). A second difference between the JAWS and NIMROD studies was the fact that the JAWS was conducted in the High

Plains region of the United States, which was subject to weather regimes very different from those found in the NIMROD experiment. By the end of the experiment, each PAM station had recorded 123,956 maximum winds, and after employing the same microburst identification algorithm used in the NIMROD study and review by JAWS meteorologists, 186 microbursts were identified during the study (Fujita, 1985:53-55).

2.1.5 Results of NIMROD and JAWS.

As a result of the immense amount of data collected in the JAWS and NIMROD study, the researchers were able to provide the meteorological community with a better understanding of downbursts. Results of these studies included the new terms “microburst” and “macroburst.” As discussed in Chapter 1, Fujita defined a “microburst” as a small downburst less than 4 km in horizontal dimension, and a “macroburst” as a downburst greater than 4 km in horizontal dimension (Fujita 1985:4,8). Other results of these studies included the identification of two different types of microburst, the “dry” microburst and the “wet” microburst. The dry microburst was typical of drier regions, often originating from high-based convective clouds. On the other hand, the wet microburst was common to regions that were more humid and originated from a much lower cloud base (Fujita, 1985:71). During the studies it was also confirmed that microbursts did not form on or near the ground; rather they descended from convective cloud bases (Fujita, 1985:72). Furthermore, microbursts could be categorized into “outflow” and “rotor” microbursts with the outflow microburst being the most common type identified in the studies (Fujita, 1985:73,74). Finally, the researchers concluded that parent storms producing microbursts were not always thunderstorms, but could be high-based cumulus or altocumulus clouds (Fujita, 1985:70).

2.1.6 Emanuel (1981).

In 1958, Squires proposed that unsaturated downdrafts introduced at cloud top, and driven by evaporative cooling, could penetrate to great depths through the cloud. Building upon this theory, Emanuel developed a similarity theory discussing the characteristics of unsaturated downdrafts initiated near cloud top (Emanuel, 1981:1541). In this similarity theory, Emanuel argued that as long as certain cloud top instability requirements were met, unsaturated downdrafts could penetrate great depths through the storm, and in some cases reach the surface. The surface-reaching downdrafts could attain velocities similar to those of buoyant updrafts, and were quite capable of causing significant damage. Finally, Emanuel even suggested the surface-reaching downdrafts might be related to downbursts (Emanuel, 1981:1556).

2.1.7 Brown, Knupp and Caracena (1982).

It was accepted as fact by the meteorological community that intense thunderstorms oftentimes produced damaging surface winds. However, the fact that damaging winds could be produced by shallow, high-based convection with little or no lightning present was not as readily accepted. Nevertheless, after observing several of these events during the summer in Colorado, Brown, Knupp and Caracena concluded these types of wind events were very common (Brown and others, 1982:272). They cited five events in eastern Colorado where damaging winds originated from high-based convection with little or no lightning present. Based on these events and others, they hypothesized that these damaging winds resulted from the fact that “weaker updrafts (common to high-based convection) produce precipitation which evaporates and melts more rapidly than that produced in clouds with strong updrafts” (Brown and others, 1982:275). This

raindrop evaporation created cooler, negatively buoyant air, which descended as a result. This descending air parcel was further assisted by the presence of a dry adiabatic sub-cloud layer extremely common to Colorado. This dry adiabatic sub-cloud layer permitted the descending air parcel to maintain its negative buoyancy and descend to the surface unmolested despite the effects of entrainment (Brown and others, 1982:274). It was this negatively buoyant air originating in shallow, high-based cumulonimbi, which often resulted in damaging winds at the surface.

2.1.8 Srivastava (1985).

Fujita's study of downbursts during JAWS and NIMROD quieted any meteorological doubt about the existence of downbursts. Therefore, the challenge that lay ahead was to discover the various environments responsible for creating and driving this meteorological phenomenon. Srivastava sought to shed light on this subject and determine whether an intense downdraft, similar to ones that produce microbursts, could be entirely driven by evaporative cooling due to raindrop evaporation. (Ultimately, Srivastava showed the majority of the microbursts identified during the JAWS project were evaporatively driven.) Moreover, he wanted to identify environmental conditions conducive to the creation of these intense downdrafts (Srivastava, 1985:1005,1022). To accomplish this goal, Srivastava numerically modeled downdraft formation using conditions similar to those encountered during JAWS (i.e., downdraft development in the sub-cloud layer of high-based cumuli common to the High Plains). He then calculated the vertical air velocities for these various environments. His "simple one-dimensional, time dependent model of an evaporatively driven downdraft" took into account the governing equations for raindrop evaporation, rain drop concentration, water substance,

thermodynamic energy and vertical air velocity (Srivastava, 1985:1004). Through application of his model he identified several conditions favoring intense downdraft development. These conditions were a sub-cloud environmental lapse rate close to dry adiabatic, high rainwater mixing ratio near cloud base, and a minimum downdraft radius of about 1 km to ensure mixing of environmental air would not weaken downdraft speeds (Srivastava, 1985:1022). Next, Srivastava was able to quantify downdraft velocities using several different parameters incorporated in his model. Of particular interest to this research was his use of reflectivity and environmental lapse rate values to compute vertical air velocities. Table 2 shows vertical velocities (m s^{-1}) computed by Srivastava at the top of a downdraft column 3,700 meters above sea level (ASL) as a function of reflectivity (dBZ) and environmental lapse rate (K km^{-1}) (Srivastava, 1985:1015). The relationship of these two parameters to downdraft velocities provided the basis for future research on downburst prediction.

Table 2. Vertical air velocities (kts) at $z=3.7$ km for Marshall-Palmer raindrop size distribution, at the top of the downdraft column, as a function of environmental lapse rate and reflectivity. Adapted from Srivastava (1985).

		Reflectivity, dBZ						
		18.7	25.5	29.5	34.2	39.6	46	51.7
Lapse Rate of Environmental Temperature ($K\ km^{-1}$)	9.5	35.0	36.9	40.8	42.7	44.7	52.3	64.1
	9		2.7	29.1	31.1	36.9	44.7	56.3
	8.5		0.5	1.6	18.1	25.3	35.0	46.6
	8		0.4	1.0	3.3	13.2	25.3	38.9
	7.5						16.3	29.1
	7							

2.1.9 Wakimoto (1985).

Using the data collected during JAWS, Wakimoto analyzed the days during which dry microbursts occurred. (Of the 186 microbursts identified during JAWS, 155 were classified as dry [Wakimoto, 1985:1134].) The purpose of this analysis was to identify and document common characteristics between the dry microburst days. This information could then be used to assist in forecasting future dry microburst events (Wakimoto, 1985:1131). Upon completion of his analysis, Wakimoto had identified four common characteristics of these dry microburst days. First, he discovered that in the morning there existed a deep dry adiabatic sub-cloud layer, and just below this layer was a shallow radiational inversion at the surface. Secondly, he discovered that the deep dry adiabatic layer extended roughly to 500 mb. (As mentioned earlier, a deep dry adiabatic layer provides greater potential for evaporative cooling resulting in a stronger negative

buoyancy force acting on the parcel of air.) Thirdly, he noted that the mean sub-cloud mixing ratio was approximately $3\text{-}5 \text{ g kg}^{-1}$, and there existed a region of moisture present in the mid-levels of the atmosphere. Finally, he noted that the convective temperature was reached during the day (Wakimoto, 1985:1138). Along with identifying these four common characteristics between dry microburst days, Wakimoto also noted that the synoptic conditions present on these days were not a major factor in setting up favorable environmental conditions for dry microbursts (Wakimoto, 1985:1141).

2.2 Radar Applications to Downdraft Forecasting

2.2.1 McCarthy and Wilson (1985).

On May 31, 1984, United Airlines Flight 633 had a near-fatal accident at Denver's Stapleton Airport. During a routine takeoff roll, the airplane suddenly lost 20 knots of airspeed. The pilot took immediate action and increased the deck angle of the plane to offset this sudden loss of airspeed. This decisive action enabled the plane to leave the end of the runway approximately five feet off the ground, with the only damage to the plane resulting from its hitting a series of antennas at the end of the runway. Subsequent investigation revealed the cause of this near-fatal accident to be due to Flight 633's encounter with a microburst during takeoff. Immediately following this accident, the Federal Aviation Administration (FAA) requested the JAWS Project to provide real time microburst forecasts and warnings at the Stapleton Airport for the remainder of the 1984 microburst season. The Classify, Locate and Avoid Wind Shear (CLAWS) Project was formed to provide this support (McCarthy and Wilson, 1985:247-248). The main purpose of CLAWS was to support the FAA with resource protection for Stapleton Airport; however, several minor objectives were to be accomplished as well by the

CLAWS Project. These other objectives included the testing of several “short term weather prediction, detection and warning concepts utilizing results from the JAWS analysis,” and to determine if these products were operationally effective for microburst prediction (McCarthy and Wilson, 1985:248). The CLAWS Project was considered a success since there was no loss of life during the rest of the 1984 microburst season, despite the detection of ten additional microbursts. Furthermore, it was estimated that the CLAWS Project, if allowed to run through an entire microburst season, would save the airlines at Stapleton Airport over \$850,000 annually in fuel costs due to accurate wind shift advisories which would prevent missed approaches and delayed departures (McCarthy and Wilson, 1985:253-254). On top of this economic benefit, and of more importance to this research, was the scientific benefit of this project. As Wilson states, “the advanced warning capability of Doppler radar to provide microburst and wind shift warnings was clearly demonstrated [during the CLAWS Project]” (McCarthy and Wilson, 1985:255). It was projects such as these that demonstrated Doppler radar’s usefulness in forecasting thunderstorm downdrafts.

2.2.2 Roberts and Wilson (1989).

Building upon the research conducted during the CLAWS Project, Roberts and Wilson studied 31 microburst-producing storms that occurred in northeastern Colorado. The intent of their study was to identify radar signatures characteristic to microburst-producing storms using Doppler radar. If common signatures could be ascertained, then a nowcast (forecast from 0-30 minutes) could be issued prior to the occurrence of a microburst. What they concluded from their research was that Doppler radar could provide a 0-10 minute warning prior to the onset of microbursts (Roberts and Wilson,

1989:285). This research would set the stage for future attempts to use other Doppler radar products to nowcast severe weather events such as microbursts.

2.2.3 Greene and Clark (1972).

Greene and Clark were two of the first meteorologists to investigate the use of digital radar data for severe weather forecasting. They proposed the digital radar had applications in determining a storm's total liquid-water content (Greene and Clark, 1972:548). At the time of their research, it was becoming widely accepted that the liquid-water content of a thunderstorm had significant meteorological importance. This was based upon the fact that any changes in the liquid-water content of a storm would also correspond to energy changes in the storm (Greene and Clark, 1972:549). For example, an increase in liquid-water content of a storm would result from increased condensation in the storm, thus corresponding to an increase of latent heat being released into the storm environment. Therefore, a sudden increase in a thunderstorm's liquid-water content could represent a strengthening storm (Greene and Clark, 1972:551). Based on these facts, Greene and Clark investigated the possibility of vertically integrating the liquid-water content of a thunderstorm using digital radar. The technique they developed using digital radar allowed them to create a three-dimensional image of a storm's total liquid-water content. With this three-dimensional product, a time series could be created by which to identify and possibly forecast severe storms based on changes in the liquid-water content. They called this three-dimensional radar product VIL (Vertically Integrated Liquid-Water Content), and even suggested that a national network of radar stations could be used to create a composite VIL product which would be helpful in forecasting the development and decay of thunderstorms (Greene and Clark,

1972:548,551). This insightful suggestion proved prophetic, considering the fact that sixteen years later, this proposed VIL product is now one of the severe weather products the WSR-88D provides to the user, and was a product used extensively in this research.

2.3 Downdraft Studies

2.3.1 Stewart (1991).

Building upon Squires' (1958) Cloud Top Penetrative Downdraft Mechanism, and Emanuel's Similarity Theory for Unsaturated Downdrafts within Clouds, Stewart proposed a quantitative technique to forecast wind gust potentials for air mass thunderstorms using VIL and TOP obtained from the WSR-57. (The WSR-57 was the non-Doppler predecessor to the WSR-88D.) Using an empirically-derived version of Emanuel's equation for maximum downward vertical velocity (m s^{-1}), and assuming 1 m^3 of dry air has a specific mass of 1 kg , Stewart developed the following equation for computing maximum surface wind gusts:

$$W=[(20.628571R_cH)-(3.125 \times 10^{-6}H^2)]^{1/2} \quad (1)$$

where

W = maximum downward vertical velocity (m s^{-1}) obtained by air parcel

R_c = storm-averaged rainwater liquid water content (g g^{-1})

H = height (m) above sea level of the 18 dBZ radar echo (Stewart 1991:1-6)

and the coefficients 20.628571 and 3.125×10^{-6} have units of m s^{-2} and s^{-2} , respectively.

Since this equation was to be used in operational forecasts, and R_c is not an easily derived parameter, Stewart replaced R_c with VIL and TOP:

$$R_c = \text{VIL} / \text{TOP} \quad (2)$$

where

R_c = storm-averaged rainwater liquid water content (g g^{-1})

VIL = Vertically Integrated Liquid Water Content (kg m^{-2})

TOP = height (m) of the 18 dBZ radar echo (Stewart 1991:6)

Substituting equation (2) into equation (1), Stewart was able to compute potential wind gust speeds for various VIL and TOP values obtained from the WSR-57. Table 3 presents the potential wind gust speeds computed for various VIL and TOP values.

Table 3. Potential wind gust (kts) as a function of VIL and TOP. Adapted from Stewart (1991).

		Echo Tops (100's feet)									
		250	300	350	400	450	500	550	600	650	700
Vertically Integrated Liquid Water (kg m^{-2})	40	49.3	46.1	42.1	36.9	29.9	19.4				
	45	53.1	50.2	46.5	41.8	35.9	27.7	13.8			
	50	56.7	53.9	50.5	46.3	40.9	34.0	24.1			
	55	60.0	57.4	54.3	50.3	45.5	39.3	31.1	18.4		
	60	63.2	60.7	57.7	54.1	49.6	44.0	36.9	27.0	6.5	
	65	66.2	63.9	61.0	57.5	53.3	48.2	41.8	33.4	20.8	
	70	69.1	66.9	64.1	60.8	56.9	52.1	46.2	38.8	28.7	9.0

In computing final predicted wind gust speeds, Stewart referenced the work of Miller (1967) who recommended vectorially adding one-third of the mean wind, between the surface and 5,000 feet, to the expected peak wind gust (Stewart 1991:7). Therefore, Stewart's method of predicting a final peak wind gust incorporated his computed values

for a given VIL and TOP using equations (1) and (2), and then vectorially adding one-third of the mean wind in the layer from the surface to 5,000 feet.

During his research Stewart looked at 143 separate cases, and using his method to determine a final predicted wind gust for each case, he discovered that 82% of the cases verified through reports of wind damage and/or actual measurement of wind gusts. For the cases that did not verify, potentially severe wind gusts were forecasted but no severe wind reports were received. However, he pointed out that there were no cases in which severe wind gusts occurred and the gust potential technique did not predict such gusts (Stewart, 1991:15,16).

This forecast technique provided forecasters with one of the first quantitative methods by which to forecast potential wind gusts for air mass thunderstorms using two common and easily acquired radar products. In fact, Stewart suggested that “warning lead times up to 20 minutes prior to the occurrence of a severe wind event are common when using this technique” (Stewart 1991:18). It should be noted, though, that his table was created and tested using WSR-57 data obtained from airmass thunderstorms occurring in the southeastern United States, and was not tested in regions where moisture may not be as prevalent.

2.3.2 Frazier (1992).

With the fielding of Table 3 and the use of Stewart’s (1991) VIL/TOP technique to forecast final wind gust potentials by the forecasting community, several National Weather Service Forecast Offices conducted studies to verify this table. The major reason studies were conducted was due to the fact that the technique was created and tested in the southeastern United States. As a result, there was concern over how

accurate this table would be in forecasting wind gusts in other regions of the United States. During the summer of 1992, Frazier conducted a study for the Pittsburgh, Pennsylvania, National Weather Service Forecast Office. The study investigated eighteen confirmed cases of severe pulse-type thunderstorms. Of these eighteen cases, three were presented in his paper. For Case 2 and Case 1, when using Stewart's (1991) method, the predicted wind gusts were off by 2 knots and 1 knot, respectively. The third documented case predicted a severe wind gust of 54 knots, but no actual wind observation was available, although wind damage was reported from the storm for which the wind gust potential was computed. As for the 15 other documented cases, no information was provided in the paper (Frazier, 1994:3-5). Frazier summarizes his results by saying, "with a few minor differences, the results of this study agree with the findings of Stewart" (Frazier, 1994:5). Frazier did note that for the best results using his eighteen case sample, the entire value of the mean wind should be added to the predicted wind gust value as opposed to Stewart's suggestion of adding just one-third the mean wind to the predicted wind gust value. Finally, Frazier cautioned that despite the encouraging results using his eighteen case samples, the technique would probably not work on all pulse-type thunderstorms. Reasons for this prediction included inaccurate VIL values due to hail contamination, and thunderstorms developing too close or too far from the radar for truly accurate interrogation by the radar (Frazier, 1994:4,5). It should be noted that Frazier's study was conducted using the WSR-57, as was Stewart's (1991) study, and not the currently fielded WSR-88D.

2.3.3 United States Air Force, Headquarters Air Weather Service (1996).

With the fielding of the WSR-88D in the early 1990's at several Department of Defense sites, the United States Air Force, Headquarters Air Weather Service, began publishing the semi-annual informational handbook Echoes. The purpose of this publication was to provide military radar operators with the most recent advances in the WSR-88D's capability to forecast severe weather. The January 1996 issue of Echoes specifically dealt with operational uses of VIL. In the issue, Stewart's (1991) and Frazier's (1994) works were cited and a wind potential gust chart (Table 4) similar to Stewart's Table 3 was published.

Table 4. Potential wind gust (kts) as a function of VIL and TOP. Adapted from Headquarters Air Weather Service (1996).

		Vertically Integrated Liquid Water-VIL (kg m^{-2})											
		15	20	25	30	35	40	45	50	55	60	65	70
Echo Tops-TOP (in 1000's of feet)	60								10	16	23	29	34
	55							12	21	27	32	36	40
	50					9	16	24	30	34	38	42	45
	45				10	20	26	31	36	40	43	46	49
	40		9	15	21	27	32	36	40	43	47	50	53
	35	13	18	23	27	32	36	41	43	47	50	53	56
	30	18	23	28	32	36	40	43	47	49	53	56	58
	25	23	28	32	36	41	44	47	49	52	55	57	59
	20	26	31	36	40	44	48	50	52	55	56	59	60
	15	29	34	38	43	47	50	53	55	56	58	61	61

In the Echoes issue that included Table 4, the author (unknown) states that Table 4 is Stewart's original table. However, Table 3 and Table 4 are not the same. Therefore, the accepted table used by military radar operators to forecast potential wind gusts using

WSR-88D VIL and TOP products is different from Stewart's empirically-based Table 3. Furthermore, Table 4 was not based on any case studies or statistical analysis, so no data set existed from which to create a modified Table 3. Therefore, this researcher can determine no scientific basis for Table 4. In addition, it should be noted Stewart's Table 3 was for use with the WSR-57 VIL and TOP products. Unfortunately, there is no mention of this fact in Echoes, and the WSR-88D operator is advised to use this table for predicting potential wind gust speeds using WSR-88D VIL and TOP products (Headquarters Air Weather Service, January 1996). However, the WSR-88D and WSR-57 are two completely different radars, as will be discussed shortly.

2.3.4 Stewart (1996).

In 1996, Stewart revisited the topic of predicting peak wind gusts associated with airmass/pulse-type thunderstorms. With the gust technique he proposed in 1991 (Stewart, 1991), which used the WSR-57, he tested to see if similar results could be produced using WSR-88D data. One main difference between the two radars is VIL resolution. For the WSR-88D, the grid resolution is 2.2 x 2.2 nm, while the WSR-57 has a grid resolution of 3 x 5 nm (Stewart, 1996; 325). The result of his tests showed the predicted wind gust speeds using the WSR-57 data and the observed wind gust speeds provided a correlation factor of 0.80 (i.e., $R=0.80$) when using his Table 3. When using WSR-88D data, the correlation factor between the predicted wind gust speeds and observed wind gust speeds was much lower with a correlation of 0.60 ($R=0.60$). (The R-value is a measure of the amount of linear relationship between variables [Devore, 1995:512]. Therefore, in these tests the R-value represents the degree of linear relationship between the technique's predicted wind gust speed and observed wind gust

speed. A R-value of one corresponds to the largest possible positive relationship.) As a result of the lower correlation values using the WSR-88D, Stewart proposed a new technique that could possibly improve forecasting potential wind gust speeds using the WSR-88D. This new technique was based on equation (1), with the exception that the storm-averaged rainwater liquid water content value (R_c) was obtained using the WSR-88D's reflectivity product to estimate the liquid water content. This was done using the conversion factor $l_z = 3.44 \times 10^{-3} Z^{4/7}$ where $l_z =$ radar-derived liquid water content (g m^{-3}), $Z =$ radar reflectivity ($\text{mm}^6 \text{m}^{-3}$). Substituting l_z into equation (1), the new equation becomes:

$$W = [(20.628571 \text{ms}^{-2} l_z H) - (3.125 \times 10^{-6} \text{s}^{-2} H^2)]^{1/2} \quad (3)$$

where

$W =$ maximum downdraft velocity (m s^{-1}) obtained by air parcel

$l_z =$ radar derived liquid water content (g m^{-3})

$H =$ height (m) above ground level of observed reflectivity (Stewart, 1996:324,325)

Figure 2 is a plot of predicted wind gust speeds using equation (3).

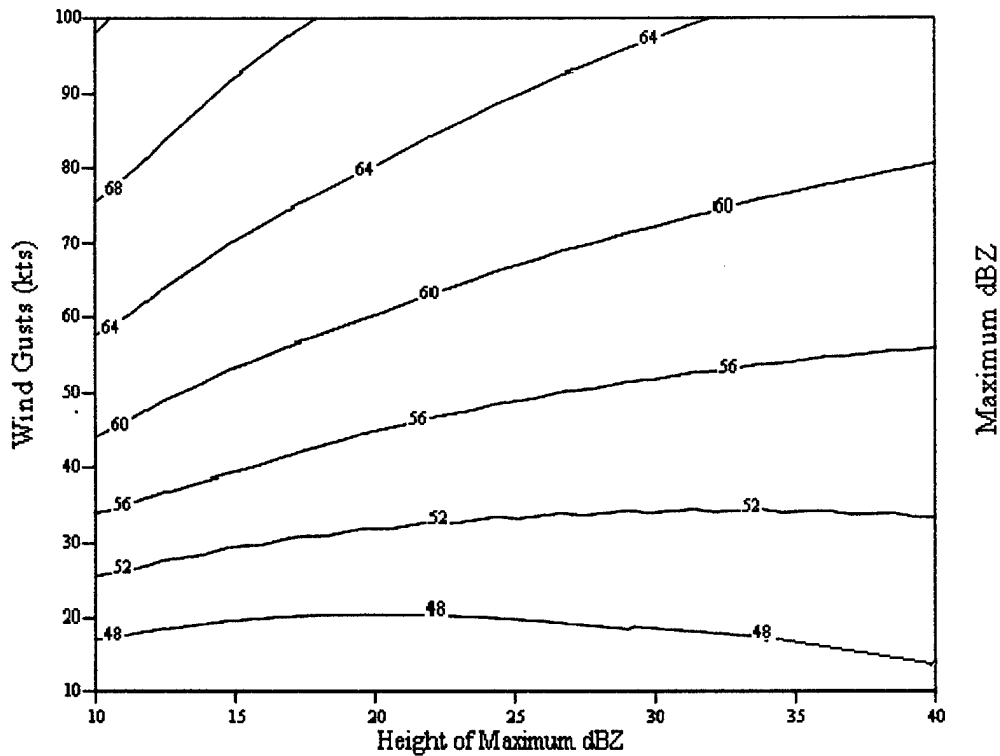


Figure 2. Plot of predicted wind gust (kts) obtained from equation (3) using Maximum dBZ and Height of Maximum dBZ values. Adapted from Stewart (1996).

Using two case studies to test the accuracy of this new Maximum Reflectivity/Height of Maximum Reflectivity technique, Stewart reported that for case one the Maximum Reflectivity/Height of Maximum Reflectivity technique forecasted, with a 14-minute lead-time, a peak wind of 63.4 knots. The actual observed wind was 63 knots. Likewise, for the second case, the Maximum Reflectivity/Height of Maximum Reflectivity technique forecasted, with a 17-minute lead-time, a peak gust of 64 knots. The actual observed wind was 62 knots. Citing only these two case studies in his paper as examples,

Stewart concluded that this “technique has shown increased skill over the VIL/TOP gust technique when using derived data from the WSR-88D radar” (Stewart, 1996:325).

2.3.5 Stewart and Vasiloff (1998).

Prior to 1998, a small number of studies (e.g., the JAWS Project and Srivastava’s (1985) microburst work) had dared to take on the unique complexities of forecasting downdrafts occurring in dry environments. However, only Srivastava’s (1995) work had attempted to forecast actual wind gust speeds occurring in a dry environment. Building on his work, Stewart and Vasiloff (1998) developed a Dry Microburst Gust Prediction (DMP) method. This DMP method was developed for use with the WSR-88D to assist in forecasting pulse-type thunderstorm downdraft speeds in a dry environment. Stewart and Vasiloff modified Srivastava’s (1985) Table 2, based on several case studies taken from the Salt Lake City area, and created Table 5.

Table 5. Potential wind gusts (kts) as a function of peak radar reflectivity (observed at or just above cloud base) and the sub-cloud lapse rate [after Srivastava (1985)] for a penetrative depth of 3800m. Adapted from Stewart (1998).

		Reflectivity Core Value, dBZ							
		15	20	25	30	35	40	45	50
Lapse Rate of Environmental Temperature (K km ⁻¹)	-10.0	41	42	43	47	52	56	60	68
	-9.8	39	40	41	46	50	53	56	64
	-9.5	35	36	37	42	44	46	51	60
	-9.0				30	33	38	44	52
	-8.5							34	44
	-8.0								36
	-7.5								26

The reflectivity values in Table 5 are for values near cloud base (i.e., within 8,000 feet of cloud base). Although Stewart points out that during the NIMROD and the JAWS Project Fujita found little correlation between a storm's maximum reflectivity value and microburst intensity (i.e., wind gust speeds), Stewart found strong correlation between maximum reflectivity at or just above cloud base and observed wind gust speeds using this technique (Stewart and Vasiloff, 1998:13). Moreover, Stewart noted that this DMP technique was a linear function. Therefore, for radar elevations other than 3800 meters (the height used in Table 5), a corresponding percentage difference needed to be added to or subtracted from the predicted wind gust value found using Table 5 (Stewart and Vasiloff, 1998:41). It was this technique, developed strictly for the dry environment, that held promise in forecasting dry microbursts at PAFB, and was one of the methods studied during this research.

3 Methodology

3.1 Data Set Selection

This thesis research is based on a concept that originated from AFSPC's Thesis Submission 96-01. In the proposal, AFSPC requested a study be conducted to assist Air Force forecasters in predicting strong convective wind gusts. This technique would incorporate WSR-88D products such as VIL, TOP, ST and reflectivity, to identify storms likely to produce severe convective wind gusts. Furthermore, this technique would also use these WSR-88D products to forecast the gust's magnitude. The original request for research specified that the study was to incorporate all AFSPC sites located in the High Plains region of the United States. Due to the magnitude of the request, and the limited time in which to conduct research, it was agreed upon after consultation with AFSPC that the research should focus on one AFSPC site. The location chosen was PAFB, Colorado.

3.1.1 Type of Convective Event.

Considering the fact that convective thunderstorms fall into several different categories, with each category containing storms capable of producing strong convective winds, it was necessary to limit the scope of this study to one thunderstorm class. Therefore, since it was already understood that strong convective wind gusts are an innate feature of supercell storms, mesoscale convective complexes, and squall lines, it was decided that airmass thunderstorms provided the greatest potential for research. In addition, all four of the techniques used to forecast downdraft wind gust speeds that were evaluated during this research dealt specifically with airmass thunderstorms. It was

hoped that this research of downdraft winds associated with airmass thunderstorms would enable development of a technique to forecast downdraft wind speeds at PAFB.

3.1.2 Time Period.

A fundamental step in any data selection process is to define a time frame for the research. This study covers the periods 1 Apr-30 Sep 96 and 1 Apr-30 Sep 97. Several factors influenced selection of these particular periods. First, during these periods the Pueblo WSR-88D (the radar servicing PAFB) was using the 9.0 WSR-88D software build. Hence, radar data from these periods was collected and analyzed using the same software, ensuring all radar products throughout this period were consistent. Secondly, convective activity prior to 1 April and after 30 September is rare at PAFB. Therefore, any convective activity that did occur prior to 1 April and after 30 September would seldom be representative of summertime convective storms, and thus data collected on these storms could potentially contaminate the data set. Finally, data for the 1998 convective season was not included in this study due to time considerations and the fact that this research was already in progress during the 1998 convective season.

3.1.3 Identification of Airmass Thunderstorm Days.

Once the time period and the type of convective event to be researched were selected, the next step in the data selection process was to identify the days during 1 Apr-30 Sep 96 and 1 Apr-30 Sep 97 when airmass thunderstorms occurred within a 10.5 nm radius of PAFB. The reason a 10.5 nm radius was selected was because it was assumed any surface winds recorded at PAFB originating from an airmass thunderstorm further than 10.5 nm would not necessarily be representative of the actual wind speed of the downdraft when it first reached the surface. Several reasons may account for the wind's

change in speed over distances greater than 10.5 nm. One reason for a change in wind speed could result from friction between the downdraft wind and the surface resulting in the slowing of the wind over distance. Also, the downdraft winds reaching PAFB from distances greater than 10.5 nm had greater potential of encountering winds originating from other thunderstorms, thus modifying the speed of the actual wind gust in ways that could not be corrected for. Finally, airmass thunderstorms outside of 10.5 nm were discounted in this study because the decrease in wind speed over distance is not necessarily a linear relationship; thus, there was no way to go back and attempt to compute the original wind speed of the downdraft upon reaching the surface. Consequently, it was assumed for purposes of this study that if an airmass thunderstorm was within 10.5 nm of PAFB, then the speed recorded by the wind sensor was considered representative of the actual downdraft wind gust when it first reached the surface. With this assumption, several filtering techniques, using various data sources, were used to identify days on which airmass thunderstorms occurred during 1 Apr-30 Sep 96 and 1 Apr-30 Sep 97.

3.1.3.1 Screening Surface Observations.

The first filtering technique used to determine the days during which airmass thunderstorms occurred at PAFB was to review every surface observation taken during the periods 1 Apr-30 Sep 96 and 1 Apr-30 Sep 97 for thunderstorms. The Air Force Combat Climatology Center (AFCCC) provided a total of 10,454 surface observations for the period identified above. Upon receipt of these surface observations, each observation was manually reviewed to see if any thunderstorms were recorded in the observation. Figure 3 is an example of a surface observation recording a thunderstorm for PAFB.

SURFACE WEATHER OBSERVATION FOR PAFB							
Date	Time (UTC)	Wind (kts)	Visibility (meters)	Weather	Sky Condition	Temp.	Dew Point Temp.
960622	0204Z	21018G23	3200	TS	OVC080	17 C	15 C

Figure 3. Sample surface observation for PAFB recording a thunderstorm (TS).

Any day recording a thunderstorm in its observation was kept as part of the data set of potential airmass thunderstorm days. However, complications developed during the review of surface observations when it was discovered the observations for 1 Apr-30 Sep 96 and 1 Apr-17 Jun 97 were recorded by an Automated Surface Observation System (ASOS). An ASOS is an unmanned observation site. As a result of this discovery, the observations for 1 Apr-30 Sep 96 and 1 Apr- 17 Jun 97 that did not record a thunderstorm became suspect. This was due to the fact that the ASOS did not record thunderstorms, but rather if there were thunderstorms near PAFB the observation was manually updated by FAA air traffic controllers at the Colorado Springs Airport to reflect the occurrence of thunderstorms. However, updating the ASOS observation was a low priority task during thunderstorm activity for the air traffic controllers; thus thunderstorms may have occurred but not necessarily have been recorded. So the concern was not whether the manually updated ASOS observations reporting thunderstorms were inaccurate, but rather that there may have been days when thunderstorms were within 10.5 nm of PAFB but FAA personnel did not record this fact on the ASOS observation (Burrill, personal communication). Therefore, lightning data for PAFB during 1 Apr- 30 Sep 96 and 1 Apr-30 Sep 97 was requested. This lightning data was used to verify the manually updated ASOS observations that did record thunderstorms, and the lightning data was

also used to identify any days where thunderstorms occurred within 10.5 nm of PAFB but were not recorded by FAA personnel in the ASOS observation.

3.1.3.2 Screening Lightning Data.

Since the ASOS was not capable of ensuring all thunderstorms occurring within 10.5 nm of PAFB were recorded in its observation, it was necessary to obtain data pertaining to any lightning flashes occurring within a 10.5-nm radius of PAFB during 1 Apr-30 Sep 96 and 1 Apr-30 Sep 97. (A single lightning flash can be comprised of several lightning strokes, and the data provided by the National Lightning Detection Network (NLDN) pertained to lightning flashes.) The AFCCC provided a lightning data set containing 54,440 cloud-to-ground lightning flashes recorded by the NLDN for 1 Apr-30 Sep 96 and 1 Apr-30 Sep 97. Figure 4 is an example of the data recorded by the NLDN for a single lightning flash.

LIGHTNING STRIKE DATA FOR PAFB									
Year	Month	Day	Hour	Minute	Second	Latitude	Longitude	Polarity	Strength (KA)
1996	4	13	17	46	7.85	38.884	-105.025	Neg	32.4

Figure 4. Sample lightning flash observation for PAFB.

This data set was manually examined to identify the days during 1 Apr-30 Sep 1996 and 1 Apr-30 Sep 1997 when lightning occurred. If a lightning flash was recorded on a given day, that day was kept in the data set of possible airmass thunderstorm days. Likewise, days not recording a lightning flash were removed from the data set of possible airmass thunderstorm days. Furthermore, any days which did not have at least one storm producing more than three lightning flashes were removed from the data set of possible

airmass thunderstorm days. The reason they were removed from the data set was because a thunderstorm producing less than three lightning flashes may not have been representative of a typical airmass thunderstorm. Despite the initial setback of potentially inaccurate surface observations, the additional use of the NLDN data ensured that any days with thunderstorms within 10.5 nm of PAFB, and the times they occurred, were identified and kept in the data set of possible airmass thunderstorm days. Given this pool of thunderstorm days, the next step was to remove any days that did not have winds greater than 15 knots during the time of thunderstorm occurrence.

3.1.3.3 Screening Surface Observations: Part II.

Employing the surface observations used in section 3.1.3.1, and using lightning data to identify the time of thunderstorm occurrence, it was identified that wind gusts equal to or in excess of 15 knots which occurred during thunderstorm activity would be of significance to this study. The reason wind gusts greater than or equal to 15 knots were of interest was because the intent of this study was to provide a technique for forecasting a large range of downdraft winds and not strictly severe winds. Therefore, by including wind speeds of 15 knots or greater, a range of speeds could be studied and included in the research and its results. However, days with wind speeds under 15 knots during thunderstorm activity were eliminated from the data set because wind speeds below this value could not necessarily be attributed solely to a thunderstorm downdraft. In fact, wind speeds under 15 knots could easily be attributed to the current synoptic pressure situation (i.e., gradient winds), boundary layer mixing, and/or local wind effects. As a result, days with wind speeds less than 15 knots during thunderstorm activity were removed from the data set of possible airmass thunderstorm days. Upon removal of these

days from the data set, the days which remained were all days during which thunderstorms occurred within 10.5 nm of PAFB during 1 Apr-30 Sep 96 and 1 Apr-30 Sep 97, which produced winds greater than or equal to 15 knots.

3.1.3.4 Screening Daily Surface Weather Maps.

Since the purpose of this research was to study downdraft wind speeds associated with airmass thunderstorms, it was necessary to reduce the current data set of thunderstorm days to include only airmass thunderstorms. This reduction was accomplished using the National Oceanic and Atmospheric Administration's (NOAA) Daily Surface Weather Maps (National Oceanic and Atmospheric Administration, 1996-1997). To determine whether a thunderstorm for a given day was of airmass origin, each day remaining in the data set was cross-checked with the day's 0700 EST Daily Surface Weather Map. Each day's surface map was examined for the presence of any synoptic scale features such as fronts, troughs, and low-pressure systems in and around the state of Colorado. The presence of such features would suggest synoptic-scale forcing and thus disqualify the thunderstorm day as being of possible airmass origin. Consequently, it would be removed from the thunderstorm data set. Furthermore, if any synoptic scale feature (such as a frontal system) was propagating towards Colorado, the following day's 0700 EST Daily Surface Weather Map was reviewed to see the current location of the system. If it appeared based on the movement of the system that the front could have affected PAFB's weather late in the previous day, it was then removed from the data set. After using this filtering technique to identify airmass thunderstorm days, thirty-three days remained in the data set for the periods 1 Apr-30 Sep 96 and 1 Apr-30 Sep 97.

3.1.3.5 Acquiring WSR-88D Data.

Of the thirty-three airmass thunderstorm days remaining in the data set, the next step was to obtain WSR-88D Level II data for these days. (WSR-88D Level II data is digitally archived WSR-88D base data. The base data products for the WSR-88D are reflectivity, mean radial velocity and spectrum width [USAF Technical Training School, Doppler Radar Glossary, 1993: 1,2]. Using these three base data products, the WSR-88D's Radar Product Generator is able to run a series of algorithms to create useable products from the base data such as VIL.) If the WSR-88D Level II data was not available for a given day, the day was eliminated from the data set. The request for WSR-88D Level II data was submitted to the AFCCC and after their review the request was forwarded to the National Climatic Data Center (NCDC) where technicians reviewed their database for the requested WSR-88D Level II data. Of the thirty-three airmass thunderstorm days for which data was requested, only twenty-two days of complete data were available from the NCDC. Therefore, these twenty-two airmass thunderstorm days were analyzed during this research. However, prior to any data analysis, it was first necessary to decide which radar products would be collected and studied during this research.

3.2 Radar Products

After an exhaustive literature review, seven radar products were identified for collection and study. These seven products are listed in Figure 5, along with their relevance to the study of forecasting surface wind gust speeds. With these seven products identified for collection and later study, the next step was to process the WSR-88D Level II data using WATADS.

RADAR PRODUCT	RESEARCH RELEVANCE
Vertically Integrated Liquid Water Content: Grid Based (VIL)	Used in TOP/VIL technique to predict maximum wind gust potential
Vertically Integrated Liquid Water Content: Cell Based	There could be a possible correlation between Cell Based VIL and maximum wind gusts
Echo Top Height (TOP)	Used in TOP/VIL technique to predict maximum wind gust potential
Storm Top Height (ST)	There could be a possible correlation between ST and maximum wind gusts
Maximum Reflectivity	Used in DMP technique and Maximum Reflectivity/Height technique to forecast maximum wind gust potential
Height of Maximum Reflectivity	Used in Maximum Reflectivity/Height technique to forecast maximum wind gust potential
Cloud Base Height AGL	Used in DMP technique to forecast maximum wind gust potential

Figure 5. Radar products collected and research relevance.

3.3 Data Collection

The WSR-88D data used in this research was collected by the Pueblo, Colorado, WSR-88D Radar Data Acquisition (RDA) unit. The RDA is the unit responsible for acquiring the three base moments of the radar (base reflectivity, mean radial velocity and spectrum width). It acquires these products by sending out S-band radio frequency (2.8-3.0x10⁶ Hz) pulses (Rinehart, 1997:350). Upon the return of these radio frequency pulses to the radar receiver, the data is immediately sent in analog form to the RDA's signal processor. At the signal processor, the analog data is converted into digital data, and then processed into base data. This processed base data is saved by archive II equipment, and then transferred in digital form to NCDC for storage (Department of Commerce, 1992:2-1,2-4). When the final data set of airmass thunderstorm days was determined for this

research, WSR-88D Level II data was ordered from the NCDC for each of the days. The NCDC transferred all available WSR-88D Level II data to 8-mm tapes.

3.4 Data Processing

With possession of the WSR-88D Level II data, the next step was to analyze the radar data for the seven radar products outlined above. The analysis of this radar data was accomplished using WATADS. The WATADS program runs on a Sun Sparc 20 workstation, with an attached 8-mm tape drive that was used to read the radar data from the 8-mm tapes to the Sun Sparc 20 hard drive. (WATADS is unable to read or process the WSR-88D Level II data stored on 8-mm tape directly from the tape. As a result, the data must first be downloaded to the hard drive before it can be examined.) Four gigabytes of hard drive space were used to store the downloaded data from the 8-mm tapes. The downloading process consisted of loading one airmass thunderstorm case to the hard drive at a time. This downloading process took on average about five hours per case. Once a case was saved to the hard drive, it was available for display using the WATADS Radar Analysis and Display System (RADS). It was with RADS that radar base data images and other WSR-88D products were displayed in graphic form. Accordingly, RADS was the display system used to assist in determining values for six of the seven radar parameters. However, prior to the interrogation of any radar data, a radar worksheet was developed to record not only values for the seven radar products, but also other relevant information pertaining to each of the airmass thunderstorms. (Appendix B contains radar worksheets for the nineteen airmass thunderstorms.)

Once a case was loaded on the hard drive and ready for interrogation, the first step was to determine which thunderstorm produced the surface wind gust recorded at PAFB.

This task was accomplished by reviewing the day's surface observations and identifying the time the maximum wind gust occurred during thunderstorm activity. Using the time of this maximum wind gust, the radar data was interrogated on RADS to determine which storm was responsible for the observed wind gust. Several ideas were considered in identifying the responsible storm. First, direction of the wind gust was crucial to identifying the correct storm. Along with direction of wind gust was the position of the storm in relation to the sensor before and at the time of maximum wind gust. Furthermore, by taking into account the speed of the wind gust and distance of the storm from the sensor, a rough estimate could be made of the storm's location when the downdraft first reached the surface and began its horizontal movement toward the wind sensor. Radar products used to determine these characteristics included base and composite reflectivity, base velocity, storm cell data and time lapses of these various radar products. Of the twenty-two airmass thunderstorm days, three were removed from the data set since no responsible storm could be accurately identified.

Upon identification of the downdraft-producing storm, values for the seven radar products crucial to this research were recorded. The first radar product to be obtained during storm interrogation was Grid Based VIL (VIL). To create this product, the radar used base reflectivity data from an entire volume scan and ran this data through the WSR-88D VIL algorithm. This VIL algorithm took into account theoretical raindrop size distributions and the relationship between reflectivity values and liquid water and was able to convert base reflectivity values, integrated throughout the entire depth of a 2.2 x 2.2 nm column over a fixed surface, into VIL values. RADS graphically displays the VIL product composed of these 2.2 x 2.2 nm grid boxes (Department of Commerce,

1992:2-98,3-34). (Appendix C contains a Grid Based VIL image as displayed on the WSR-88D.) Using individually displayed VIL volume scans and time lapses of several VIL volume scans prior to the occurrence of the storm's maximum wind gust, a maximum Grid Based VIL value for the gust-producing storm was identified. This value was then recorded on the radar worksheet.

The second radar product to be investigated was Cell Based VIL. This product is similar to Grid Based VIL, except Cell Based VIL is created by vertically integrating the base reflectivity values of the storm cell centroid throughout the entire depth of the storm. Therefore, the algorithm determines a VIL value for the center of the storm, as opposed to Grid Based VIL that determines a VIL value for a 2.2 x 2.2 nm vertical column. Since the storm centroid is considered the region of highest reflectivity, the Cell Based VIL is considered the maximum VIL value for the storm. Unlike Grid Based VIL, Cell Based VIL is not displayed in graphic form, but rather it is displayed in the WSR-88D algorithm table. It was from the WATADS WSR-88D VIL algorithm table that Cell Based VIL was read and recorded.

The third radar product to be ascertained for the wind gust-producing storm was Echo Top (TOP). TOP is the height in a storm above which all reflectivity values are less than 18.5 dBZ (USAF Technical Training School, PUP Operator, July 1993:7-14). Although WATADS, through the use of RADS, has the ability to display many of the original radar products from the WSR-88D, TOP was not one these products. However, since TOP was used in several previous wind gust studies, and no work had been conducted specifically for the High Plains using TOP, it was necessary to obtain a TOP value for the storm under study. After several consultations with the National Severe

Storms Laboratory's (NSSL) WATADS algorithm personnel, a method was created by which to adjust the fundamental WATADS algorithm to obtain a TOP value for each storm. This adjustment allowed the NSSL Storm Cell Identification and Tracking (SCIT) algorithm to be modified to identify the height of the 18 dBZ layer of a storm. This height was then recorded as the TOP value of the storm. To ensure accuracy of the modified NSSL SCIT algorithm, the TOP value was double-checked using several base reflectivity cross sections for the storm in question. (Appendix C contains a TOP image as displayed on the WSR-88D.)

The fourth radar product to be investigated was Storm Top (ST). Storm Top is a product similar to TOP, except ST was designed to identify the maximum height of the 30 dBZ reflectivity level of a storm. The ST value for a storm was determined using WATADS' WSR-88D algorithm. As with TOP, the ST value processed by the WSR-88D algorithm was checked against values obtained from a series of base reflectivity products and base reflectivity cross sections in order to ensure the accuracy of the WSR-88D algorithm.

The fifth radar product to be investigated was the maximum reflectivity value of the storm prior to the occurrence of the maximum observed wind gust at the surface. The maximum reflectivity value was obtained using RADS and a series of base reflectivity, composite reflectivity and reflectivity cross-section products for several volume scans prior to the time of the observed wind gust. The pixel representing the maximum reflectivity value was then identified using these reflectivity products and the maximum reflectivity value recorded. (Appendix C contains a Composite Reflectivity image as displayed on the WSR-88D from which the maximum reflectivity value can be obtained.)

The sixth radar parameter to be examined and recorded was the height of the maximum reflectivity value. Peterson Air Force Base is at an elevation of 6,250 ft, so the height of maximum reflectivity was recorded above ground level (AGL) for two reasons. First, the height values computed in WATADS were AGL so no conversion was necessary. Secondly, Stewart's (1991 and 1996) VIL/TOP and Maximum dBZ/Height of Maximum dBZ techniques used heights AGL. This value was computed for a storm using WATADS' WSR-88D algorithm. As with TOP and ST, the height of the maximum reflectivity value was compared with various reflectivity slices and reflectivity cross sections for the volume scan from which the maximum reflectivity value was taken in an attempt to ensure the accuracy of the WSR-88D algorithm.

The final radar parameter to be recorded was the storm's cloud base height (AGL) taken for the same time as the maximum reflectivity value. Again, the WSR-88D algorithm computed this value for each air mass thunderstorm. Finally, this value was compared to several reflectivity cross sections to ensure the accuracy of the WSR-88D algorithm and recorded on the radar worksheet.

One non-radar product was needed for use in verifying Stewart and Vasiloff's (1998) DMP technique. This non-radar product was the sub-cloud temperature lapse rate. To obtain this value, the 1200Z atmospheric sounding profile for Denver, Colorado was requested from the AFCCC. Upon receipt of this data, the atmospheric soundings for the nineteen air mass thunderstorm days of interest were hand plotted on the Skew T, Log P thermodynamic diagram. The sub-cloud temperature lapse rate was then calculated for each of the nineteen thunderstorms using the Skew T, Log P diagram, and recorded on the radar worksheet. The 1200Z versus the 0000Z atmospheric sounding was used to

calculate the sub-cloud temperature lapse rate because the majority of airmass thunderstorm activity occurred prior to 0000Z. Furthermore, since the majority of airmass thunderstorms occurred prior to 0000Z, it was quite possible the 0000Z sounding may have represented a modified environmental lapse rate resulting from thunderstorm activity occurring prior to 0000Z. As a result, the 1200Z sounding was in all likelihood more representative of the sub-cloud temperature lapse rate during which thunderstorm activity occurred.

Although these seven radar products and one non-radar product were of greatest interest to this study, several other parameters also needed to be computed and/or recorded. With the exception of having to compute the distance from the thunderstorm to the wind sensor, the values for these other parameters were obtained directly from Level II data, PAFB surface observations or the Skew T, Log P diagram. Since WATADS only provided the azimuth and range of the storm from the RDA, it was necessary to convert the thunderstorm's azimuth and range from the RDA to a latitude and longitude for the storm. With this latitude and longitude, the distance from the thunderstorm to the wind sensor was computed using the latitude and longitude of both locations. The computed distances were then recorded in the radar worksheet.

3.5 Development of Research Method

With the data collected for all nineteen airmass thunderstorms, the next step was to evaluate and possibly modify several wind gust prediction techniques discussed in the literature review for employment at PAFB. Furthermore, the collected data, specifically the seven radar products and sub-cloud temperature lapse rate, were tested to see if some possible correlation existed between their values. The existence of a possible correlation

between values could assist in a forecasting technique being developed with which to accurately forecast downdraft winds for PAFB and possibly other High Plains locations. The first technique to be evaluated was Stewart's (1991) VIL/TOP technique. The second technique to be evaluated was Headquarters AWS' (1996) VIL/TOP technique. The third technique to be evaluated was Stewart's (1996) Maximum dBZ/Height of Maximum dBZ technique. The fourth technique to be evaluated was Stewart and Vasiloff's (1998) DMP technique. Upon completion of the evaluations of these four techniques, the next plan of action for this research was to attempt and modify these techniques if they were not accurate forecasters of downdraft wind speeds at PAFB. Finally, the last aspect of this research was to conduct a statistical analysis of the collected radar products and the sub-cloud temperature lapse rate to possibly identify a new relationship between these products and observed downdraft wind speeds which would be useful in forecasting downdraft wind speeds at PAFB.

4 Results and Analysis

4.1 Description of Data Set

The final data set used in this research was composed of nineteen airmass thunderstorms, each of which occurred within 10.5 nm of PAFB. Of these nineteen airmass thunderstorms, seven occurred in 1996 and twelve in 1997. Although the month of April was analyzed for thunderstorms during both years, none were recorded in April. The average range of the thunderstorms to PAFB was 4.9 nm. The closest storm and furthest storms were 0.5 nm and 10.4 nm, respectively. The average thunderstorm range from the RDA was 36.9 nm with the closest storm recorded at 30 nm and the furthest recorded at 44 nm. Twelve of the days had thunderstorms occurring in a hybrid microburst environment, seven cases occurred in a dry microburst environment, and no cases occurred in the wet microburst environment. For all nineteen days, the surface observation did not record hail for any of the storms, and the radar reported only a slight possibility of hail for four of the storms. This suggested that for the nineteen cases the WSR-88D products were not contaminated by hail; thus, there should not have been any excessively high radar reflectivity values and VIL values resulting from hail contamination. Finally, of the nineteen storms, only one produced a possible microburst with a wind gust of 46 knots being recorded.

During the research, seven radar products were collected for each of the nineteen storms in the data set. The products collected were VIL, Cell Based VIL, TOP, ST, Maximum dBZ, Height of Maximum dBZ and Cloud Base Height. For each of these products, the mean, median, variance, standard deviation, maximum value and minimum

value were computed for each storm. The results of these computations are presented in Table 6.

Table 6. Summary statistics for collected radar products.

	VIL-Cell Based (kg/m ²)	VIL-Grid Based (kg/m ²)	Echo Top (1000's ft)	Storm Top (1000's ft)	Maximum dBZ	Maximum dBZ Height (1000's ft)	Cloud Base Height (1000's ft)
Minimum Value	1	1	16	11.7	36	2.7	2.6
Maximum Value	32	37	35	28	57.5	13	8
Mean	11.3	13.1	25	18.7	48.1	6.6	5
Median	8	9	24	18.1	48.5	6.5	4.8
Standard Deviation	10.5	11.6	5.8	4.8	6.8	2.2	1.8
Variance	101.4	133.5	3.37E+04	2.3E+04	45.9	4.8E+03	3.3E+03

In addition, the Pearson correlation and P-values for the seven radar products were computed to identify any possible relationships between products. A correlation value greater than or equal to 0.8 suggested a strong positive relationship existed between products. In addition, a correlation value between 0.5 and 0.8 suggested a moderate positive relationship existed, and a correlation value less than or equal to 0.5 implied a weak positive relationship between products (Devore, 1995:216). The P-value is considered the smallest level for which the data being studied is still statistically significant (Devore, 1995:335). For this research a P-value less than 0.05 suggested that

the data being studied was statistically significant. The Pearson correlation and P-values are displayed in Table 7.

Table 7. Pearson correlation (top value in each block) and P-values (bottom value) for collected radar products.

Correlation P-Value	VIL- Grid Based	VIL-Cell Based	Echo Top	Storm Top	Maximum dBZ	Height of Maximum dBZ
VIL- Cell Based	0.9160 0.0000		0.6257 0.0126	0.7816 0.0006	0.8635 0.0000	-0.1055 0.7082
Echo Top	0.6877 0.0046	0.6257 0.0126		0.8135 0.0002	0.5039 0.0555	-0.1765 0.5292
Storm Top	0.7830 0.0006	0.7816 0.0006	0.8135 0.0002		0.5764 0.0245	-0.2751 0.3211
Maximum dBZ	0.8533 0.0001	0.8635 0.0000	0.5039 0.0555	0.5764 0.0245		-0.1408 0.6168
Height of Maximum dBZ	-0.2046 0.4646	-0.1055 0.7082	-0.1765 0.5292	-0.2751 0.3211	-0.1408 0.6168	
Height of Cloud Base	-0.0118 0.9668	0.1556 0.5796	0.2976 0.2813	0.1437 0.6094	-0.0865 0.7591	0.3636 0.1828

Although the intent of this research was to study the application of WSR-88D products to forecasting downdraft wind speeds, one non-radar parameter was collected during this research in order to evaluate Stewart and Vasiloff's (1998) DMP technique. This non-radar parameter was the sub-cloud temperature lapse rate, and as discussed in Chapter 3, it was computed for each of the nineteen storms using the Skew T, Log P diagram. The mean, median, variance, standard deviation, maximum value and minimum value were computed and are displayed in Table 8.

Table 8. Summary statistics for sub-cloud temperature lapse rate ($K km^{-1}$).

Sample Size	Minimum Value	Maximum Value	Mean	Median	Standard Deviation	Variance
19	5.4	11.3	8.3	8.5	1.7	2.7

4.2 Evaluation of Techniques

The first objective of this research was to evaluate several existing methods used to predict potential downdraft wind speeds associated with airmass thunderstorms.

Therefore, once the collection of radar and Skew T, Log P data was completed, the next step in the research process was to calculate the predicted thunderstorm downdraft wind speeds for each of the four methods. Once the calculation of the downdraft wind speeds, which are realized as the observed wind gust speeds upon the downdraft reaching the surface, was completed for all four techniques, they were then compared with the observed wind gust speeds.

4.2.1 Stewart's VIL/TOP Technique (1991).

The first method for which predicted downdraft wind speeds were computed was for Stewart's (1991) VIL/TOP method. To accomplish this, VIL and TOP values for each airmass thunderstorm were substituted into equation (1) and a wind gust was calculated. To obtain the final potential wind gust for the airmass thunderstorm using this technique, one-third of the surface to 5,000 feet mean wind was vectorially added to the wind gust obtained using equation (1). Of the nineteen thunderstorms under study, this technique was able to provide a predicted wind gust value for eleven of these storms. The final predicted wind gust speeds are recorded in Table 9.

Table 9. Predicted and observed wind gust speeds.

Date	Observed Wind at PAFB (kts)	Predicted Wind (kts): Stewart's (1991) VIL/TOP	Predicted Wind (kts): Headquarters AWS' (1996) VIL/TOP	Predicted Wind (kts): Stewart's (1996) dBZ/Height	Predicted Wind (kts): Stewart and Vasiloff's (1998) DPM	Type of Environment
1 Jun 96	36	No Forecast	No Forecast	No Forecast	55.2	Hybrid
10 Jun 96	46	34.1	36.4	28.6	48.0	Dry
14 Jun 96	30	27.2	28.3	29.9	No Forecast	Hybrid
17 Jun 96	29	35.4	41.7	30.2	59.8	Dry
21 Jun 96	22	26.9	33.3	16.0	42.3	Hybrid
27 Jun 96	23	No Forecast	No Forecast	10.8	46.4	Dry
28 Aug 96	31	43.9	43.8	29.3	No Forecast	Hybrid
6 May 97	15	No Forecast	No Forecast	4.4	No Forecast	Dry
18 May 97	25	Missing Data	Missing Data	7.2	No Forecast	Hybrid
18 Jun 97	23	4.1	No Forecast	9.3	57.2	Hybrid
19 Jun 97	33	9.2	No Forecast	12.1	54.1	Hybrid
26 Jun 97	28	No Forecast	No Forecast	17.5	45.4	Dry
27 Jun 97	23	Missing Data	Missing Data	16.4	>37.1	Hybrid
4 Jul 97	23	No Forecast	No Forecast	7.5	47.4	Dry
26 Jul 97	19	25.4	35.5	30.0	>60.8	Hybrid
31 Jul 97	29	21.8	No Forecast	25.7	No Forecast	Hybrid
2 Aug 97	24	6.4	No Forecast	17.4	No Forecast	Hybrid
24 Aug 97	18	No Forecast	No Forecast	10.5	47.2	Dry
11 Sep 97	25	15.6	No Forecast	14.6	No Forecast	Hybrid

As discussed in the literature review, Stewart's (1991) VIL/TOP technique was created in an effort to forecast maximum surface wind gusts associated with airmass thunderstorm downdrafts. The technique was built around an empirically-derived equation and tested using data from the WSR-57. Stewart tested 143 cases and verified "by reported wind damage and/or severe wind gusts (measured or estimated)" 82% of these cases (Stewart, 1991:15). Applying this technique to wind gust prediction for

airmass thunderstorms near PAFB, the following results were obtained. A “successful potential wind gust forecast” was a case where the forecasted wind gust was within ± 5 kts of the observed wind gust. A “missed potential wind gust forecast” was a case where the forecasted wind gust was not within ± 5 kts of the observed value. A “no potential wind gust forecast” was a case where the prediction technique was unable to obtain a potential wind gust speed for a thunderstorm using the data collected from that thunderstorm. Applying these definitions, the successful potential wind gust forecast rate for Stewart’s VIL/TOP potential wind gust technique was 11.8%. The no forecast rate was 35.3%. The missed potential wind gust forecast rate, not including no forecasts, was 52.9%. If no forecasts were counted as a missed potential wind gust forecast, the missed potential wind gust forecast rate became 88.2%. For all cases when the predicted wind gust value was within ± 5 kts of the forecasted value, the environment was a hybrid microburst environment; thus, there were no cases when a successful potential wind gust forecast occurred in a dry microburst environment. The mean absolute error between the observed wind gust and the predicted wind gust for this technique was 11.1 kts and the root mean-squared error was 12.8 kts. (Both values can be considered the typical magnitude of error between the forecasted and observed values.) Finally, the bias for this technique (i.e., the difference between the mean forecasted wind value and mean observed wind value) was -3.7 knots. This suggested that on average the VIL/TOP technique forecasted wind gust potential values that were too low (Wilks, 1995:251-254). The mean absolute error, the root mean-squared error, and bias are displayed in Table 10.

Table 10. Mean absolute error, root mean-squared error and bias for the four potential wind gust prediction techniques.

	Stewart's (1991) VIL/TOP Prediction Technique	Headquarters AWS' (1996) VIL/TOP Prediction Technique	Stewart's (1996) dBZ/Height of Maximum dBZ Prediction Technique	Stewart and Vasiloff's (1998) DMP Technique
Mean Absolute Error (kts)	11.1	10.8	9.6	23.2
Root Mean- Squared Error (kts)	12.8	11.7	11.3	25.2
Bias (kts)	-3.7	10.1	-8.8	23.7

Figure 6 is a scatter plot of the observed wind gust speeds and the predicted wind gust speeds using Stewart's (1991) VIL/TOP technique. A strong linear relationship between the observed and predicted wind gust speeds would be identified by the plotted points lying near the plotted regression line. Given this fact, it did not appear from the scatter plot that a linear relationship existed between the observed wind gust speeds and the predicted wind gust speeds. Furthermore, a correlation value of 0.3786 was computed which suggested that there was not a strong linear relationship between the predicted wind gust speeds and the observed wind gust speeds.

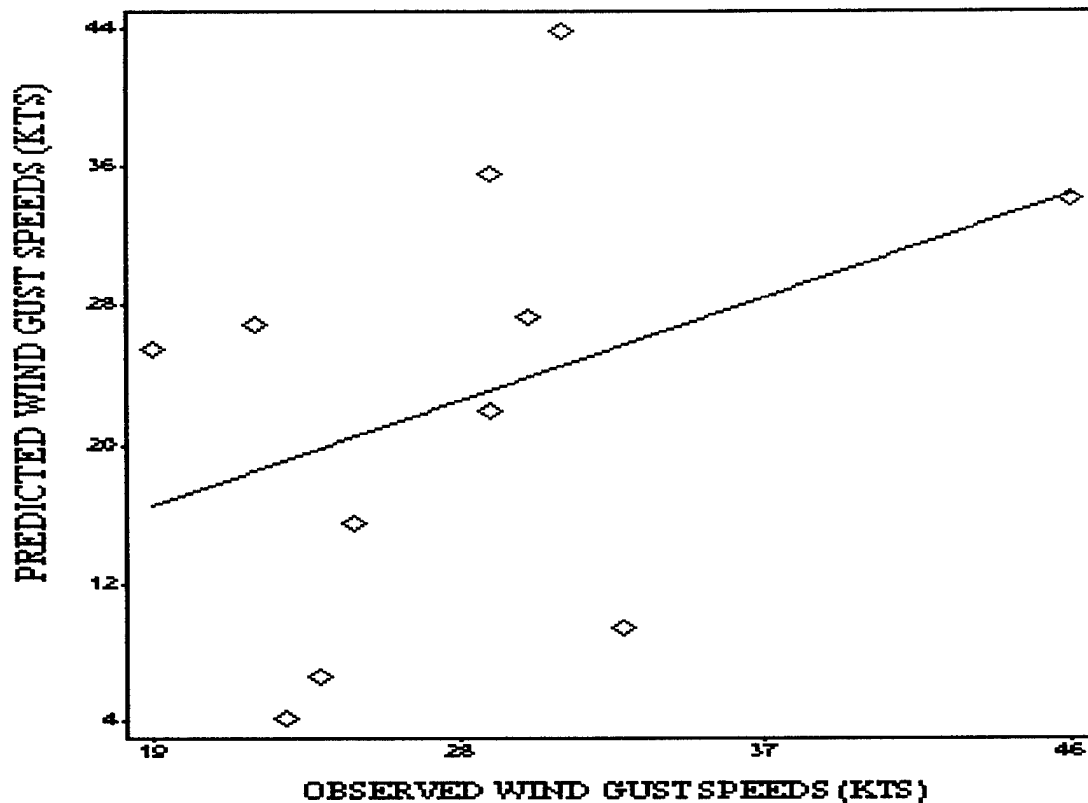


Figure 6. Scatter plot of computed wind speeds using Stewart's (1991) VIL/TOP technique versus observed wind speeds.

The reason Stewart's (1991) VIL/TOP technique did not perform well in predicting the observed wind gust speeds was probably due to several reasons. Stewart developed and tested his empirical equation using case studies originating from the southeastern and southern United States in typically wet microburst environments. Furthermore, he tested this method using data from the WSR-57 and not the WSR-88D. With this in mind, the reason this technique was still tested for PAFB and its typically dry environment results from the fact that this method has been used operationally throughout much of the United States. Moreover, this technique was the basis for Headquarters AWS' (1996) VIL/TOP technique that was fielded without specific mention of the type of environment in which

it should or should not be used. Hence, the AWS technique has been used operationally by Air Force forecasters at PAFB, and thus evaluation of Stewart's (1991) VIL/TOP technique was of interest to this research.

4.2.2 Headquarters AWS' VIL/TOP Technique (1996).

The second technique to be evaluated for operational use during this research was Headquarters AWS' (1996) VIL/TOP technique. To compute the predicted wind gust potential associated with an airmass thunderstorm downdraft using the AWS VIL/TOP technique, the VIL and TOP values for a given storm were used with AWS' Wind Gust Potential (WGP) chart (Table 4) to obtain a wind gust potential speed. In cases where the VIL and TOP values fell between values on the WGP chart, the predicted wind gust speed was linearly interpolated from the chart. Once the wind gust speed was computed from the chart, the total surface to 5,000 feet mean wind was added to the wind speed, and this value became the final predicted wind gust speed obtained by this technique. The AWS VIL/TOP technique was unable to predict a potential wind gust speed for thirteen of the storms. The final predicted wind gust speeds are recorded in Table 9.

Using the same definitions for successful potential wind gust forecast, missed potential wind gust forecast and no potential wind gust forecast as used in the evaluation of Stewart's (1991) VIL/TOP technique, the following results were obtained from the data set of seventeen thunderstorms for which both VIL and TOP could be obtained. The AWS VIL/TOP technique obtained a successful potential wind gust forecast rate of 5.9%. Unfortunately, the technique had difficulty producing a forecasted wind gust potential for several storms in the data set and consequently had a no potential wind gust forecast rate of 64.7%. The missed potential wind gust forecast rate, not including no forecasts was

29.4%, and if no forecasts were counted the missed potential wind gust forecast rate climbed to 94.1%. The one successful potential wind gust forecast that did occur did so in a hybrid microburst environment. The mean absolute error between the observed wind gust and the predicted wind gust using this technique was 10.8 kts, and the root mean-squared error was 11.7 kts. Finally, the bias for this technique was 10.1 knots. This suggested that on average the AWS VIL/TOP technique forecasted potential wind gust speeds that were too high. The mean absolute error, the root mean-squared error, and bias are displayed in Table 10.

Figure 7 is a scatter plot of the observed wind gust speeds and predicted wind gust speeds using the AWS' VIL/TOP technique. From the scatter plot, it did not appear that a linear relationship existed between the observed wind gust speeds and the predicted wind gust speeds. Furthermore, a Pearson correlation value of 0.1401 was computed, and this value showed that there was little if any linear relationship between the predicted wind gust speeds and the observed wind gust speeds. Moreover, a P-value of 0.7912 further supported this observation and suggested that the correlation value had no statistical significance.

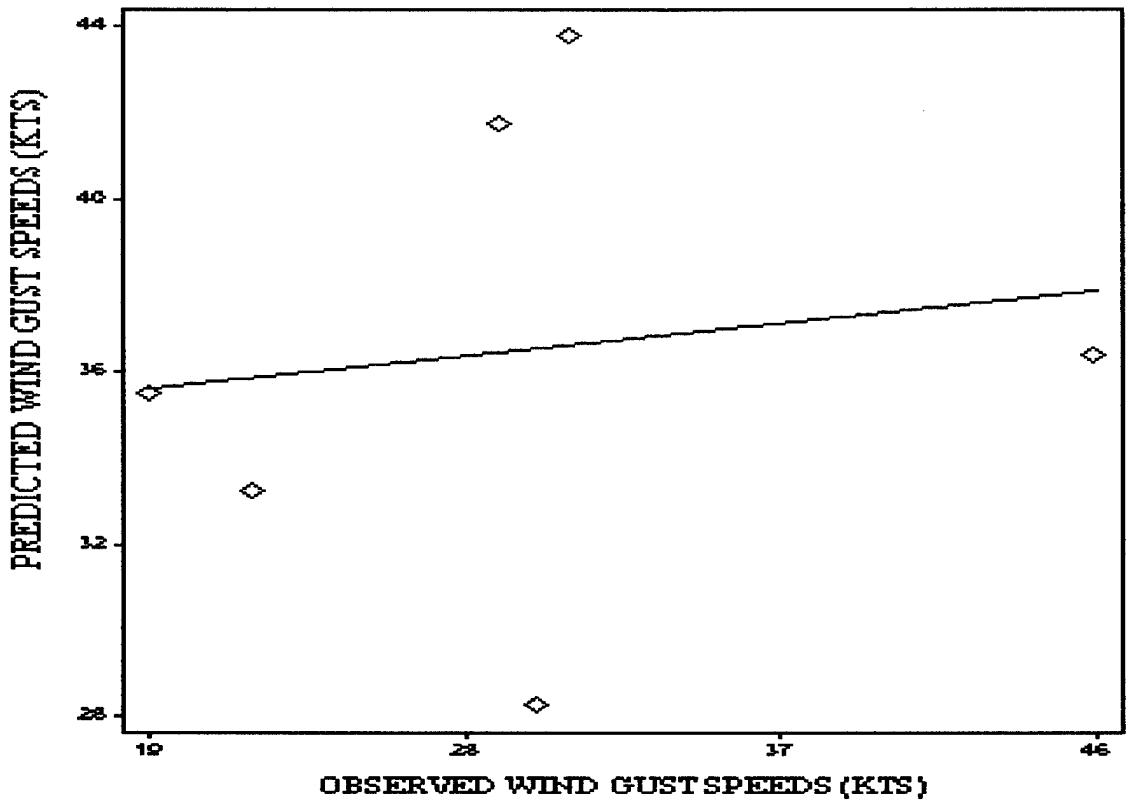


Figure 7. Scatter plot of computed wind speeds using Headquarters AWS' (1996) VIL/TOP technique versus observed wind speeds.

It was of no surprise to this researcher that the AWS' VIL/TOP technique was not accurate in forecasting the observed wind gust speeds. As was discovered during the literature review portion of this research, and was explained in section 2.3.3, this technique was not based on any case studies or statistical analysis. Furthermore, no data set existed from which to develop this technique; thus, for all practical purposes this technique has no scientific basis. Fittingly, the results from the evaluation of the AWS' VIL/TOP technique, based on this study's data set, reinforced this fact.

4.2.3 Stewart's Maximum dBZ/Height of Maximum dBZ Technique (1996).

The third method to be assessed during this research was Stewart's (1996) Maximum dBZ/Height of Maximum dBZ technique. This method was developed in order to forecast potential maximum wind gusts originating from airmass thunderstorms using the WSR-88D. The forecasting technique was originally developed and tested in the wet microburst environment, and no research was discovered which had shown evidence that this technique had been tested in either the dry or hybrid microburst environments. Consequently, it was selected for study and evaluation during this research.

To compute the potential wind gust speeds, the values of the maximum dBZ and the height of this maximum dBZ for a given storm were entered into equation (3) and a potential wind gust speed was calculated. Since no correction factor was necessary when using this technique (i.e., no mean wind speed was added to this value), the speed computed using equation (3) was the final predicted wind gust speed and was recorded in Table 9. This method predicted a wind gust speed for eighteen of the nineteen storms in this study.

Once the wind gust speeds were calculated, they were then evaluated against the observed surface wind gust speeds. The successful potential wind gust forecast rate computed for this prediction technique was 21%. Furthermore, no potential wind gust forecast rate was only 5.3%. Finally, the missed potential wind gust forecast rate not including no forecasts was 73.7%, while the missed potential wind gust forecast rate including no forecasts was 79%. The mean absolute error between the observed wind gust and the predicted wind gust was 9.6 kts, the root mean-squared error was 11.3 kts

and the bias for this technique was -8.8 knots. This negative bias suggested that on average the Maximum dBZ/Height of Maximum dBZ technique forecasted potential wind gust speeds that were generally too low. The mean absolute error, the root mean-squared error, and bias are also displayed in Table 10.

Figure 8 is a scatter plot of these computed winds and the observed winds. From the scatter plot, it did not appear that a linear relationship existed between the observed wind gust speeds and the predicted wind gust speeds. Furthermore, a Pearson correlation value of 0.5371 was computed. The correlation value supported the fact that there did not appear to be a linear relationship between the predicted wind gust speeds for the Maximum dBZ/Height of Maximum dBZ technique and the observed wind gust speeds.

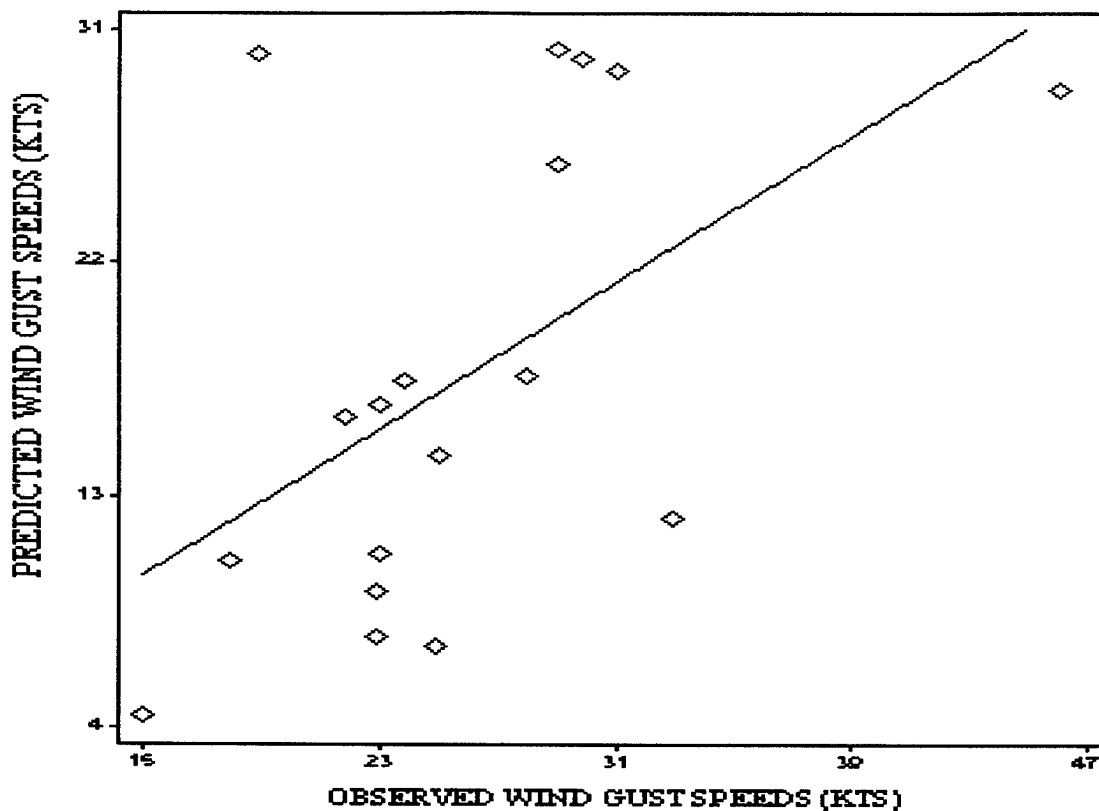


Figure 8. Scatter plot of computed wind speeds using Stewart's (1996) Maximum dBZ/Height of Maximum dBZ technique versus observed wind speeds.

4.2.4 Stewart and Vasiloff's Dry Microburst Prediction Technique (1998).

The final method studied, and the only method developed for and previously tested in the dry microburst environment, was Stewart and Vasiloff's DMP technique. To compute potential wind gust speeds using Stewart and Vasiloff's (1998) DMP technique, the sub-cloud temperature lapse rate and maximum dBZ occurring near cloud base (i.e., within 8,000 feet of cloud base) were used with Table 5 to find the potential wind gust speed associated with an airmass thunderstorm. In cases where the sub-cloud

temperature lapse rate and maximum dBZ occurring near cloud base fell between values on the table, the potential wind gust speeds were interpolated and extrapolated from the table. This calculated speed was then multiplied by a correction factor of 1.031 to adjust for the difference in elevation between PAFB and Salt Lake City for which Table 5 was originally created. (In their paper, Stewart and Vasiloff discuss the fact that their DMP technique is a linear function. As a result, for downdraft heights different from the 3800 m on which their table is based, "a corresponding percentage difference must be added to or subtracted from the predicted gust value" taken from their table [Stewart and Vasiloff, 1998: 41]. In the case of PAFB, the mean terrain is 118 m lower than the mean terrain used in Stewart and Vasiloff's study. As a result of this difference, the correction factor by which all computed potential wind gust speeds obtained from Table 5 had to be multiplied by was 1.031 [i.e., $3918/3800$] to correct for this 118 m difference [Stewart, e-mail].) The predicted wind gust speeds obtained from Table 5 and multiplied by the correction factor for PAFB are recorded in Table 9. This technique was unable to predict a wind gust potential for seven of the nineteen storms.

Evaluation of this technique against the observed wind gust speeds attained a successful potential wind gust forecast rate of 5.3%. The no potential wind gust forecast rate was 36.8%. The missed potential wind gust forecast rate not including no forecasts was 57.9%, while the miss rate including no forecasts was 94.7%. The mean absolute error between the observed wind gust and the predicted wind gust was 23.2 kts, the root mean-squared error was 25.2 kts and the bias for this technique was 23.7 knots. This suggests on average that the DMP technique forecasted potential wind gust speeds that

were too high. The mean absolute error, the root mean-squared error, and bias are also displayed in Table 10.

Figure 9 is a scatter plot of the predicted wind speeds versus the observed wind speeds using the DMP technique.

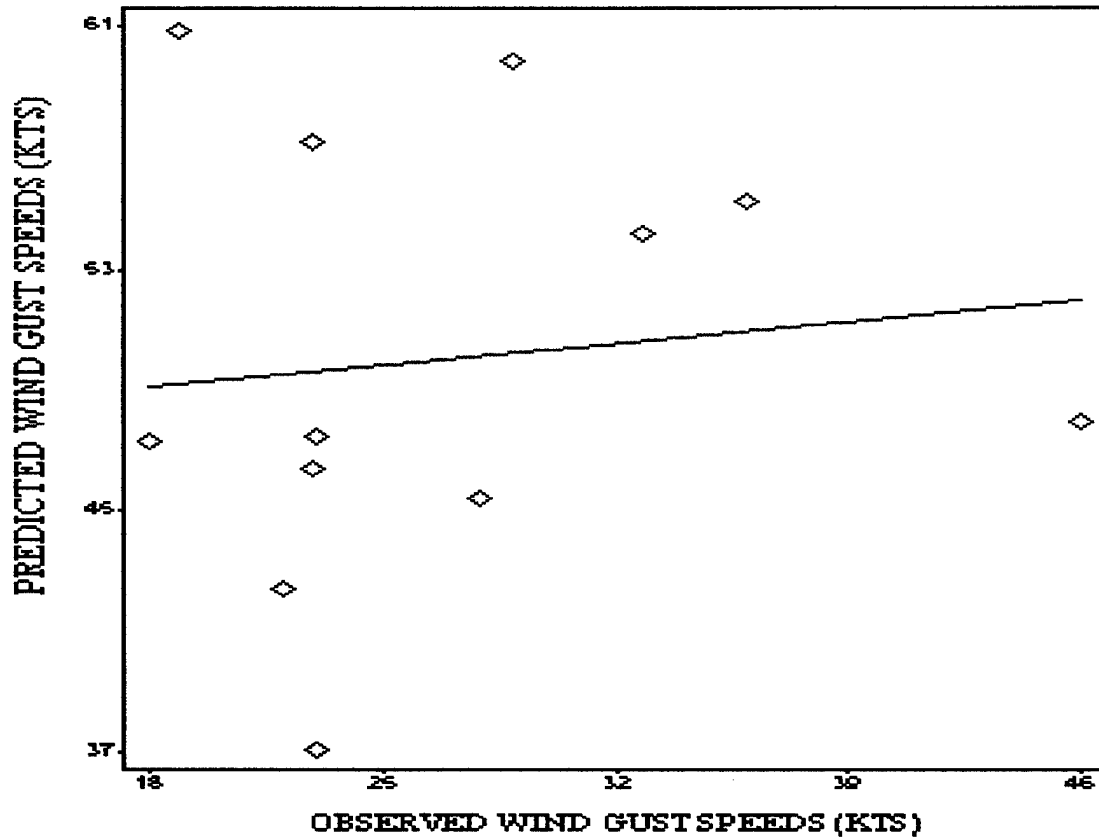


Figure 9. Scatter plot of the computed wind speeds using Stewart and Vasiloff's (1998) DMP technique versus observed wind speeds.

The Pearson correlation and P-value computed for this technique and the observed wind gust speeds were 0.1131 and 0.7263, respectively. These values suggest that analogous

to the other three techniques, no linear relationship appeared to exist between the DMP technique's predicted wind gust speeds and the observed wind gust speeds.

4.3 Description of Wind Data Set

The potential wind gust speeds computed using the four methods discussed above were included in Table 9 along with the observed wind gust for each thunderstorm studied. Once these potential wind gust speeds were obtained for the four techniques, these speeds along with the observed wind gust speeds were subjected to statistical analysis. As with the radar and Skew T, Log P products, the mean, median, variance, standard deviation, maximum value and minimum value were computed for each technique's predicted wind gust speeds. The results of the statistical analysis are presented in Table 11.

Table 11. Summary statistics for predicted and observed wind gust speeds (kts).

	Observed Wind Gust	Predicted Wind Gust Stewart(1991) VIL/TOP	Predicted Wind Gust Headquarters AWS' (1996) VIL/TOP	Predicted Wind Gust Stewart(1996) dBZ/Height	Predicted Wind Gust Stewart and Vasiloff's (1998) DMP
Minimum Value	15	4.1	28.3	4.4	37.1
Maximum Value	46	43.9	43.8	30.2	60.8
Mean	26.4	22.7	36.5	17.6	50.1
Median	25	25.4	35.9	16.2	47.7
Standard Deviation	7.1	12.8	5.6	9.0	7.3
Variance	50.0	163.1	31.8	81.2	53.3

4.4 Regression of Wind Techniques

One of the original intents of this research was to evaluate several potential wind gust prediction techniques and determine their usefulness in predicting downdraft wind speeds for airmass thunderstorms at PAFB. Based upon this evaluation, if a technique was not accurate in wind gust prediction, then the next step was to attempt to modify the existing technique. This technique modification would be based upon the identification of a common bias between the forecasted wind gusts or some other statistically significant relationship between forecasted and observed wind gust speeds. If no relationship could be identified to modify the technique, the final goal of this research was to use statistical regression to find a possible relationship between the collected radar and Skew T, Log P products, and develop a new forecasting technique for PAFB based on the results of this regression.

As reported above, the results of the evaluation of the four potential wind gust prediction techniques left considerable room for improvement. Evaluation of the four wind gust prediction techniques employing data collected during this research suggests that not one of the four techniques can be considered accurate in forecasting downdraft wind speeds associated with airmass thunderstorms at PAFB. Therefore, the next step was to run a statistical regression using the radar and Skew T, Log P products used in each of the four techniques to ascertain if any relationship could be discerned between these products and the observed wind gust speeds.

4.4.1 Regression of VIL and TOP.

Both Stewart's (1991) and Headquarters AWS' (1996) VIL/TOP technique incorporated VIL and TOP as the only independent variables in their technique by which

to forecast a maximum wind gust potential. Therefore, a statistical regression was run strictly on these two products in an attempt to identify a possible relationship between these products and the observed wind gust speed. However, prior to running the statistical regression, a scatter plot was created for VIL and TOP versus the observed wind gust speed to identify if a possible linear relationship existed between these products and the observed wind gust speeds. Figures 10 and 11 are the scatter plots for VIL and TOP versus the observed wind gust speeds, respectively.

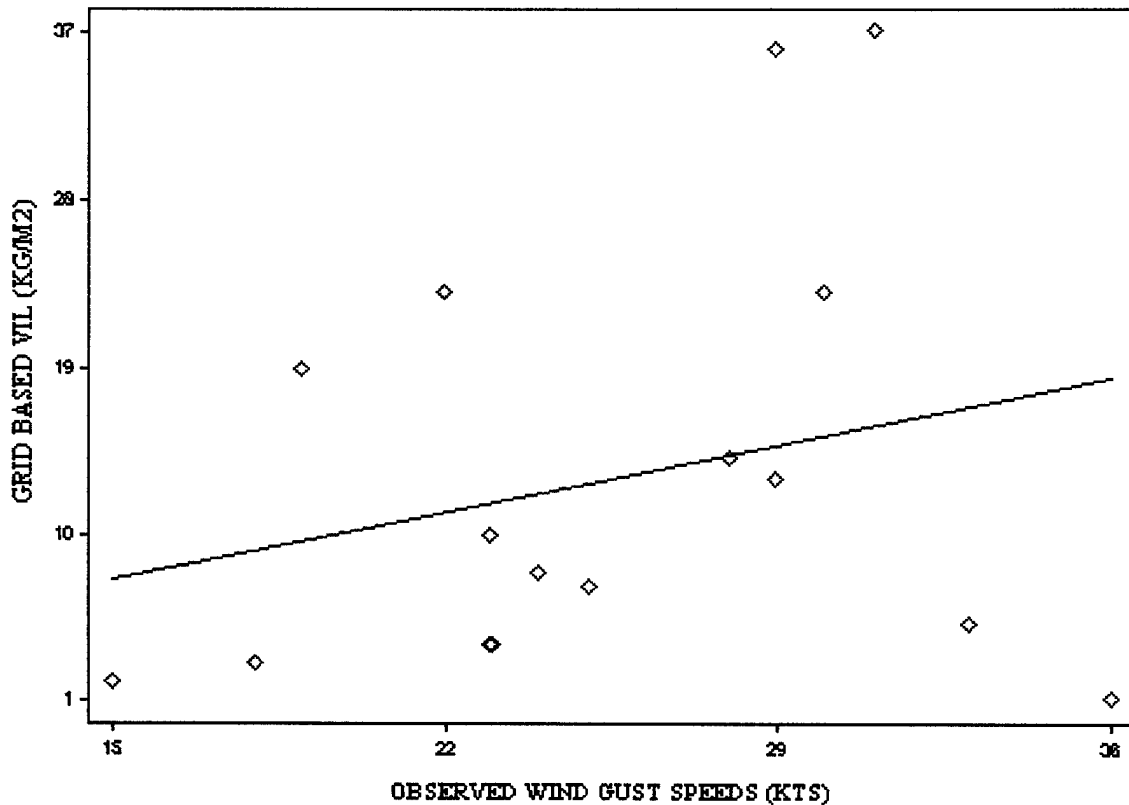


Figure 10. Scatter plot of Grid Based VIL versus observed wind speeds.

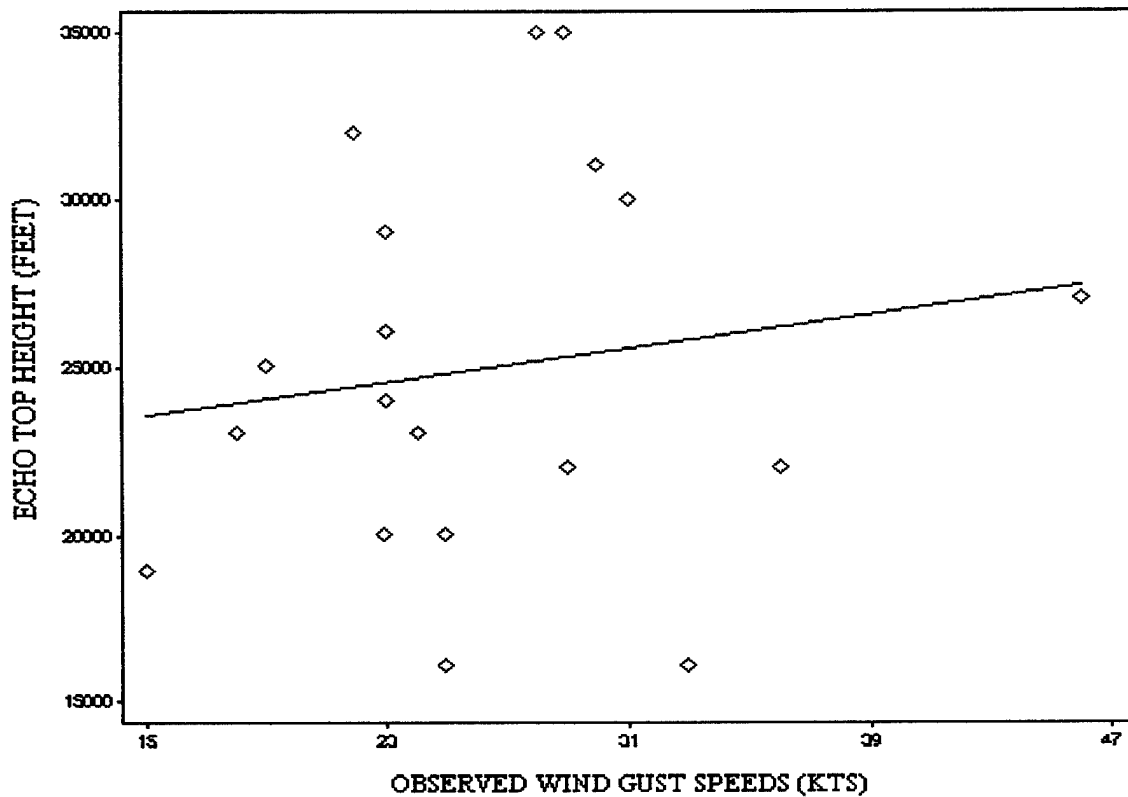


Figure 11. Scatter plot of EchoTop Height versus observed wind speeds.

As can be seen from both these figures, the plotted VIL and TOP points do not appear to have any sort of linearity to them since a straight line would not pass smoothly through their set of points. Despite the lack in appearance of a linear relationship in the scatter plots, linear statistical regression was conducted to ensure there was not a linear relationship. The resultant R^2 values for VIL and TOP were 0.065 and 0.023, respectively. A R^2 value of 1 would suggest the variation in the observed wind was completely explained by the linear regression model. A R^2 value of 0 would suggest the variation in the observed wind was not explained at all by the regression model to include the influence of the VIL and TOP products. In fact, if R^2 is small, another regression model should be investigated to find one that can more effectively explain the variation in

observed wind gust speeds (Devore, 1995:489). The extremely low values of R^2 suggested that the linear regression model, when used with either of these products, does not explain the variability in the observed wind gust speeds.

In addition to the linear regression model used above, four other statistical regression models were used, incorporating VIL and TOP as their independent variables, to test for a possible relationship with the observed wind gust speeds. The four statistical regression models used were the first-order regression model, second-order no-interaction regression model, first-order interaction model and the full quadratic regression model. Figure 12 shows the general formulas for these models where x_1 is VIL and x_2 is TOP.

REGRESSION MODEL	EQUATION
First-Order Model	$Y = \beta_0 + \beta_1 x_1 + \beta_2 x_2 + \epsilon$
Second-Order No-Interaction Model	$Y = \beta_0 + \beta_1 x_1 + \beta_2 x_2 + \beta_3 x_1^2 + \beta_4 x_2^2 + \epsilon$
First-Order Interaction Model	$Y = \beta_0 + \beta_1 x_1 + \beta_2 x_2 + \beta_3 x_1 x_2 + \epsilon$
Full Quadratic Model	$Y = \beta_0 + \beta_1 x_1 + \beta_2 x_2 + \beta_3 x_1^2 + \beta_4 x_2^2 + \beta_5 x_1 x_2 + \epsilon$

Figure 12. Statistical nonlinear regression models used.

Table 12 shows the results of these regressions, specifically the R^2 values computed for each of the multiple regression models.

Table 12. Results of the multiple regression model using VIL and TOP products.

REGRESSION MODEL:	First-Order Model	Second-Order No-Interaction Model	First-Order Interaction Model	Full Quadratic Model
R^2 VALUE:	0.072	0.145	0.091	0.169

Examining the R^2 values in Table 12, it was apparent based on their low values (i.e., values < 0.4) that the four regression models were not very useful in explaining the relationship between VIL and TOP with the observed wind gust speeds collected during this study. Therefore, based on the results of these statistical regression models, VIL and TOP do not appear to be useful by themselves, or effective in explaining the variation in the observed surface wind gust speeds caused by airmass thunderstorm downdrafts at PAFB. Moreover, this lack of relationship prevents an effective statistical forecasting technique from being developed using VIL and TOP to forecast potential downdraft wind gust speeds.

4.4.2 Regression of Maximum dBZ and Height of Maximum dBZ.

As was the case with Stewart's (1991) VIL/TOP technique, Stewart's (1996) Maximum dBZ/Height of Maximum dBZ technique was not accurate in forecasting potential wind gust speeds associated with airmass thunderstorm downdrafts for PAFB when using the data collected during this research. Careful assessment of the scatter plots of Maximum dBZ and Height of Maximum dBZ with observed wind gusts, Figures 13 and 14, showed a linear relationship did not appear to exist between these variables and the observed wind gust speeds.

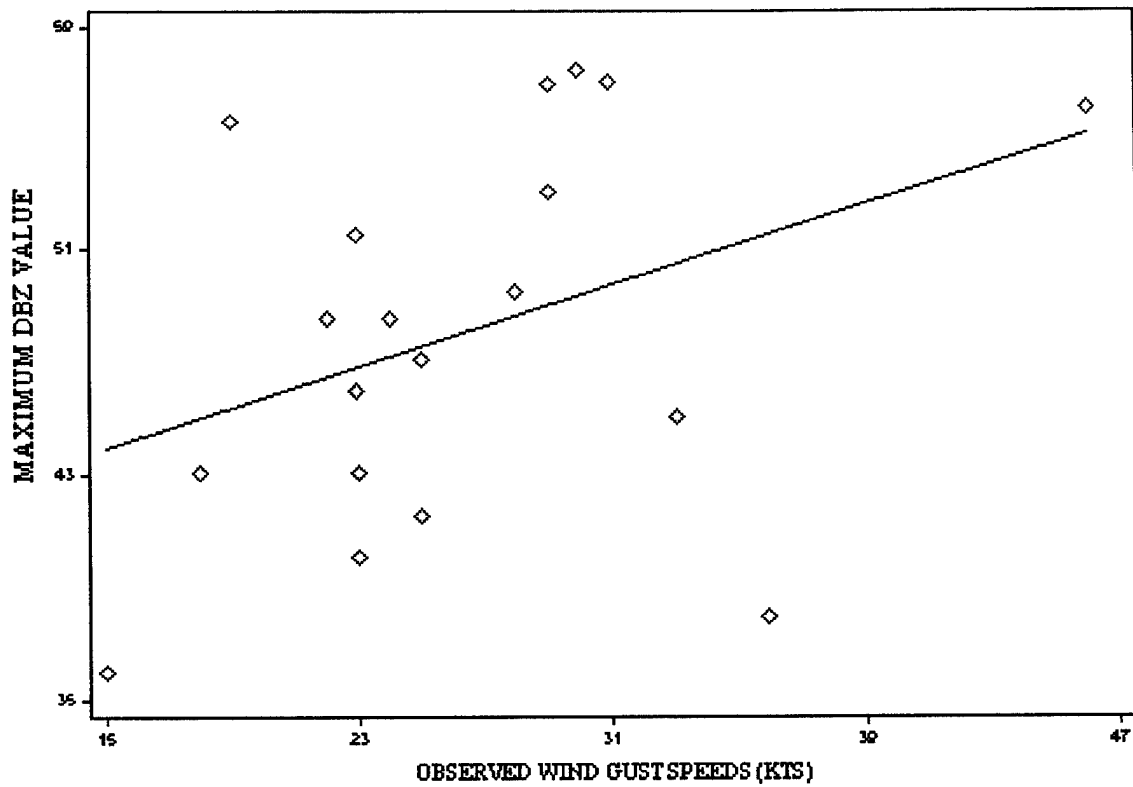


Figure 13. Scatter plot of Maximum dBZ value versus observed wind speeds.

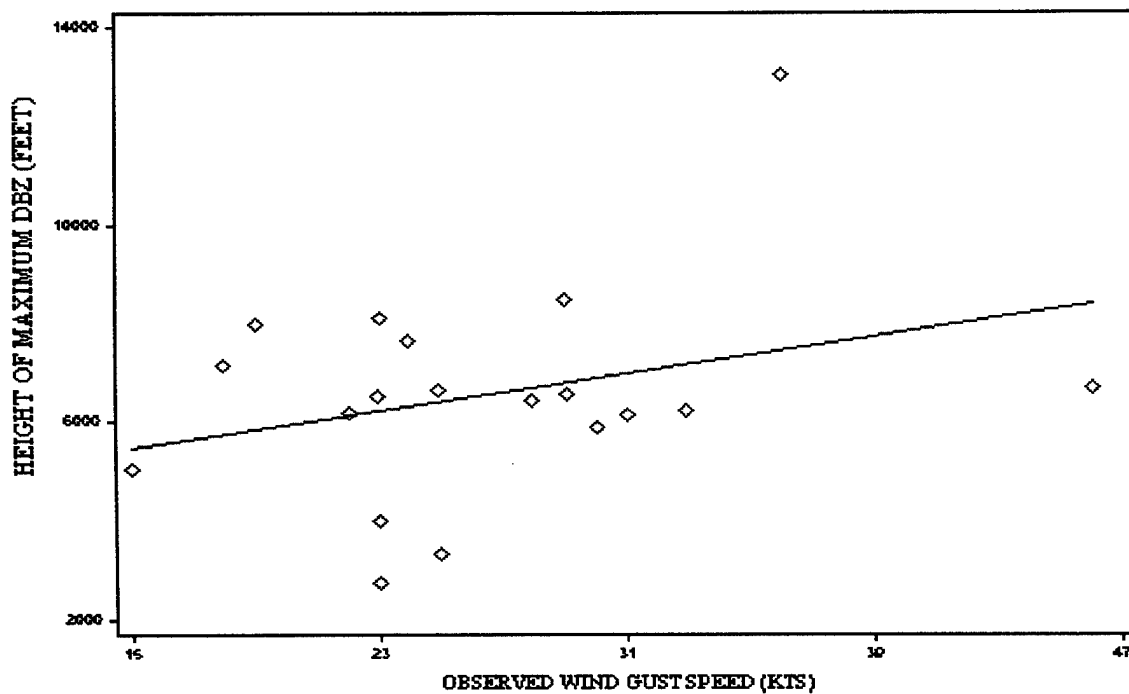


Figure 14. Scatter plot of Height of Maximum dBZ versus observed wind speeds.

A linear regression model was used to test this assessment, and R^2 values of 0.142 and 0.093 were obtained for Maximum dBZ and the Height of Maximum dBZ, respectively. These R^2 values supported the notion that a linear relationship did not exist between these products and the observed wind gust speeds. Furthermore, because of the lack of linearity, the same regression models used to test Stewart's (1991) VIL/TOP technique were applied here also. The results of these regressions are displayed in Table 13.

Table 13. Results of multiple regression model using Maximum dBZ and Height of Maximum dBZ products.

REGRESSION MODEL:	First-Order Model	Second-Order No-Interaction Model	First-Order Interaction Model	Full Quadratic Model
R² VALUE:	0.258	0.340	0.354	0.368

Based on the computed R^2 values presented in Table 13, it appeared the regression model, using the Maximum dBZ and the Height of Maximum dBZ products as independent variables, explained some of the variation in the observed wind gust speeds. However, most of the variation still appears to be unexplained by this regression model. Moreover, in the case of the full quadratic regression model that attained the highest R^2 value out of the four regression models, the P-value was 0.253. A P-value of 0.253, when a value of 0.05 or less is desired, suggested this regression model was not statistically significant and could not be used to accurately forecast downdraft wind speeds. Therefore, forecasting downdraft wind speeds solely using Maximum dBZ and the Height of Maximum dBZ products did not appear to provide an accurate forecast and another prediction method should be researched.

4.4.3 Regression of Maximum dBZ and Sub-Cloud Temperature Lapse Rate.

The last technique to be studied during this research was Stewart and Vasiloff's (1998) DMP technique. The two products used by this model to forecast potential wind gust speeds were Maximum dBZ at or just near cloud base and the sub-cloud temperature lapse rate. Since Maximum dBZ was already tested with the last prediction technique to identify a possible linear relationship with the observed wind gust speeds, only the sub-cloud temperature lapse rate needed to be tested. Using a linear regression model with the sub-cloud lapse rate as the independent variable, a R^2 value of 0.058 was obtained. This R^2 value suggested that a linear relationship did not exist between the sub-cloud lapse rate and the observed wind gust speeds. Therefore, the next step was to apply the same statistical regression models used to evaluate the other prediction techniques using the Maximum dBZ and sub-cloud lapse rate as independent variables, and the observed wind gust speed as the dependent variable. The resultant R^2 values for these regression models are displayed in Table 14.

Table 14. Results of multiple regression model using Maximum dBZ and sub-cloud temperature lapse rate products.

REGRESSION MODEL:	First-Order Model	Second-Order No-Interaction Model	First-Order Interaction Model	Full Quadratic Model
R² VALUE:	0.146	0.314	0.148	0.329

It should be noted that the full quadratic regression model provided a R^2 value of 0.329, which suggested a possible relationship between the Maximum dBZ and the sub-cloud temperature lapse rate with variations in the observed downdraft speed. Unfortunately, a P-value of 0.228 was computed which suggested that the model was not statistically

significant and could not be used to accurately forecast downdraft wind gusts based on the data collected during this research. Consequently, this lack of relationship prevents an effective statistical forecasting technique from being developed using Maximum dBZ and the sub-cloud temperature lapse rate to forecast potential downdraft wind gust speeds at PAFB.

4.5 Regression of Radar Products

As shown in this research, the four techniques used to forecast potential downdraft wind speeds did not prove to be very accurate when applied to airmass thunderstorms occurring at PAFB. Furthermore, with the inability to modify the existing techniques using statistical analysis, the final step was to try and use statistical analysis to find a possible relationship between downdraft wind speeds and other radar products collected from the airmass thunderstorms. The other products to be examined were Cell Based VIL, ST, and Cloud Base Height. Figures 15, 16 and 17 are the scatter plots of these products and the observed wind gusts, respectively. From these scatter plots it appears a linear regression model would not be the regression model to use in order to find a possible relationship between these products and the observed wind gusts. This is due to the fact that for all three cases, the plotted points do not lie in a straight line and therefore do not appear to possess a linear relationship. Consequently, the four regression models used earlier were also used with these three radar products as well as with the other radar and Skew T, Log P products. Since a data sample of at least ten cases is desired for every one independent variable used in a regression model, only two products would be regressed in a model at a time based on this research's sample size of nineteen cases (Reynolds. 1998, personal interview).

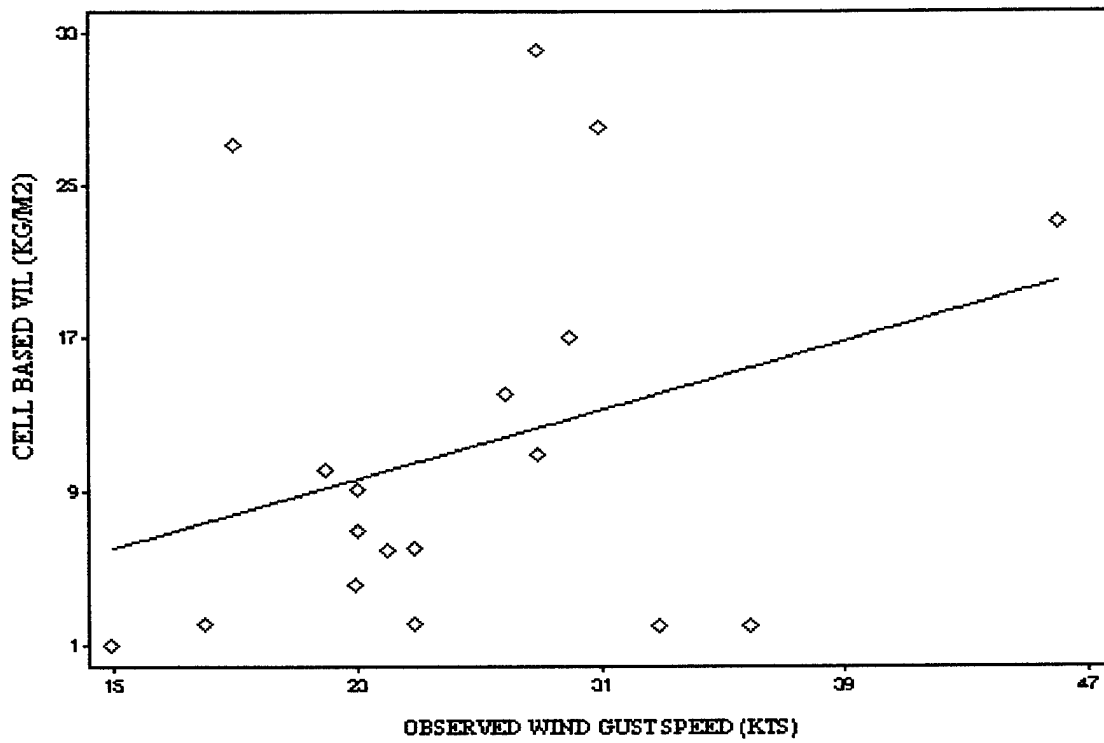


Figure 15. Scatter plot of Cell Based VIL versus observed wind speeds.

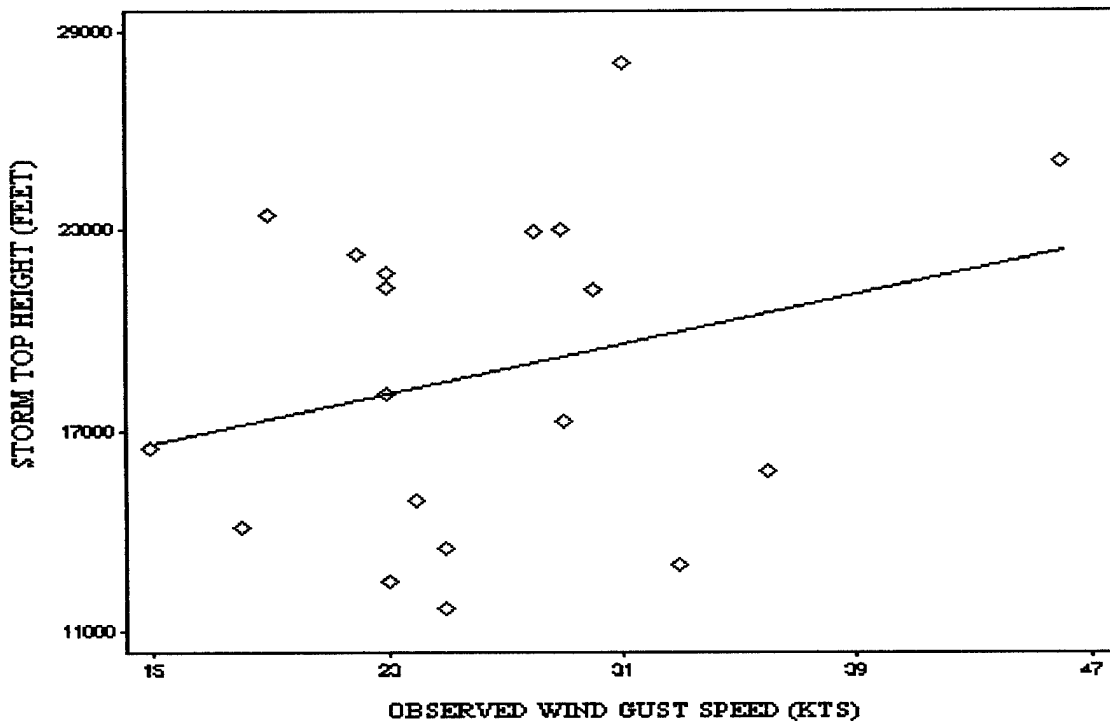


Figure 16. Scatter plot of Storm Top Heights versus observed wind gust speeds.

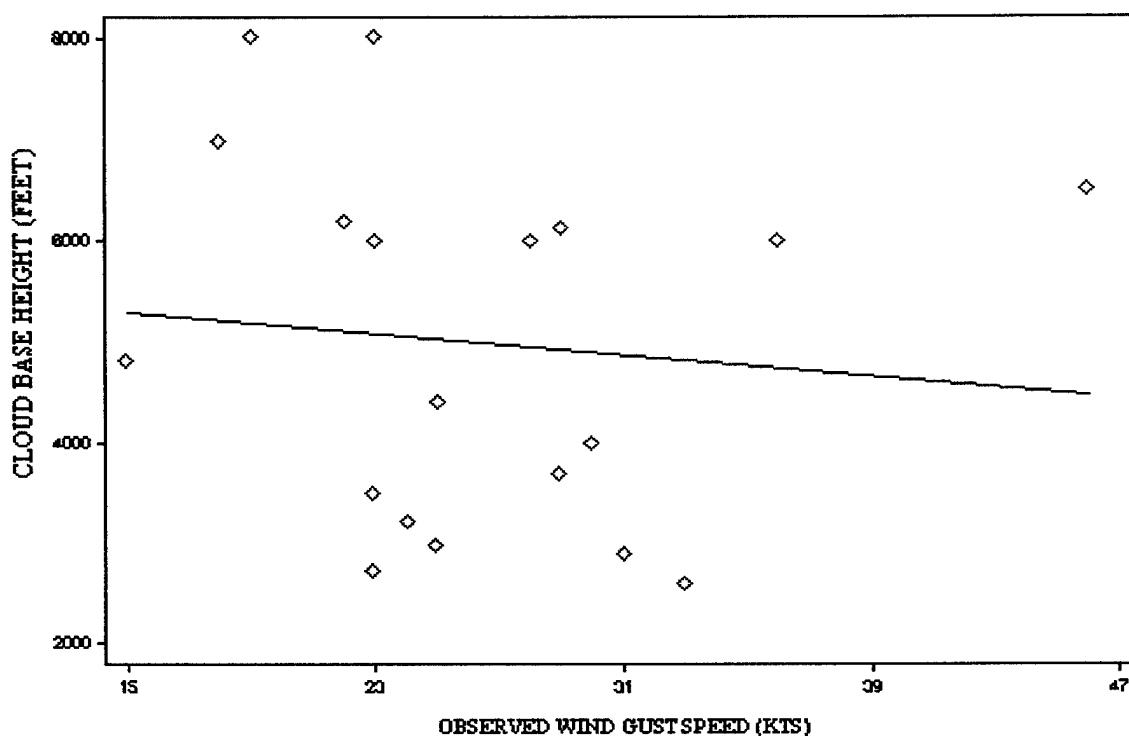


Figure 17. Scatter plot of Cloud Base Heights versus observed wind speeds.

This condition permitted 112 regression models to be tested using the statistical analysis program Statistix, including the three regression models (i.e., VIL and TOP, Maximum dBZ and Height of Maximum dBZ, and Maximum dBZ and sub-cloud temperature lapse rate) tested earlier, in an attempt to find a possible relationship between these eight products and observed wind gust speeds. The R^2 values of these 112 regression models for the various product combinations are presented in Table 15. These regression models and corresponding R^2 values < 0.4 suggested the regression models were not very effective in explaining the relationship between the products and observed downdraft wind speeds.

Table 15. Results of multiple regression model using VIL, Cell Based VIL, TOP, ST, Maximum dBZ, Height of Maximum dBZ, Cloud Base Height and sub-cloud temperature lapse rate products.

Radar and Skew-T, Log P Products	First Order Regression Model R² Value	Second Order No-Interaction Regression Model R² Value	First Order Interaction Regression Model R² Value	Quadratic Regression Model R² Value
Grid Based VIL/Cell Based VIL	0.072	0.203	0.093	0.255
Grid Based VIL/TOP	0.072	0.145	0.091	0.169
Grid Based VIL/ST	0.101	0.119	0.113	0.121
Grid Based VIL/Maximum dBZ	0.082	.191	0.137	0.219
Grid Based VIL/Maximum dBZ Height	0.295	0.383	0.481	0.495
Grid Based VIL/Cloud Base Height	0.195	0.227	0.208	0.230
Grid Based VIL/Lapse Rate	0.137	0.302	0.176	0.352
Cell Based VIL/TOP	0.114	0.152	0.117	0.231
Cell Based VIL/ST	0.105	0.204	0.130	0.205
Cell Based VIL/Maximum dBZ	0.133	0.159	0.157	0.299
Cell Based VIL/Maximum dBZ Height	0.209	0.285	0.335	0.360
Cell Based VIL/Cloud Base Height	0.129	0.183	0.132	0.186
Cell Based VIL/Lapse Rate	0.134	0.194	0.171	0.277
TOP/ST	0.089	0.152	0.153	0.181
TOP/Maximum dBZ	0.145	0.176	0.153	0.186
TOP/Maximum dBZ Height	0.125	0.155	0.129	0.157
TOP/Cloud Base Height	0.043	0.054	0.056	0.062
TOP/Lapse Rate	0.077	0.164	0.099	0.247
ST/Maximum dBZ	0.143	0.206	0.203	0.207
ST/Maximum dBZ Height	0.189	0.304	0.189	0.304
ST/Cloud Base Height	0.095	0.216	0.117	0.259
ST/Lapse Rate	0.136	0.227	0.189	0.257
Maximum dBZ/Maximum dBZ Height	0.258	0.340	0.354	0.368
Maximum dBZ/Cloud Base Height	0.149	0.193	0.150	0.193
Maximum dBZ/Lapse Rate	0.146	0.314	0.148	0.329
Maximum dBZ Height/Cloud Base Height	0.173	0.192	0.179	0.251
Maximum dBZ Height/Lapse Rate	0.168	0.293	0.195	0.293
Cloud Base Height/Lapse Rate	0.058	0.225	0.207	0.240

One exception to this observation was the use of Grid Based VIL and Height of Maximum dBZ with the full quadratic regression model. Grid Based VIL and Height of Maximum dBZ when used as independent variables, and the observed wind gust speeds used as the dependent variable in the full quadratic regression model, returned a R^2 value of 0.495. The following is the full quadratic regression equation that obtained this R^2 value:

$$V_o = \beta_0 + \beta_1 x_1 + \beta_2 x_2 + \beta_3 x_1^2 + \beta_4 x_2^2 + \beta_5 x_1 x_2 \quad (4)$$

where

V_o is the observed downdraft wind gust speed (m s^{-1}),

$$\beta_0 = 0.2253,$$

$$\beta_1 = 2.1243,$$

$$\beta_2 = 0.0036,$$

$$\beta_3 = -0.0059,$$

$$\beta_4 = -6.1\text{E-}8,$$

$$\beta_5 = -0.0003,$$

x_1 = Grid Based VIL (kg m^{-2}), and

x_2 = Height of Maximum dBZ (meters).

A R^2 value of 0.495 suggested that Grid Based VIL and Height of Maximum dBZ, when used with this full quadratic regression model, had some merit in explaining the variation between the observed and predicted downdraft wind gust speeds. Table 16 displays the values for Grid Based VIL, Height of Maximum dBZ, the observed wind gust speed, and

the regression model's predicted wind gusts using the values for Grid Based VIL and Height of Maximum dBZ from sixteen of the nineteen thunderstorms. (It is important to note that Grid Based VIL values were obtained for sixteen of the nineteen thunderstorms under study. Therefore, sixteen cases were used in the development of this full quadratic regression model.)

Table 16. Observed and predicted wind gust speeds computed using Grid Based VIL, Height of Maximum dBZ and equation (4).

Date of Thunderstorm	Observed Wind Gust Speed (kts)	Quadratic Model's Predicted Wind Gust Speed (kts)	Grid Based VIL (kg/m²)	Height of Maximum dBZ (1000's ft)
1 Jun 1996	36	35.9	1	13
14 Jun 1996	30	29.1	23	5.9
17 Jun 1996	29	27.6	36	6.5
21 Jun 1996	22	28.1	23	6.2
27 Jun 1996	23	25.4	4	8.1
28 Aug 1996	31	30.4	37	6.1
6 May 1997	15	18.4	2	5
18 Jun 1997	23	23.0	10	2.7
19 Jun 1997	33	22.6	5	6.2
26 Jun 1997	28	25.7	14	6.4
4 Jul 1997	23	22.8	4	6.5
26 Jul 1997	19	23.1	19	8
31 Jul 1997	29	23.9	13	8.5
2 Aug 1997	24	24.7	8	7.6
24 Aug 1997	18	23.6	3	7.1
11 Sep 1997	25	23.8	7	6.6

Although the R^2 value of 0.495 suggested that this regression model provided some value in explaining the relationship between the observed and predicted downdraft wind gust speeds, it was still necessary to determine the validity of this regression model. The first test to ensure the model's validity was to construct a residual plot using the model's residual values. The residual plot for the regression model is shown in Figure 18.

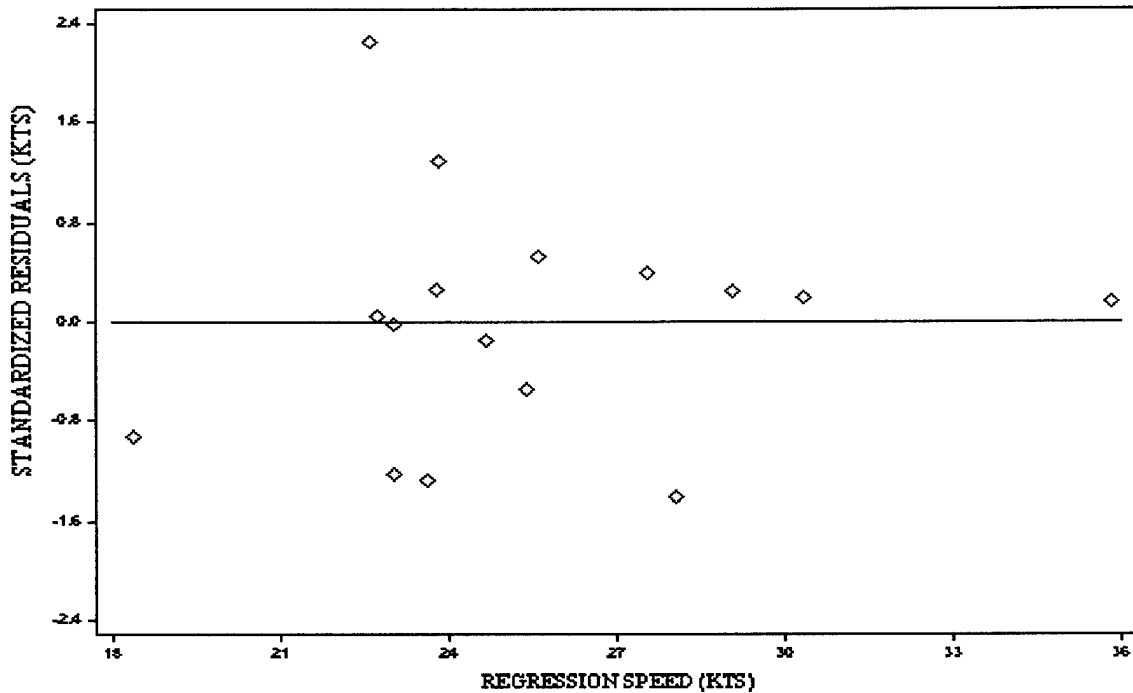


Figure 18. Regression residual plot for equation (4).

This residual plot shows no distinct pattern created by the plotted residuals. Furthermore, this random distribution of residual values, and the fact that all but one of the residuals falls within +2 and -2 on the residual plot, suggested that the model was valid (Devore, 1995:525). The next test to ensure model validity was to plot the predicted wind gust speeds with the observed wind gust speeds for each thunderstorm. The plot of the predicted and observed wind gust speeds is presented in Figure 19. If the regression line for this plot had a 45 degree slope, then this would show the regression model was an accurate predictor of the observed wind gusts. For the regression model used, the slope of the regression line was approximately 22 degrees. This slope provided a good fit for the observed and predicted wind gust speeds, and suggested the model was a good predictor of the observed data.

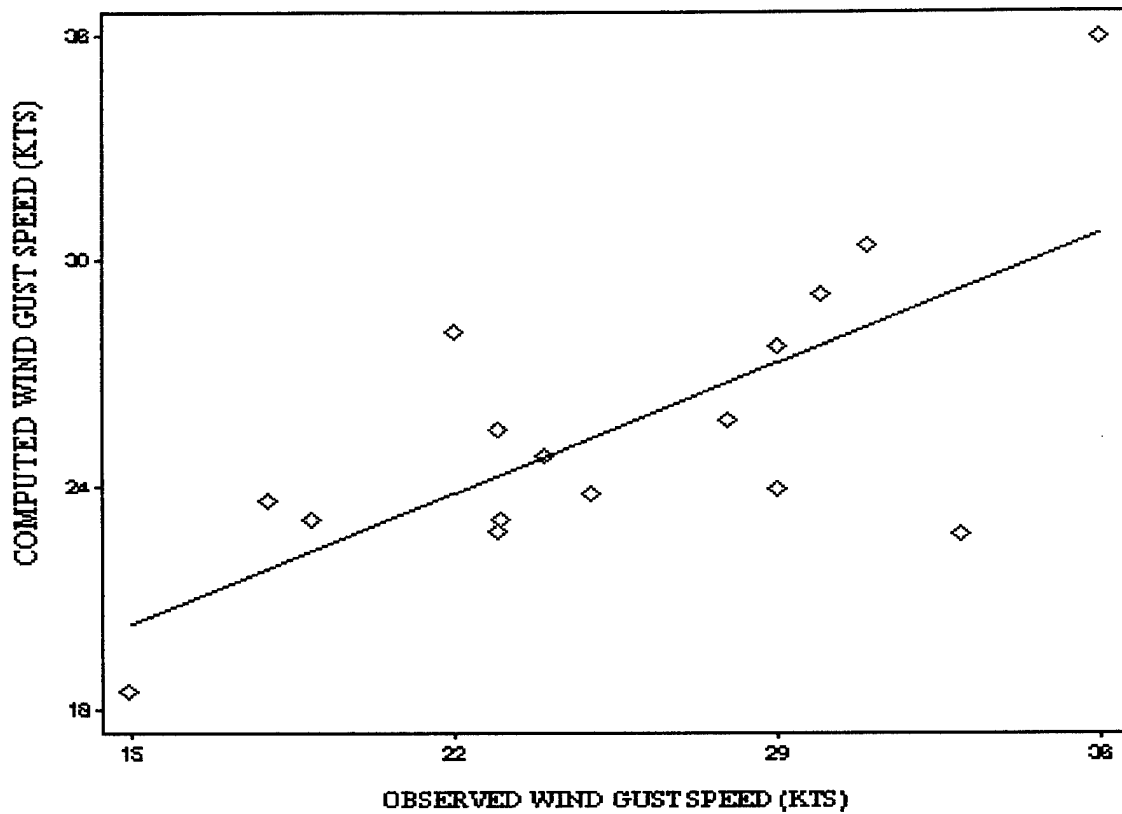


Figure 19. Plot of observed wind speeds versus computed wind speeds using equation (4).

The final test to ensure the model's validity was to plot the model's residuals and check for normality. Figure 20 is a Wilk-Shapiro/Rankit Plot of the residuals for this regression model. The plot, along with the Wilk-Shapiro statistic of 0.99, strongly suggested the normality of the residuals and further supported the validity of the model.

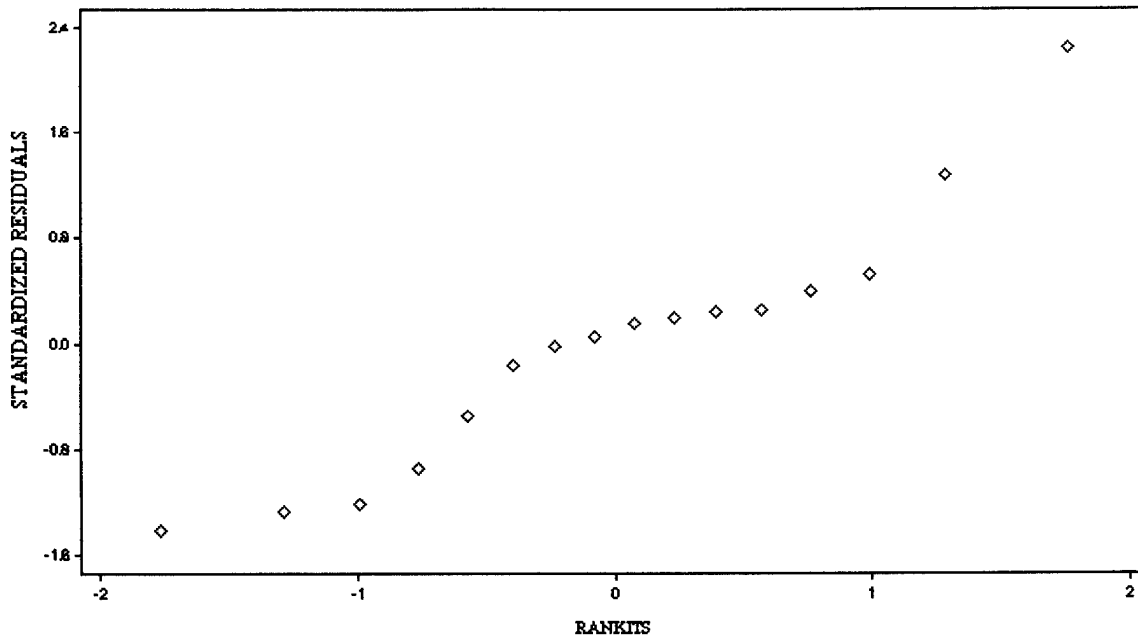


Figure 20. Wilk-Shapiro/Rankit Plot for residuals of equation (4).

All tests conducted for this model support the validity of the full quadratic regression model in predicting downdraft wind speeds based on the data collected during this research. With the check for model validity completed, the model was then checked for statistical significance. To check the statistical significance of this model, the P-value was computed and a value of 0.171 was obtained. This value suggested that the model does possess some statistical significance, and that Grid Based VIL and Height of Maximum dBZ when used with the full quadratic regression model showed potential in predicting downdraft wind speeds.

To test the skill of this regression model developed using the statistical analysis program Statistix, the predicted wind gust speeds were compared to the observed wind gust speeds, and a successful potential wind gust forecast, a missed potential wind gust

forecast and no potential wind gust forecast percentage rate was computed for the sixteen thunderstorm days. The regression model's computed wind gust potential had a successful potential wind gust forecast rate of 75%. Furthermore, there was a 0% no forecast rate, and a missed potential wind gust forecast rate of 25%. Based on this data set, equation (4) using Grid Based VIL and Height of Maximum dBZ values obtained during this research was more effective in forecasting downdraft wind speeds than the other four prediction techniques discussed earlier.

A second regression equation identified as showing promise in effectively explaining the relationship between observed downdraft wind gusts using Grid Based VIL and Height of Maximum dBZ was the first-order interaction regression model. Once again the statistical analysis program Statistix was used with Grid Based VIL and Height of Maximum dBZ entered as the independent variables and observed wind gust speeds as the dependent variable in the first-order interaction regression model. This regression model returned a R^2 value of 0.481. The following is the first-order interaction regression equation that obtained this R^2 value:

$$V_o = \beta_0 + \beta_1 x_1 + \beta_2 x_2 + \beta_3 x_1 x_2 \quad (5)$$

where

V_o is the observed downdraft wind gust speed ($m\ s^{-1}$),

$\beta_0 = 6.9725$,

$\beta_1 = 1.5616$,

$\beta_2 = 0.0023$,

$\beta_3 = -0.0002$,

x_1 =Grid based VIL (kg m^{-2}), and

x_2 =Height of Maximum dBZ.

Although this equation's R^2 value was slightly less than the R^2 value obtained for the full quadratic regression model, the P-value associated with this first-order interaction model was 0.0426. This value suggested that the model was statistically more significant than the full quadratic regression model when using the same independent and dependent variables. Therefore, the first-order interaction model might be a more appropriate model to explain the variation of the observed wind gust speeds when using Grid Based VIL and Height of Maximum dBZ products. Table 17 displays the values for Grid Based VIL, Height of Maximum dBZ, the observed wind gust speed, and the first-order interaction regression model's predicted wind gust speeds using equation (5).

Table 17. Observed and predicted wind gust speeds computed using Grid Based VIL, Height of Maximum dBZ and equation (5).

Date of Thunderstorm	Observed Wind Gust Speed (kts)	First-Order Interaction Model's Predicted Wind Gust Speed (kts)	Grid Based VIL (kg/m²)	Height of Maximum dBZ (1000's ft)
1 Jun 1996	36	36.3	1	13
14 Jun 1996	30	27.9	23	5.9
17 Jun 1996	29	28.7	36	6.5
21 Jun 1996	22	27.1	23	6.2
27 Jun 1996	23	25.3	4	8.1
28 Aug 1996	31	31.0	37	6.1
6 May 1997	15	19.7	2	5
18 Jun 1997	23	23.2	10	2.7
19 Jun 1997	33	22.7	5	6.2
26 Jun 1997	28	24.8	14	6.4
4 Jul 1997	23	22.9	4	6.5
26 Jul 1997	19	23.1	19	8
31 Jul 1997	29	23.7	13	8.5
2 Aug 1997	24	24.4	8	7.6
24 Aug 1997	18	23.8	3	7.1
11 Sep 1997	25	23.6	7	6.6

Prior to making any further conclusions, the validity of this model was checked. To test the validity of this regression model, a residual plot using the model's residuals, and a plot of the model's predicted wind gust speeds versus the observed wind gust speeds for each thunderstorm needed to be constructed. Furthermore, the model's residuals needed to be tested for normality. Figures 21, 22 and 23 are the plots of these three tests, respectively. It can be seen from Figure 21 that no distinct pattern was produced by the plotted residuals. Furthermore, this random distribution of residual values, and the fact that all but one residual falls within +2 and -2 on the residual plot, suggested the model was valid (Devore, 1995:525).

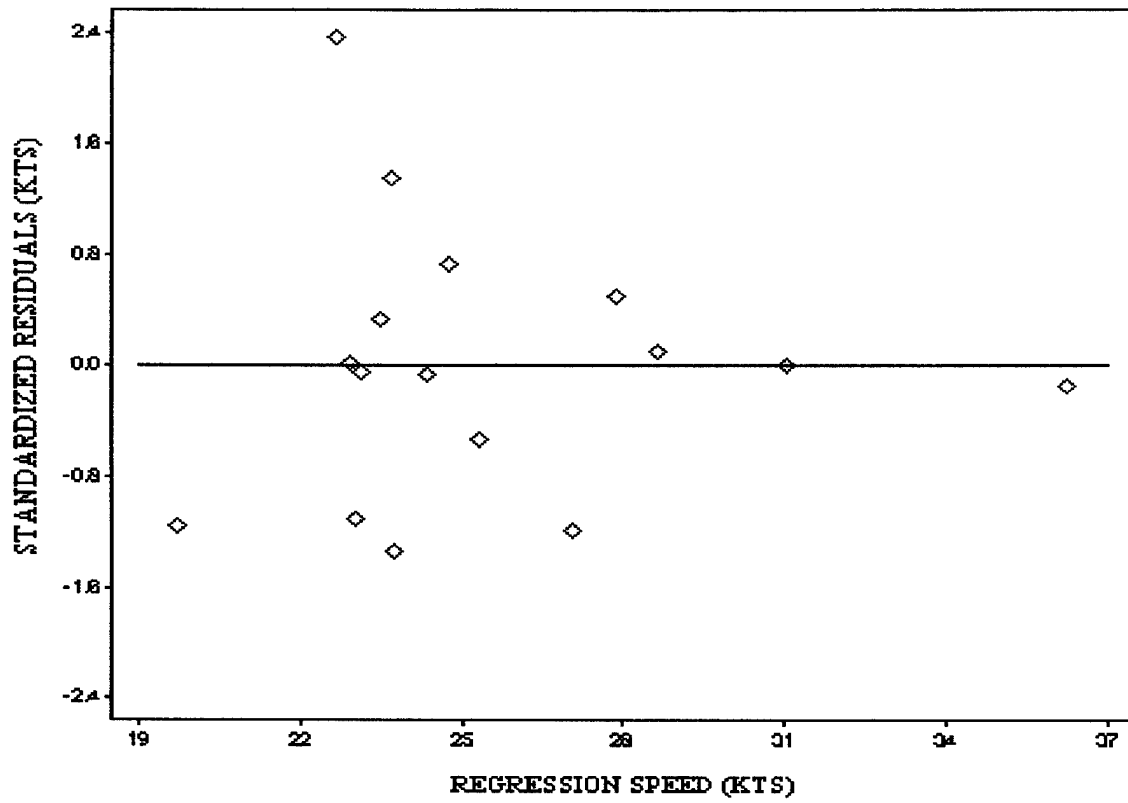


Figure 21. Regression residual plot for equation (5).

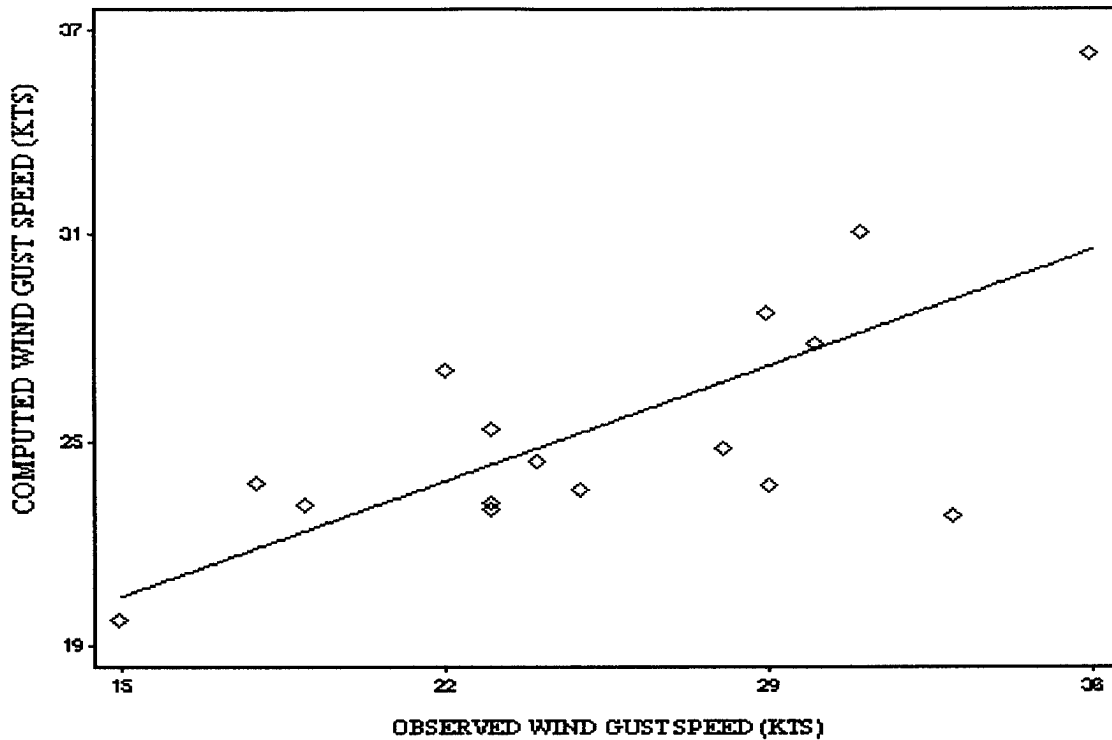


Figure 22. Plot of observed wind speeds versus computed wind speeds using equation (5).

Figure 22 displays a plot of the predicted and observed wind gust speeds, and this plot shows a regression line slope of 15 degrees. As mentioned before, if the regression line for this plot had a 45 degree slope, then this would show the regression model was an accurate predictor of the observed wind gusts. Therefore, this slope provides a tolerable fit for the observed and predicted wind gust speeds, and suggests that the model was a fair predictor of the observed data. The final test to ensure model validity was to plot the model's residuals and check for normality. Figure 23 is a Wilks-Shapiro/Rankit Plot of the residuals for this regression model. The plot and corresponding Wilk-Shapiro statistic of 0.922 shows the normality of the residuals and further supports the validity of the model.

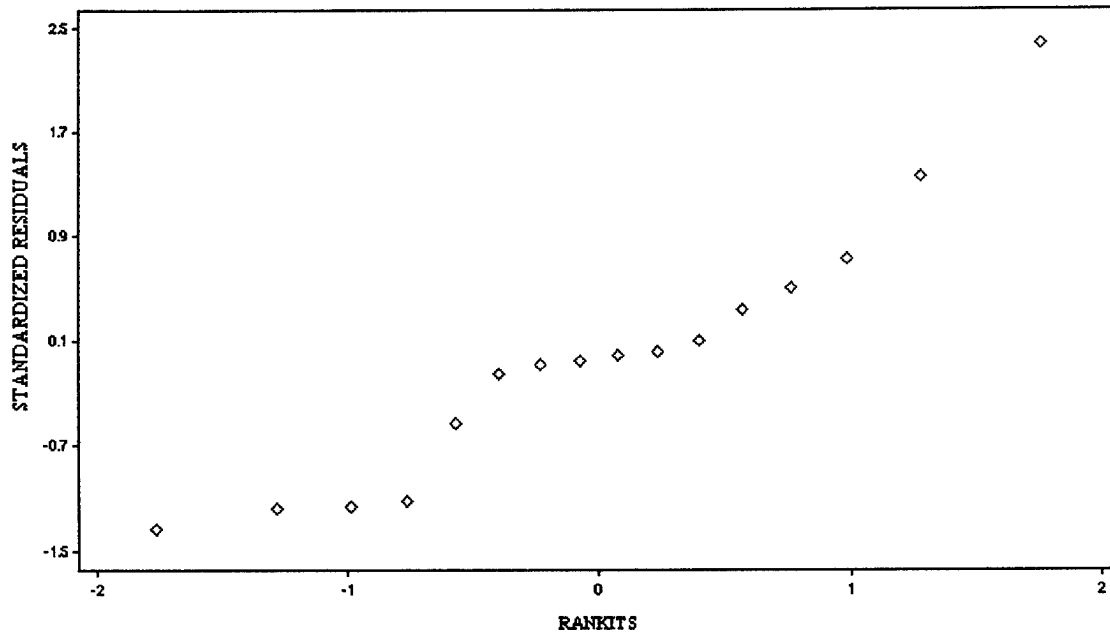


Figure 23. Wilk-Shapiro/Rankit Plot for residuals of equation (5).

All three tests conducted for this model support the validity of the first-order interaction regression model in the prediction of downdraft wind speeds when using the data collected during this research. With the validity of the model proven, the final step in this research was to compare the model's predicted wind gust speeds with the observed wind gust speeds. The results of this evaluation revealed that if the first-order interaction regression model had been used with the obtained values of Grid Based VIL and Height of Maximum dBZ then it would have attained a successful potential wind gust forecast rate of 75%, a missed potential wind gust forecast rate of 25%, and 0% no potential wind gust forecast rate. As with the full quadratic regression equation, had this regression equation been used with this data set, it would have out forecasted the other four techniques reviewed in this research. Therefore, the fact that the model is valid, the model is statistically significant based on its P-value of .0426, and the model has a

successful potential wind gust forecast rate of 75% suggested that the Grid Based VIL and Height of Maximum dBZ products hold potential in forecasting downdraft wind speeds, and should be subjected to further study using a new and larger data set of airmass thunderstorm days.

4.6 Validation of the Developed Regression Models

For the two nonlinear regression models developed above, the entire data set of sixteen airmass thunderstorms was used in the creation of these regression models. The reason the entire data set was used resulted from the fact that the airmass thunderstorm data set from which to create these regression models was very small. However, in any regression model development a validation of the regression model should be conducted. Consequently, a new full quadratic regression model and first-order interaction regression model using Grid Based VIL and Height of Maximum dBZ as independent variables and observed wind gusts as dependent variables were created and a validation of these new regression models was conducted.

The first step in building the new regression models with the intent of validating the models was to withhold part of the data set. It was determined based on a sample size of sixteen airmass thunderstorms that two thunderstorm cases would be held out of the model development in order to validate the model later. The two cases withheld were chosen using the random number generator function in MATHCAD, and cases four and thirteen were selected. (The two days representing cases four and thirteen were 21 Jun 96 and 31 Jul 97, respectively.) With these two cases removed from the data set, a new full quadratic regression model and first-order interaction regression model were built using the remaining fourteen thunderstorm cases. Through use of the statistical analysis

program Statistix, the following full quadratic regression model was created based on this data set of fourteen airmass thunderstorms:

$$V_o = \beta_0 + \beta_1 x_1 + \beta_2 x_2 + \beta_3 x_1^2 + \beta_4 x_2^2 + \beta_5 x_1 x_2 \quad (6)$$

where

V_o is the observed downdraft wind gust speed (m s^{-1}),

$\beta_0 = -12.5416$,

$\beta_1 = 3.3637$,

$\beta_2 = 0.0064$,

$\beta_3 = -0.0101$,

$\beta_4 = -1.932\text{E-}7$,

$\beta_5 = -4.33\text{E-}4$,

$x_1 = \text{Grid Based VIL (kg m}^{-2}\text{), and}$

$x_2 = \text{Height of Maximum dBZ (meters).}$

A R^2 value of 0.650 was computed and suggested that Grid Based VIL and Height of Maximum dBZ, when used with this full quadratic regression model, had strong value in explaining the variation between the observed and predicted downdraft wind speeds. Furthermore, a P-value of 0.083 was obtained for this full quadratic regression model which suggested that this model possessed some statistical significance. The next step was to create a prediction interval for the regression model and compare the two withheld cases against this prediction interval to determine if the new model was valid. Using the statistical analysis program Statistix, a 95% prediction interval was created for the full

quadratic regression model for the two cases. For case four, the lower bound and upper bound for the 95% prediction interval was 17.6 kts and 41.9 kts, respectively. The predicted wind gust speed was 29.7 kts. For case thirteen the lower bound and upper bound for the 95% prediction interval was 8.8 kts and 34.7 kts, respectively. The predicted wind gust speed was 21.7 kts. What the 95 % prediction interval represented for these two cases was the interval created by these upper and lower bounds would “hook” the independently observed wind gust speed 95% of the time. However, in both cases the prediction interval was extremely large, which suggested the full quadratic regression model was not as strong a regression model as desired.

The next step was to then to build a first-order regression model using the same fourteen airmass thunderstorm cases as were used in development of the full quadratic regression model. Using Statistix, the following regression model was created:

$$V_o = \beta_0 + \beta_1 x_1 + \beta_2 x_2 + \beta_3 x_1 x_2 \quad (7)$$

where

V_o is the observed downdraft wind gust speed ($m\ s^{-1}$),

$\beta_0 = 5.5828$,

$\beta_1 = 2.0614$,

$\beta_2 = 0.0025$,

$\beta_3 = -2.868E-4$,

$x_1 =$ Grid based VIL ($kg\ m^{-2}$), and

$x_2 =$ Height of Maximum dBZ.

A R^2 value of 0.5954 was computed and this value suggested that Grid Based VIL and Height of Maximum dBZ, when used with this first-order interaction regression model, had some merit in explaining the variation between the observed and predicted downdraft wind gust speeds. Furthermore, a P-value of 0.024 was obtained for this first-order interaction regression model which suggested that this model possessed statistical significance and should not be disregarded. The next step was to create a prediction interval for the regression model and test the two withheld thunderstorm cases against this prediction interval to determine if this model was valid. Using the statistical analysis program Statistix, a 95% prediction interval was created for the regression model using the withheld cases. For case four, the lower bound and upper bound for the 95% prediction interval was 17.3 kts and 37.9 kts, respectively. The predicted wind gust speed was 27.6 kts. For case thirteen, the lower bound and upper bound for the 95% prediction interval was 10.6 kts and 33.3 kts, respectively. The predicted wind gust speed was 21.9 kts. As in the case with the full quadratic regression model, the prediction interval for the first-order interaction regression model was extremely large, yet still smaller than the prediction intervals computed for the full quadratic regression model. This prediction interval suggested the first-order interaction regression model was still not as strong of a regression model as desired, but was more suitable than the full quadratic regression model. Likewise, although this equation's R^2 value was slightly less than the R^2 value obtained for the full quadratic regression model, the P-value associated with this first-order interaction model was 0.024. This small P-value suggested that the first-order interaction regression model was more statistically significant than the full quadratic regression model when using the same independent and dependent variables. Therefore,

the first-order interaction model would be the more appropriate model to explain the variation of the observed wind gust speeds when using Grid Based VIL and Height of Maximum dBZ products.

4.7 A Second Validation of the Developed Regression Models

The conclusion that the first-order interaction regression model was a more appropriate model than the full quadratic regression model to explain the variation in observed wind gust speeds was further supported by conducting a second validation of the models developed in section 4.5. For this second validation, new full quadratic and first-order interaction regression models were built using fifteen of the sixteen thunderstorm cases. The one thunderstorm case withheld was used to validate the newly built regression models. For both the full quadratic and first-order interaction regression models, sixteen models were built based on a data set of fifteen thunderstorms, with a different thunderstorm case being withheld for each of the sixteen regression models.

For the sixteen models built using the full quadratic regression model, the corresponding R^2 and P-values were computed and are displayed in Table 18. A mean R^2 value of 0.503 and a mean P-value of 0.222 were calculated for the full quadratic model. As was the case with the results from the first validation conducted for the full quadratic regression model, the individual R^2 values and the mean R^2 value revealed that the newly developed full quadratic regression models exhibited some strength in explaining the variation in observed wind gust speeds. However, the individual P-values and the mean P-value were significantly larger than the desired 0.05 value; thus, these P-values suggested the full quadratic model was not statistically significant in explaining the

variation of observed wind gust speeds when using this research's data set and may not be useful in explaining the variation in observed wind gust speeds.

Table 18. Results of sixteen full quadratic regression models using Grid Based VIL and Height of Maximum dBZ.

Withheld Thunderstorm Day	R²	P-value
1 June 1996	.337	.513
14 June 1996	.475	.248
17 June 1996	.489	.225
21 June 1996	.586	.106
27 June 1996	.504	.204
28 August 1996	.461	.270
6 May 1997	.394	.393
18 June 1997	.488	.227
19 June 1997	.715	.026
26 June 1997	.502	.207
4 July 1997	.488	.227
26 July 1997	.527	.173
31 July 1997	.566	.126
2 August 1997	.494	.218
24 August 1997	.518	.184
11 September 1997	.498	.212

This was not the case when for the sixteen models built using the first-order interaction regression model. The R² and P-values computed for these sixteen regression models are displayed in Table 19. The mean R² value and mean P-value were 0.483 and 0.067, respectively. A mean R² value of 0.483 suggested the first-order interaction models showed strength in describing the variation in observed wind gust speeds. Furthermore, a mean P-value of 0.067, though slightly larger than the desired 0.05, supported the fact that the first-order interaction regression model was statistically significant based on this research's data set. Based on these results, prediction intervals for the sixteen first-order interaction regression equations were computed and are displayed in Table 19. Similar to the results from the first validation method, the

prediction intervals for the first-order interaction regression model were larger than desired, and suggested that the first-order interaction regression model was not as strong of a regression model as desired.

Table 19. Results of sixteen first-order interaction regression models using Grid Based VIL and Height of Maximum dBZ.

Withheld Thunderstorm Day	R²	P-value	95% Prediction Interval
1 June 1996	.319	.222	7.2,69.2
14 June 1996	.469	.065	16.1,38.9
17 June 1996	.467	.066	15.5,41.4
21 June 1996	.529	.035	17.2,38.4
27 June 1996	.486	.054	14.5,36.7
28 August 1996	.444	.081	17.4,44.8
6 May 1997	.394	.125	9.7,32.4
18 June 1997	.474	.061	8.1,38.6
19 June 1997	.686	.004	13.2,29.6
26 June 1997	.497	.049	13.8,35.3
4 July 1997	.474	.061	11.7,34.2
26 July 1997	.489	.053	12.9,38.3
31 July 1997	.548	.028	10.3,33.2
2 August 1997	.478	.059	13.3,35.5
24 August 1997	.496	.049	14.1,34.9
11 September 1997	.485	.055	12.4,34.4

However, the R² values and P-values for this model support the conclusion of the first validation test. This conclusion was that the first-order interaction model is more appropriate than the full quadratic regression model in explaining the variation of the observed wind gust speeds when using Grid Based VIL and Height of Maximum dBZ products. This conclusion is based on the thunderstorm data set used in this research and the first-order interaction regression model developed during this research. Although this model appears to hold promise in explaining the variation in observed wind speeds, the model should be tested with a larger data set before any definitive conclusions are drawn about the usefulness of this model.

5 Conclusion

5.1 Problem Statement Review

During the summer of 1996, AFSPC units issued nearly 65% of their weather warnings for downdraft related winds, making it the most frequent challenge to forecasters. Couple this with the fact that during the period of Jun-Aug 96, four Air Force installations suffered over \$4.8 million in damage from convective winds, and it was clear a technique was needed to assist Air Force forecasters in forecasting this meteorological phenomenon.

Up to the time of this research, several techniques had been developed utilizing the WSR-88D to forecast downdraft wind speeds, particularly wind speeds associated with downbursts. However, only limited research had been conducted on ways to forecast downdraft wind speeds in the High Plains region of the United States. Furthermore, little research had been conducted on ways to forecast downdraft winds at speeds less than those associated with traditional downbursts. The ability of Air Force forecasters to accurately predict downdraft wind speeds would assist in significantly improving weather warning and advisory predictions and false alarm rates. As a result, the intent of this research was to evaluate and build upon existing techniques, and moreover, to investigate new ways WSR-88D products, specifically VIL, TOP, ST and reflectivity, could be used by Air Force forecasters to more accurately forecast downdraft wind speeds at PAFB, Colorado.

5.2 Review of Methodology

Based on the research objectives, the overall approach of this research consisted of three phases. The first phase was to identify all airmass thunderstorms which occurred within 10.5 nm of PAFB during 1 Apr-30 Sep 96 and 1 Apr-30 Sep 97 and produced winds that were equal to or in excess of 15 knots. This was accomplished through the rigorous screening of surface observations, lightning flash data, and surface synoptic weather maps. These data sources were used to ensure the thunderstorms which occurred within 10.5 nm of PAFB were not synoptically induced, and had winds that were greater than or equal to 15 knots at the time of convective activity. The airmass thunderstorm days that remained comprised the data set from which the radar data was requested.

The next phase was to order and interrogate archived WSR-88D Level II data from the Pueblo, Colorado WSR-88D corresponding to the airmass thunderstorms days identified in phase one. Upon receipt of the Level II data, each case was analyzed with WATADS to identify the thunderstorm responsible for the observed wind gust occurring at PAFB. Identification of the downdraft-producing thunderstorm required meticulous interrogation of the Level II data. Once the downdraft-producing thunderstorm was identified, the values for the radar products of interest were collected.

The final phase was to conduct a statistical analysis of the collected radar products. This phase included the evaluation of the existing downdraft prediction techniques for PAFB and the possible modification of these techniques if they were not accurate forecasters of downdraft wind speeds at PAFB. Furthermore, the final step of this statistical analysis included the use of other WSR-88D products to possibly identify a

new relationship between the radar products collected and observed downdraft wind speeds.

5.3 Review of Results

The research conducted was based on a data set of nineteen airmass thunderstorms occurring within 10.5 nm of PAFB during 1 Apr-30 Sep 96 and 1 Apr-30 Sep 97 for which observed winds were greater than or equal to 15 knots. From this data set of thunderstorms, the following results were obtained.

The results of the evaluations of Stewart's (1991) VIL/TOP technique, Headquarters AWS' (1996) VIL/TOP technique, Stewart's (1996) Maximum dBZ/Height of Maximum dBZ method and Stewart and Vasiloff's (1998) DMP technique are presented in Table 1. As can be discerned from the table, these techniques were not very accurate in forecasting downdraft wind speeds associated with airmass thunderstorms at PAFB using the data collected during this research. In fact, based on the data collected and analyzed, it is recommended that none of the four techniques should be used in forecasting downdraft wind speeds for airmass thunderstorms occurring near PAFB.

The results obtained from the evaluation of the four potential wind gust prediction techniques were unexpected. From prior research, it was anticipated that the techniques would show some proficiency in forecasting downdraft wind speeds, and only minor modification would be required for application in the High Plains region of the United States, specifically PAFB. Since this was not the case, and no specific forecasting bias could be identified between the predicted and observed wind gust speeds, the next step in the modification of the four techniques was statistical regression. Unfortunately, the multiple regression analysis of the four techniques was unable to identify a relationship

between the radar products and the observed wind gusts. As a result, modification of the gust prediction techniques for forecasting purposes at PAFB could not be accomplished.

The last objective of this research was to investigate the use of radar products, other than those used in the four wind gust prediction techniques, to forecast downdraft wind speeds at PAFB. Once again, statistical regression was used to identify a possible relationship between these radar products and observed wind gust speeds. After 112 regression models were developed and tested, two models, a full quadratic regression model and a first-order interaction regression model, that both incorporated VIL and Height of Maximum dBZ to explain the variation in observed wind gust speeds showed promise. Both regression models were shown to be valid and statistically significant. Furthermore, the two regression models developed using VIL and Height of Maximum dBZ as independent variables and the observed wind gust speed as the dependent variable, would have predicted a wind speed within ± 5 kts of the observed wind speed 75% of the time for the thunderstorms studied during this research. Although the sample set consisted of only sixteen airmass thunderstorms, the results suggested that the two regression models hold some potential in forecasting downdraft wind speeds associated with airmass thunderstorms for PAFB. However, the results obtained from these two regression models should not be considered conclusive until tested with a larger data set.

5.4 Possible Sources of Error

There are four possible sources of error for this research. The first of these sources dealt with having only one wind sensor available to record downdraft wind speeds. A second possible source of error was the potential impact due to the gaps that exist between WSR-88D elevation scans. Another source of error involved computing the

sub-cloud temperature lapse rate using an atmospheric sounding valid for a location 50 miles away. Finally, and undoubtedly the most important possible source of error was the small size of the research data set.

The fact that only one wind sensor was available for use during this research required the assumption be made that downdrafts originating from thunderstorms within 10.5 nm of PAFB did not lose significant speed prior to reaching the PAFB wind sensor. Although this is not an invalid assumption, it was still possible the downdraft slowed by a few knots due to friction experienced at the surface. Furthermore, the downdraft could also have slowed due to interaction with other thunderstorm downdrafts. Despite thorough radar interrogation that attempted to identify and discard cases where thunderstorm downdrafts may have interacted, it was still possible cases with interacting downdrafts remained in the data set. Finally, in some rare cases the thunderstorm downdraft may have experienced a ring vortex that would have accelerated the downdraft upon reaching the surface (Fujita, 1985:14).

A radar related source of error dealt with the potential impact caused by the gaps which exist between WSR-88D elevation scans. Although this should not have been a major source of error, it was quite possible that if the thunderstorm's TOP, ST, height of maximum dBZ and/or cloud base fell between radar elevation scans, the radar would have truncated the product's height to the top of the lower elevation scan. Furthermore, if the base reflectivity product was truncated this would have caused the thunderstorm's VIL values to be underestimated since VIL is a reflectivity-derived product. Although this truncation of heights may only cause minor differences between actual and WSR-

88D reported heights, it was still a possible source of error during the data collection stage of this research.

A third possible source of error dealt with calculating the sub-cloud temperature lapse rate for the airmass thunderstorms. The atmospheric sounding data used to compute the sub-cloud temperature lapse rate for PAFB was obtained from a radiosonde sounding site 50 miles from PAFB. Even though this was the closest radiosonde sounding site, it was quite possible that the sub-cloud temperature lapse rate calculated using this data may have been in some cases different from the actual sub-cloud temperature lapse rate at PAFB. Consequently, this would have been a source of error for this research.

A final source of error was the small size of the airmass thunderstorm data set. Although thirty-three airmass thunderstorms were identified for possible study, archived WSR-88D data was available for only twenty-two of these storms. Furthermore, of these twenty-two airmass thunderstorms only nineteen could be accurately identified as the gust-producing storm. Therefore, the results of the evaluation of the four potential wind gust prediction techniques and the results of the statistical analysis conducted using this data set may not be the same results obtained if a larger airmass thunderstorm data set was used. Although the model's validity and statistical significance have been verified, and the model had success in predicting downdraft wind speeds for the data set of airmass thunderstorms, further research still needs to be conducted using a larger data set of airmass thunderstorms to ensure this is a reproducible model. As a result, the smallness of the data set should be considered a possible source of error.

5.5 Recommendations

As a result of this research, several recommendations pertaining to forecasting downdraft wind speeds at PAFB and possible future research are provided. First, it is recommended that the Air Force cease using Headquarters AWS' (1996) VIL/TOP technique. As was discussed earlier, this technique was based on Stewart's (1991) VIL/TOP technique. However, Stewart's (1991) VIL/TOP technique was developed using data from the WSR-57 and not the WSR-88D. Furthermore, the AWS VIL/TOP technique is a modification of Stewart's technique, yet this modification is not based on any case studies or statistical analysis. Consequently, the technique has no scientific basis. Finally, the AWS VIL/TOP technique's achieved a successful potential wind gust forecast rate of only 5.3% for PAFB; thus, for this reason alone should not be used by Air Force forecasters at PAFB.

The second recommendation is Stewart's (1991) VIL/TOP technique, Stewart's (1996) Maximum dBZ/Height of Maximum dBZ technique and Stewart and Vasiloff's (1998) DMP technique should be evaluated with a larger airmass thunderstorm data set in an effort to see if results similar to those of this research can be obtained. Furthermore, any future evaluations using a larger data set should include airmass thunderstorms which did not produce microbursts (i.e., null cases). It appears from this research that the failure of these three techniques to accurately predict downdraft wind speeds at PAFB may result from the fact that these techniques were developed and tested without null cases. This suggests that these techniques may be useful for cases when microbursts occur, but lack proficient prediction skill when null cases are included in the data set. Moreover, future research should include null cases because forecasters will not know

whether a downburst is going to occur until it happens; thus, future research needs to include null cases to ensure any technique developed can be used operationally.

However until more research can be conducted on these techniques, it is recommended based on the data set used in this research, that these three techniques be used with caution and skepticism when used to predict downdraft wind speeds for airmass thunderstorms at PAFB.

The third recommendation is the two regression models developed and tested during this research should be tested with a larger airmass thunderstorm data set.

Although the two regression models performed well with the available data set, only through verification with a larger data set can these regression models be determined conclusive in predicting downdraft wind speeds for airmass thunderstorms at PAFB.

The fourth recommendation is future research on downdraft wind speed prediction should not be limited to WSR-88D products. The results of this research suggest that to accurately predict downdraft wind speeds, other meteorological information (e.g., thermodynamic parameters), as well as WSR-88D data, are needed in order to develop a valid prediction technique. Although the two regression models developed in this research show potential for forecasting downdraft wind speeds at PAFB and should be evaluated using a larger data set of airmass thunderstorms, any future research should not rely solely on WSR-88D products. It is hypothesized by this researcher that any future technique which predicts downdraft wind speeds at PAFB with great skill will not only have to take into account WSR-88D products but other meteorological parameters as well.

The final recommendation is that future research pertaining to forecasting downdraft wind speeds should focus on the soon-to-be-fielded WSR-88D Damaging Downburst Prediction and Detection Algorithm (DDPDA). From an operational perspective, radar operators will most likely use this algorithm instead of the techniques evaluated in this research because of the expected ease the DDPDA will afford them. For this reason, research that can evaluate and identify the strengths and weaknesses of the DDPDA for a given location will provide greater benefit to Air Force forecasters.

Appendix A: Acronyms

AFCCC: Air Force Combat Climatology Center

AFSPC: Air Force Space Command

AGL: Above Ground Level

ASL: Above Sea Level

ASOS: Automated Surface Observation System

AWS: Air Weather Service

CLAWS: Classify, Locate and Avoid Wind Shear

dBZ: Radar reflectivity factor measured in decibels and normalized by $1 \text{ mm}^6 \text{ m}^{-3}$

DMP: Dry Microburst Gust Prediction

EST: Eastern Standard Time

FAA: Federal Aviation Administration

JAWS: Joint Airport Weather Studies

NCDC: National Climatic Data Center

NEXRAD: Next Generation Weather Radar

NIMROD: Northern Illinois Meteorological Research On Downbursts

NLDN: National Lightning Detection Network

NOAA: National Oceanic and Atmospheric Administration

NSSL: National Severe Storms Laboratory

PAFB: Peterson Air Force Base, Colorado

PAM: Portable Automated Mesonet

RADS: Radar Analysis and Display System

SCIT: Storm Cell Identification and Tracking

ST: Radar height of the 30-dBZ echo

TOP: Radar height of the 18.5-dBZ echo

VIL: Vertically Integrated Liquid Water Content

WATADS: WSR-88D Algorithm Testing and Display System

WGP: Wind Gust Potential

WSR-57: Weather Surveillance Radar -1957

WSR-88D: Weather Surveillance Radar -1988 Doppler

Appendix B: Radar Worksheets

Date	1 June 1996
Volume Scan	25
Storm ID Number (NSSL algorithm)	-
Storm ID Number (WSR-88D algorithm)	28
Azimuth/Range	312/37
Storm LAT/LON	38.861N/104.755W
Distance from Wind Sensor	2.8 nm
Storm Motion/Speed	217/19kts
Time of Maximum Wind Gust	0201z
Direction/Speed of Maximum Gust	300/36kts
Time of Maximum VIL	0144z
Maximum VIL: Cell Based	2
Maximum VIL: Grid Based	1
Echo Top Height (AGL)	22,000'
Storm Top Height (AGL)	15,800'
Maximum dBZ	38
Height of Maximum dBZ (AGL)	13,000'
Cloud Base Height (AGL)	6,000'
Mean Wind/Direction Sfc-5000ft	8.2 kts/235°
Sub-Cloud Lapse Rate	10.1°C/km
Predicted Wind Gust Stewart(1991) VIL/TOP	Can't Be Computed
Predicted Wind Gust AWS(1996) VIL/TOP	Can't Be Computed
Predicted Wind Gust Stewart(1996) dBZ/H	Can't Be Computed
Predicted Wind Gust Dry Microburst (1998)	55.2 kts
Type of Environment	Hybrid
Hail Present (Y/N)	No

Date	10 June 1996
Volume Scan	93
Storm ID Number (NSSL algorithm)	22
Storm ID Number (WSR-88D algorithm)	54
Azimuth/Range	305/37
Storm LAT/LON	38.805N/104.814W
Distance from Wind Sensor	3.9 nm
Storm Motion/Speed	308/23kts
Time of Maximum Wind Gust	2334z
Direction/Speed of Maximum Gust	300/46kts
Time of Maximum VIL	2318z
Maximum VIL: Cell Based	23
Maximum VIL: Grid Based	-
Echo Top Height (AGL)	27,000'
Storm Top Height (AGL)	25,000'
Maximum dBZ	56
Height of Maximum dBZ (AGL)	6,700'
Cloud Base Height (AGL)	6,500'
Mean Winds/Direction Sfc-5000ft	8.4 kts/280°
Sub-Cloud Lapse Rate	8.2°C/km
Predicted Wind Gust Stewart(1991) VIL/TOP	34.1 kts
Predicted Wind Gust AWS(1996) VIL/TOP	36.4 kts
Predicted Wind Gust Stewart(1996) dBZ/H	28.6 kts
Predicted Wind Gust Dry Microburst (1998)	48.0 kts
Type of Environment	Dry
Hail Present (Y/N)	No

Date	14 June 1996
Volume Scan	201
Storm ID Number (NSSL algorithm)	-
Storm ID Number (WSR-88D algorithm)	33
Azimuth/Range	310/30
Storm LAT/LON	38.770N/104.658W
Distance from Wind Sensor	4.5 nm
Storm Motion/Speed	176/10kts
Time of Maximum Wind Gust	2124z
Direction/Speed of Maximum Gust	110/30kts
Time of Maximum VIL	2115z
Maximum VIL: Cell Based	17
Maximum VIL: Grid Based	23
Echo Top Height (AGL)	31,000'
Storm Top Height (AGL)	21,200'
Maximum dBZ	57.5
Height of Maximum dBZ (AGL)	5,900'
Cloud Base Height (AGL)	4,000'
Mean Wind/Direction Sfc-5000ft	3.3 kts/200°
Sub-Cloud Lapse Rate	6.7°C/km
Predicted Wind Gust Stewart(1991) VIL/TOP	27.2 kts
Predicted Wind Gust AWS(1996) VIL/ TOP	28.3 kts
Predicted Wind Gust Stewart(1996) dBZ/H	29.9 kts
Predicted Wind Gust Dry Microburst (1998)	Can't Be Computed
Type of Environment	Hybrid
Hail Present (Y/N)	Possible

Date	17 June 1996
Volume Scan	347
Storm ID Number (NSSL algorithm)	12
Storm ID Number (WSR-88D algorithm)	-
Azimuth/Range	326/35.8
Storm LAT/LON	38.944N/104.595W
Distance from Wind Sensor	10.0 nm
Storm Motion/Speed	267/16kts
Time of Maximum Wind Gust	2211z
Direction/Speed of Maximum Gust	020/29kts
Time of Maximum VIL	2148z
Maximum VIL: Cell Based	32
Maximum VIL: Grid Based	36
Echo Top Height (AGL)	35,000'
Storm Top Height (AGL)	23,000'
Maximum dBZ	57
Height of Maximum dBZ (AGL)	6,500'
Cloud Base Height (AGL)	6,100'
Mean Wind/Direction Sfc-5000ft	8.9 kts/220°
Sub-Cloud Lapse Rate	8.6°C/km
Predicted Wind Gust Stewart(1991) VIL/TOP	35.4 kts
Predicted Wind Gust AWS(1996) VIL/ TOP	41.7 kts
Predicted Wind Gust Stewart(1996) dBZ/H	30.2 kts
Predicted Wind Gust Dry Microburst (1998)	59.8 kts
Type of Environment	Dry
Hail Present (Y/N)	Possible

Date	20/21 June 1996
Volume Scan	416
Storm ID Number (NSSL algorithm)	59
Storm ID Number (WSR-88D algorithm)	49
Azimuth/Range	314/34
Storm LAT/LON	38.842N/104.690W
Distance from Wind Sensor	2.6 nm
Storm Motion/Speed	324/33kts
Time of Maximum Wind Gust	21/0300z
Direction/Speed of Maximum Gust	330/22kts
Time of Maximum VIL	21/0250z
Maximum VIL: Cell Based	10
Maximum VIL: Grid Based	23
Echo Top Height (AGL)	32,000'
Storm Top Height (AGL)	22,200'
Maximum dBZ	48.5
Height of Maximum dBZ (AGL)	6,200'
Cloud Base Height (AGL)	6,200'
Mean Wind/Direction Sfc-5000ft	9.3 kts/260°
Sub-Cloud Lapse Rate	8.5°C/km
Predicted Wind Gust Stewart(1991) VIL/TOP	26.9 kts
Predicted Wind Gust AWS(1996) VIL/ TOP	33.3 kts
Predicted Wind Gust Stewart(1996) dBZ/H	16.0 kts
Predicted Wind Gust Dry Microburst (1998)	42.3 kts
Type of Environment	Hybrid
Hail Present (Y/N)	No

Date	26/27 June 1996
Volume Scan	140
Storm ID Number (NSSL algorithm)	53
Storm ID Number (WSR-88D algorithm)	-
Azimuth/Range	299/42
Storm LAT/LON	38.787N/104.952W
Distance from Wind Sensor	10.4 nm
Storm Motion/Speed	193/21kts
Time of Maximum Wind Gust	27/0000z
Direction/Speed of Maximum Gust	200/23kts
Time of Maximum VIL	2342z
Maximum VIL: Cell Based	-
Maximum VIL: Grid Based	4
Echo Top Height (AGL)	20,000'
Storm Top Height (AGL)	12,500'
Maximum dBZ	43
Height of Maximum dBZ (AGL)	8,100'
Cloud Base Height (AGL)	8,000'
Mean Wind/Direction Sfc-5000ft	7.9 kts/200°
Sub-Cloud Lapse Rate	9.3°C/km
Predicted Wind Gust Stewart(1991) VIL/TOP	Can't Be Computed
Predicted Wind Gust AWS(1996) VIL/ TOP	Can't Be Computed
Predicted Wind Gust Stewart(1996) dBZ/H	10.8 kts
Predicted Wind Gust Dry Microburst (1998)	46.4 kts
Type of Environment	Dry
Hail Present (Y/N)	No

Date	28 August 1996
Volume Scan	226
Storm ID Number (NSSL algorithm)	38
Storm ID Number (WSR-88D algorithm)	17
Azimuth/Range	320/33
Storm LAT/LON	38.870N/104.620W
Distance from Wind Sensor	6.2 nm
Storm Motion/Speed	309/14kts
Time of Maximum Wind Gust	2148z
Direction/Speed of Maximum Gust	010/31kts
Time of Maximum VIL	2136z
Maximum VIL: Cell Based	28
Maximum VIL: Grid Based	37
Echo Top Height (AGL)	30,000'
Storm Top Height (AGL)	28,000'
Maximum dBZ	57
Height of Maximum dBZ (AGL)	6,100'
Cloud Base Height (AGL)	2,900'
Mean Wind/Direction Sfc-5000ft	6.1 kts/290°
Sub-Cloud Lapse Rate	6.5°C/km
Predicted Wind Gust Stewart(1991) VIL/TOP	43.9 kts
Predicted Wind Gust AWS(1996) VIL/ TOP	43.8 kts
Predicted Wind Gust Stewart(1996) dBZ/H	29.3 kts
Predicted Wind Gust Dry Microburst (1998)	Can't Be Computed
Type of Environment	Hybrid
Hail Present (Y/N)	Possible

Date	6 May 1997
Volume Scan	294
Storm ID Number (NSSL algorithm)	33
Storm ID Number (WSR-88D algorithm)	-
Azimuth/Range	310/43
Storm LAT/LON	38.908N/104.872W
Distance from Wind Sensor	8.5 nm
Storm Motion/Speed	274/19kts
Time of Maximum Wind Gust	1854z
Direction/Speed of Maximum Gust	200/15kts
Time of Maximum VIL	1845z
Maximum VIL: Cell Based	1
Maximum VIL: Grid Based	2
Echo Top Height (AGL)	19,000'
Storm Top Height (AGL)	16,500'
Maximum dBZ	36
Height of Maximum dBZ (AGL)	5,000'
Cloud Base Height (AGL)	4,800'
Mean Wind/Direction Sfc-5000ft	-
Sub-Cloud Lapse Rate	11.3°C/km
Predicted Wind Gust Stewart(1991) VIL/TOP	Can't Be Computed
Predicted Wind Gust AWS(1996) VIL/ TOP	Can't Be Computed
Predicted Wind Gust Stewart(1996) dBZ/H	4.4 kts
Predicted Wind Gust Dry Microburst (1998)	Can't Be Computed
Type of Environment	Dry
Hail Present (Y/N)	No

Date	18 May 1997
Volume Scan	410
Storm ID Number (NSSL algorithm)	8
Storm ID Number (WSR-88D algorithm)	72
Azimuth/Range	317/41
Storm LAT/LON	38.948N/104.766W
Distance from Wind Sensor	8.0 nm
Storm Motion/Speed	262/27kts
Time of Maximum Wind Gust	0128z
Direction/Speed of Maximum Gust	020/25kts
Time of Maximum VIL	0108z
Maximum VIL: Cell Based	2
Maximum VIL: Grid Based	-
Echo Top Height (AGL)	20,000'
Storm Top Height (AGL)	11,700'
Maximum dBZ	41.5
Height of Maximum dBZ (AGL)	3,300'
Cloud Base Height (AGL)	3,000'
Mean Wind/Direction Sfc-5000ft	18.0 kts/250°
Sub-Cloud Lapse Rate	5.8°C/km
Predicted Wind Gust Stewart(1991) VIL/TOP	Can't Be Computed
Predicted Wind Gust AWS(1996) VIL/ TOP	Can't Be Computed
Predicted Wind Gust Stewart(1996) dBZ/H	7.2 kts
Predicted Wind Gust Dry Microburst (1998)	Can't Be Computed
Type of Environment	Hybrid
Hail Present (Y/N)	No

Date	18 June 1997
Volume Scan	183
Storm ID Number (NSSL algorithm)	13
Storm ID Number (WSR-88D algorithm)	-
Azimuth/Range	310/34
Storm LAT/LON	38.813N/104.723W
Distance from Wind Sensor	0.5 nm
Storm Motion/Speed	255/8kts
Time of Maximum Wind Gust	2320z
Direction/Speed of Maximum Gust	030/23kts
Time of Maximum VIL	2306z
Maximum VIL: Cell Based	9
Maximum VIL: Grid Based	10
Echo Top Height (AGL)	26,000'
Storm Top Height (AGL)	21,700'
Maximum dBZ	46
Height of Maximum dBZ (AGL)	2,700'
Cloud Base Height (AGL)	2,700'
Mean Wind/Direction Sfc-5000ft	8.7 kts/255°
Sub-Cloud Lapse Rate	9.7°C/km
Predicted Wind Gust Stewart(1991) VIL/TOP	4.1 kts
Predicted Wind Gust AWS(1996) VIL/ TOP	Can't Be Computed
Predicted Wind Gust Stewart(1996) dBZ/H	9.3 kts
Predicted Wind Gust Dry Microburst (1998)	57.2 kts
Type of Environment	Hybrid
Hail Present (Y/N)	No

Date	19 June 1997
Volume Scan	237
Storm ID Number (NSSL algorithm)	65
Storm ID Number (WSR-88D algorithm)	48
Azimuth/Range	311/34
Storm LAT/LON	38.820N/104.715W
Distance from Wind Sensor	0.9 nm
Storm Motion/Speed	265/12kts
Time of Maximum Wind Gust	2134z
Direction/Speed of Maximum Gust	030/33kts
Time of Maximum VIL	2118z
Maximum VIL: Cell Based	2
Maximum VIL: Grid Based	5
Echo Top Height (AGL)	16,000'
Storm Top Height (AGL)	13,000'
Maximum dBZ	45
Height of Maximum dBZ (AGL)	6,200'
Cloud Base Height (AGL)	2,600'
Mean Wind/Direction Sfc-5000ft	11.2 kts/280°
Sub-Cloud Lapse Rate	9.6°C/km
Predicted Wind Gust Stewart(1991) VIL/TOP	9.2 kts
Predicted Wind Gust AWS(1996) VIL/ TOP	Can't Be Computed
Predicted Wind Gust Stewart(1996) dBZ/H	12.1 kts
Predicted Wind Gust Dry Microburst (1998)	54.1 kts
Type of Environment	Hybrid
Hail Present (Y/N)	No

Date	26 June 1997
Volume Scan	318
Storm ID Number (NSSL algorithm)	-
Storm ID Number (WSR-88D algorithm)	67
Azimuth/Range	307/35
Storm LAT/LON	38.799N/104.764W
Distance from Wind Sensor	1.8 nm
Storm Motion/Speed	298/8kts
Time of Maximum Wind Gust	2254z
Direction/Speed of Maximum Gust	300/28kts
Time of Maximum VIL	2241z
Maximum VIL: Cell Based	14
Maximum VIL: Grid Based	14
Echo Top Height (AGL)	35,000'
Storm Top Height (AGL)	22,900'
Maximum dBZ	49.5
Height of Maximum dBZ (AGL)	6,400'
Cloud Base Height (AGL)	6,000'
Mean Wind/Direction Sfc-5000ft	12.4 kts/180°
Sub-Cloud Lapse Rate	8.5°C/km
Predicted Wind Gust Stewart(1991) VIL/TOP	Can't Be Computed
Predicted Wind Gust AWS(1996) VIL/ TOP	Can't Be Computed
Predicted Wind Gust Stewart(1996) dBZ/H	17.5 kts
Predicted Wind Gust Dry Microburst (1998)	45.4 kts
Type of Environment	Dry
Hail Present (Y/N)	No

Date	27 June 1997
Volume Scan	360
Storm ID Number (NSSL algorithm)	24
Storm ID Number (WSR-88D algorithm)	19
Azimuth/Range	311/37
Storm LAT/LON	38.853N/104.764W
Distance from Wind Sensor	2.6 nm
Storm Motion/Speed	-
Time of Maximum Wind Gust	1954z
Direction/Speed of Maximum Gust	350/23kts
Time of Maximum VIL	1920z
Maximum VIL: Cell Based	7
Maximum VIL: Grid Based	-
Echo Top Height (AGL)	24,000'
Storm Top Height (AGL)	18,100'
Maximum dBZ	51.5
Height of Maximum dBZ (AGL)	4,000'
Cloud Base Height (AGL)	3,500'
Mean Wind/Direction Sfc-5000ft	3.6 kts/210°
Sub-Cloud Lapse Rate	8.0°C/km
Predicted Wind Gust Stewart(1991) VIL/TOP	Can't Be Computed
Predicted Wind Gust AWS(1996) VIL/ TOP	Can't Be Computed
Predicted Wind Gust Stewart(1996) dBZ/H	16.4 kts
Predicted Wind Gust Dry Microburst (1998)	> 37.1 kts
Type of Environment	Hybrid
Hail Present (Y/N)	No

Date	4 July 1997
Volume Scan	89
Storm ID Number (NSSL algorithm)	-
Storm ID Number (WSR-88D algorithm)	33
Azimuth/Range	315/34
Storm LAT/LON	38.849N/104.681W
Distance from Wind Sensor	3.1 nm
Storm Motion/Speed	-
Time of Maximum Wind Gust	2254z
Direction/Speed of Maximum Gust	050/23kts
Time of Maximum VIL	2235z
Maximum VIL: Cell Based	4
Maximum VIL: Grid Based	4
Echo Top Height (AGL)	29,000'
Storm Top Height (AGL)	21,200'
Maximum dBZ	40
Height of Maximum dBZ (AGL)	6,500'
Cloud Base Height (AGL)	6,000'
Mean Wind/Direction Sfc-5000ft	8.7 kts/210°
Sub-Cloud Lapse Rate	9.5°C/km
Predicted Wind Gust Stewart(1991) VIL/TOP	Can't Be Computed
Predicted Wind Gust AWS(1996) VIL/TOP	Can't Be Computed
Predicted Wind Gust Stewart(1996) dBZ/H	7.5 kts
Predicted Wind Gust Dry Microburst (1998)	47.4 kts
Type of Environment	Dry
Hail Present (Y/N)	No

Date	26 July 1997
Volume Scan	110
Storm ID Number (NSSL algorithm)	66
Storm ID Number (WSR-88D algorithm)	40
Azimuth/Range	313/37
Storm LAT/LON	38.869N/104.746W
Distance from Wind Sensor	3.2 nm
Storm Motion/Speed	-
Time of Maximum Wind Gust	1954z
Direction/Speed of Maximum Gust	110/19kts
Time of Maximum VIL	1948z
Maximum VIL: Cell Based	27
Maximum VIL: Grid Based	19
Echo Top Height (AGL)	25,000'
Storm Top Height (AGL)	23,400'
Maximum dBZ	55.5
Height of Maximum dBZ (AGL)	8,000'
Cloud Base Height (AGL)	8,000'
Mean Wind/Direction Sfc-5000ft	8.5 kts/280°
Sub-Cloud Lapse Rate	9.4°C/km
Predicted Wind Gust Stewart(1991) VIL/TOP	25.4 kts
Predicted Wind Gust AWS(1996) VIL/TOP	35.5 kts
Predicted Wind Gust Stewart(1996) dBZ/H	30.0 kts
Predicted Wind Gust Dry Microburst (1998)	>60.8 kts
Type of Environment	Hybrid
Hail Present (Y/N)	Possible

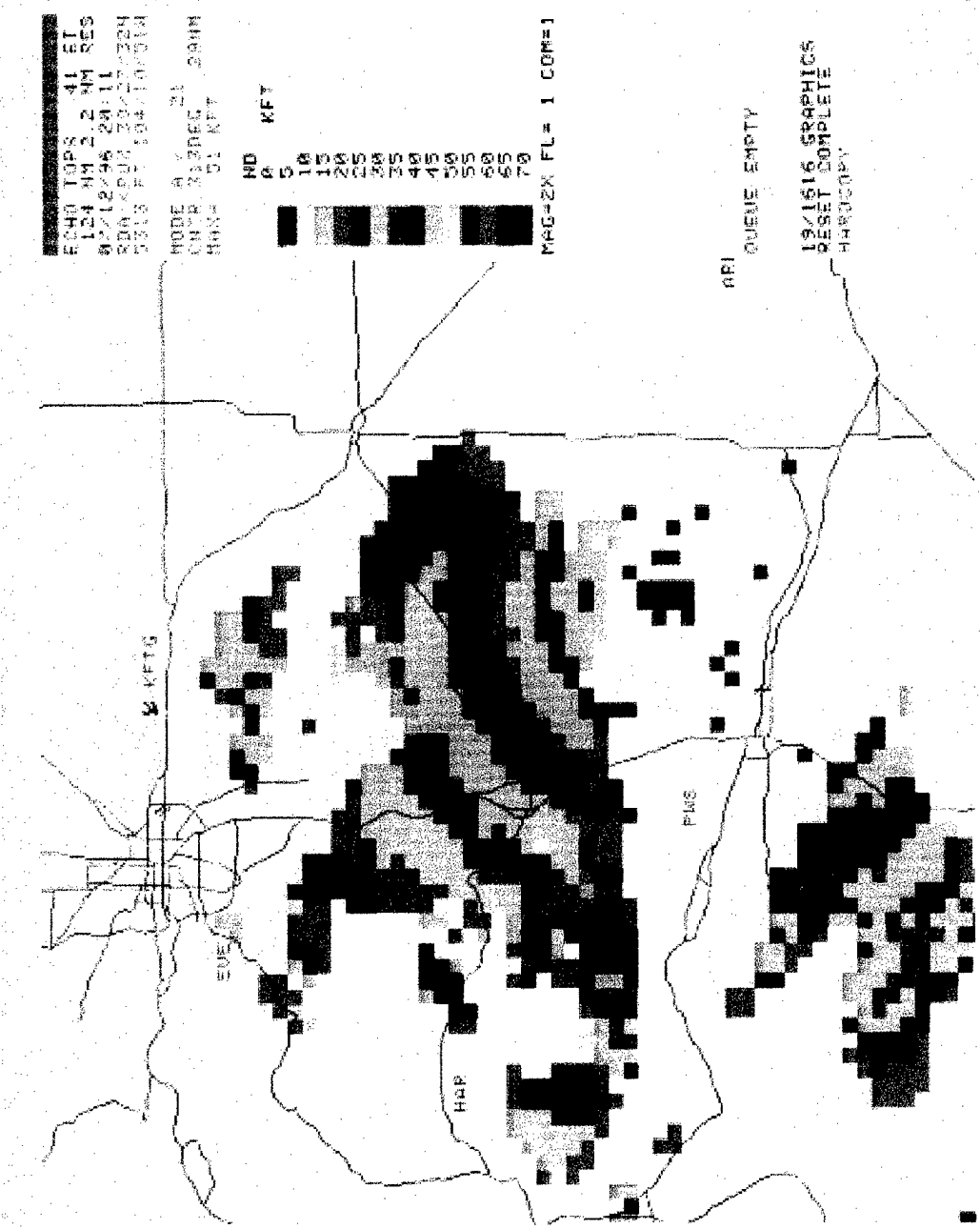
Date	31 July 1997
Volume Scan	179
Storm ID Number (NSSL algorithm)	55
Storm ID Number (WSR-88D algorithm)	6
Azimuth/Range	312/44
Storm LAT/LON	38.938N/104.867W
Distance from Wind Sensor	9.6 nm
Storm Motion/Speed	311/8kts
Time of Maximum Wind Gust	1/0054z
Direction/Speed of Maximum Gust	350/29kts
Time of Maximum VIL	0032z
Maximum VIL: Cell Based	11
Maximum VIL: Grid Based	13
Echo Top Height (AGL)	22,000'
Storm Top Height (AGL)	17,300'
Maximum dBZ	53
Height of Maximum dBZ (AGL)	8,500'
Cloud Base Height (AGL)	3,700'
Mean Wind/Direction Sfc-5000ft	4.7 kts/230°
Sub-Cloud Lapse Rate	6.0°C/km
Predicted Wind Gust Stewart(1991) VIL/TOP	21.8 kts
Predicted Wind Gust AWS(1996) VIL/TOP	Can't Be Computed
Predicted Wind Gust Stewart(1996) dBZ/H	25.7 kts
Predicted Wind Gust Dry Microburst (1998)	Can't Be Computed
Type of Environment	Hybrid
Hail Present (Y/N)	No

Date	2 August 1997
Volume Scan	343
Storm ID Number (NSSL algorithm)	-
Storm ID Number (WSR-88D algorithm)	96
Azimuth/Range	311/40
Storm LAT/LON	38.885N/104.813W
Distance from Wind Sensor	5.5 nm
Storm Motion/Speed	-
Time of Maximum Wind Gust	2241z
Direction/Speed of Maximum Gust	310/24kts
Time of Maximum VIL	2233z
Maximum VIL: Cell Based	6
Maximum VIL: Grid Based	8
Echo Top Height (AGL)	23,000'
Storm Top Height (AGL)	14,900'
Maximum dBZ	48.5
Height of Maximum dBZ (AGL)	7,600'
Cloud Base Height (AGL)	3,200'
Mean Wind/Direction Sfc-5000ft	8.9 kts/180°
Sub-Cloud Lapse Rate	5.4°C/km
Predicted Wind Gust Stewart(1991) VIL/TOP	6.4 kts
Predicted Wind Gust AWS(1996) VIL/TOP	Can't Be Computed
Predicted Wind Gust Stewart(1996) dBZ/H	17.4 kts
Predicted Wind Gust Dry Microburst (1998)	Can't Be Computed
Type of Environment	Hybrid
Hail Present (Y/N)	No

Date	24 August 1997
Volume Scan	121
Storm ID Number (NSSL algorithm)	23
Storm ID Number (WSR-88D algorithm)	82
Azimuth/Range	317/38
Storm LAT/LON	38.912N/104.721W
Distance from Wind Sensor	5.7 nm
Storm Motion/Speed	-
Time of Maximum Wind Gust	0154z
Direction/Speed of Maximum Gust	320/18kts
Time of Maximum VIL	0125z
Maximum VIL: Cell Based	2
Maximum VIL: Grid Based	3
Echo Top Height (AGL)	23,000'
Storm Top Height (AGL)	14,100'
Maximum dBZ	43
Height of Maximum dBZ (AGL)	7,100'
Cloud Base Height (AGL)	7,000'
Mean Wind/Direction Sfc-5000ft	7.8 kts/360°
Sub-Cloud Lapse Rate	9.3°C/km
Predicted Wind Gust Stewart(1991) VIL/TOP	Can't Be Computed
Predicted Wind Gust AWS(1996) VIL/TOP	Can't Be Computed
Predicted Wind Gust Stewart(1996) dBZ/H	10.5 kts
Predicted Wind Gust Dry Microburst (1998)	47.2 kts
Type of Environment	Dry
Hail Present (Y/N)	No

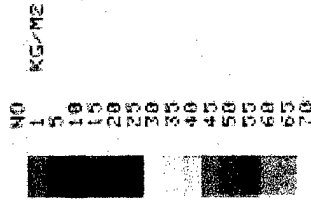
Date	11 September 1997
Volume Scan	297
Storm ID Number (NSSL algorithm)	23
Storm ID Number (WSR-88D algorithm)	-
Azimuth/Range	304/36
Storm LAT/LON	38.784N/104.804W
Distance from Wind Sensor	3.9 nm
Storm Motion/Speed	310/8kts
Time of Maximum Wind Gust	2054z
Direction/Speed of Maximum Gust	290/25kts
Time of Maximum VIL	2044z
Maximum VIL: Cell Based	6
Maximum VIL: Grid Based	7
Echo Top Height (AGL)	16,000'
Storm Top Height (AGL)	13,400'
Maximum dBZ	47
Height of Maximum dBZ (AGL)	6,600'
Cloud Base Height (AGL)	4,400'
Mean Wind/Direction Sfc-5000ft	6.0 kts/180°
Sub-Cloud Lapse Rate	6.6°C/km
Predicted Wind Gust Stewart(1991) VIL/TOP	15.6 kts
Predicted Wind Gust AWS(1996) VIL/TOP	Can't Be Computed
Predicted Wind Gust Stewart(1996) dBZ/H	14.6 kts
Predicted Wind Gust Dry Microburst (1998)	Can't Be Computed
Type of Environment	Hybrid
Hail Present (Y/N)	No

Appendix C: Sample WSR-88D Images

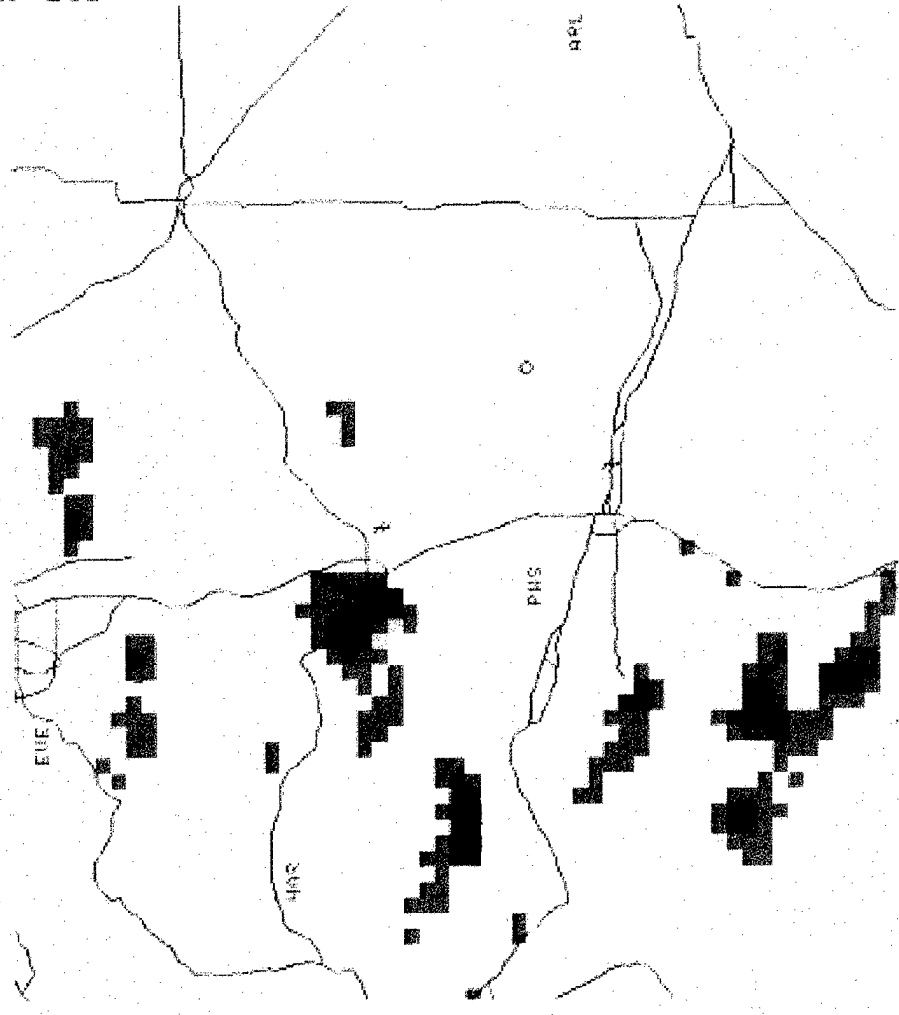


TOP image as displayed on the WSR-88D from which Echo Top heights can be obtained.

19/1616 18:17
 U INT LOD 57 VIL
 129 NR 2 2 NR
 07/12/96 20:16
 RORRPOX 2827282H
 5317 FT 11421145IN
 MODE A 21
 CMTS 300DEC 22HM
 MAKE 48 K24M3



MAG=2X FL=1 COM=1
 OUL 53 M HC
 OUL 020-ME TU



QUEUE EMPTY

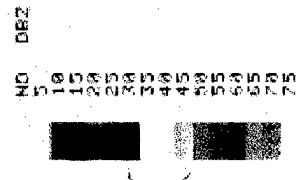
19/1616 GRAPHICS
 RESET COMPLETE
 HIGH COPY

OVERLAYS OFF

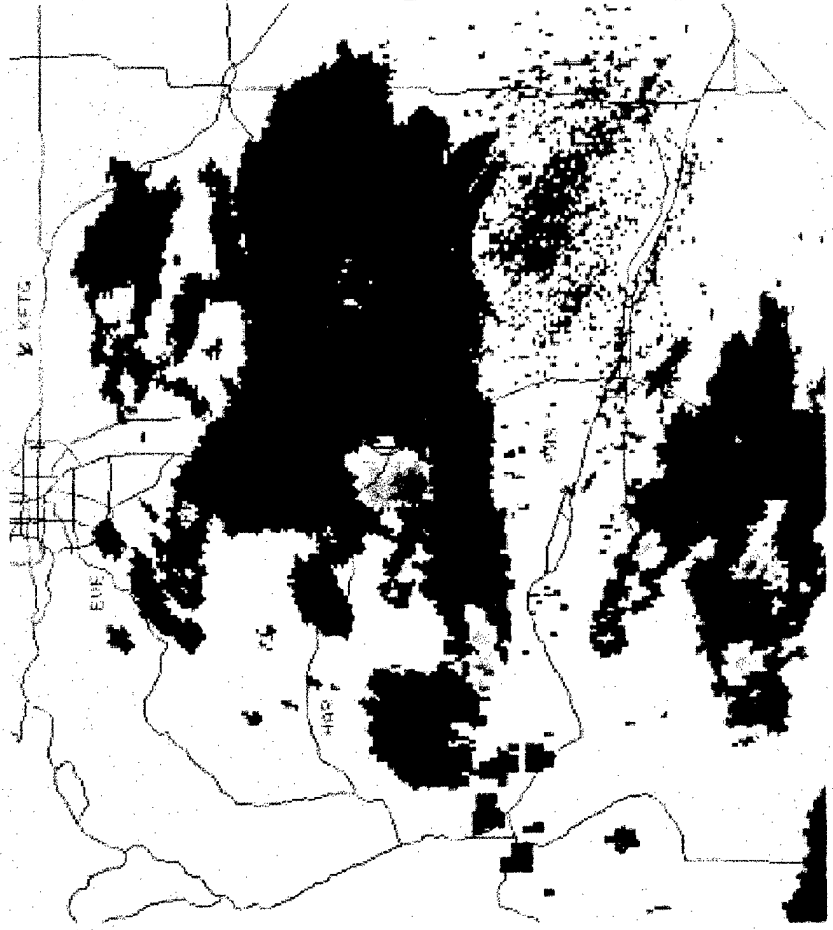
VIL image as displayed on the WSR-88D from which Grid Based VIL values can be obtained.

MI 12749 1811M
 CME REF 54 07 CR
 124 NR 54 07 RES
 87-12296 08-16
 RPT PER 20 00 22N
 SET PT 104 10 53R

MODE 0 21
 DATE 081000 0810M
 MAG 53 DBZ



MAG=2X FL= 2 COM=1



RPT (209)
 QUEUE EMPTY

12/16/15 GRAPHICS
 READY COMPLETE
 HARD COPY

Composite Reflectivity image as displayed on the WSR-88D from which Maximum Reflectivity values can be obtained.

Bibliography

- Brown, John M., Kevin R. Knupp, and Fernando Caracena. "Destructive Winds from Shallow, High-Based Cumulonimbi," Proceedings of the 12th Conference on Severe Local Storms: 272-275. San Antonio, Texas: American Meteorological Society, 1981.
- Burrill, Don. Civilian Weather Observer for the Colorado Springs Airport. Telephone Interview. 21 December 1998.
- Department of Commerce. Doppler Radar Meteorological Observations: WSR-88D Unit Description and Operational Applications. FCM-H11D-1991. Washington: GPO, April 1992.
- Devore, Jay L. Probability and Statistics for Engineering and the Sciences (Fourth Edition). Pacific Grove, California: Brooks/Cole Publishing Company, 1995.
- Emanuel, Kerry A. "A Similarity Theory for Unsaturated Downdrafts within Clouds," Journal of the Atmospheric Sciences: 1541-1557 (August 1981).
- Foster, Donald S. "Thunderstorm Gusts Compared with Computed Downdraft Speeds," Monthly Weather Review: 91-94 (March 1958).
- Frazier, Mark. "The Prediction of Thunderstorm Wind Gusts Based on Vertically Integrated Water Content and Storm Echo Tops," Eastern Region Technical Attachment Number 94-7B: 1-9 (July 1994).
- Fujita, Theodore T. The Downburst Microburst and Macrobust. Chicago: University of Chicago Press, 1985.
- Greene, Douglas R. and Robert A. Clark. "Vertically Integrated Liquid Water: A New Analysis Tool," Monthly Weather Review, 7: 548-552 (1972).
- Huschke, Ralph E. Glossary of Meteorology. Boston: American Meteorological Society, 1989.
- Headquarters Air Weather Service. "Operational Uses of VIL," Echoes, 16: 1-12 (January 1996).
- McCarthy, John and James Wilson. "The Classify, Locate, and Avoid Wind Shear (CLAWS) Project at Denver's Stapleton International Airport: Operational Testing of Terminal Weather Hazard Warnings with an Emphasis on Microburst Wind Shear," Proceedings of the 2nd International Conference on the Aviation Weather System: 247-256. Montreal, Canada: American Meteorological Society, 1985.

Miller, R.C. "Notes on analysis and Severe Storm Forecasting Procedures of the Military Warning Center," USAF Air Weather Service Manual Number 200: (1967)

National Oceanic and Atmospheric Administration. Daily Weather Maps. 1 April-30 September 1996, 1 April-30 September 1997. Washington D.C.: Department of Commerce, 1996-1997.

National Weather Service Training Center Hydrometeorology and Management Division. Thunderstorms, Silver Springs, Maryland: September 1993.

Read, W. L. and J. T. Elmore. "Summer Season Severe Downbursts in North Texas: Forecast and Warning Techniques Using Current National Weather Service Technology," Proceedings of the 12th Conference on Weather Analysis and Forecasting: 142-147. Monterey: American Meteorological Society, 1989.

Reynolds, Daniel E. Professor of Statistics. Air Force Institute of Technology, Wright-Patterson AFB, OH. Personal Interview. December 1998.

Rinehart, Ronald E. Radar for Meteorologists (Third Edition). Fargo: Knight Printing Company, 1997.

Roberts, Rita D. and James W. Wilson. "A Proposed Microburst Nowcasting Procedure Using Single-Doppler Radar," Journal of Applied Meteorology: 285-303 (April 1989).

Squires, P. "Penetrative Downdraughts in Cumuli," Tellus, 10: 381-389 (1958).

Srivastava, R. C. "A Simple Model of Evaporatively Driven Downdraft: Application to Microburst Downdraft," Journal of the Atmospheric Sciences: 1004-1023 (May 1985).

Stewart, Stacy R. "The Prediction of Pulse-Type Thunderstorm Gusts Using Vertically Integrated Liquid Content (VIL) and the Cloud Top Penetrative Downdraft Mechanism," NOAA Technical Memorandum NWS SR-136: 1-20 (October 1991).

---- "Wet Microbursts: Predicting Peak Wind Gusts Associated with Summertime Pulse-Type Thunderstorms," Proceedings of the 15th Conference on Weather Analysis and Forecasting: 324-327. Norfolk, Virginia: American Meteorological Society, 1996.

---- Meteorologist Instructor, NEXRAD Operational Support Facility, Norman, OK.
E-mail Correspondence. 13 November 1998.

---- and Steve Vasiloff. "Dry Microburst Prediction and Detection by Doppler Radar."
Excerpt from unpublished article, 1-52.
<http://www.osf.noaa.gov/otb/working/dmb/storybrd.htm>. 24 July 1998.

USAF Technical Training School. Doppler Radar Glossary. E4OST2524-009. Keesler
AFB: AETC, July 1993.

---- PUP Operator. E3OZR15W3-014. Keesler AFB: AETC, April 1993.

Wakimoto, Roger M. "Forecasting Dry Microburst Activity over the High Plains,"
Monthly Weather Review. 1131-1143 (July 1985).

Wilks, Daniel S. Statistical Methods in the Atmospheric Sciences. San Diego: Academic
Press, 1995.

Vita

Captain Travis A. Steen was born 27 May 1970 in Mankato, Minnesota. He graduated from Iowa State University with a Bachelor of Science degree in Meteorology in December 1992. He was commissioned through the Detachment 250 AFROTC at Iowa State University.

His first assignment was at Camp Red Cloud, Republic of Korea where he was the Division Weather Officer for the U.S. Army's 2nd Infantry Division from March 1993 to March 1994. He was reassigned to the 21st Operational Support Squadron, Detachment A, Cheyenne Mountain Air Force Base, Colorado where he served as an Air Force Space Command weather briefer. He was reassigned to Peterson Air Force Base, Colorado in July 1994 to serve as the United States Space Command/NORAD/Air Force Space Command CINC weather briefer. In August 1997, he entered the Graduate Meteorology program, School of Engineering, Air Force Institute of Technology.

Permanent Address: 1570F Bromley Drive
Fairborn, OH 45324